NASA TECHNICAL MEMORANDUM

NASA TM X-2748

CASE FILE COPY

AERODYNAMIC CHARACTERISTICS OF A 55° CLIPPED-DELTA-WING ORBITER MODEL AT MACH NUMBERS FROM 1.60 TO 4.63

by A. B. Blair, Jr., and Josephine Grow

Langley Research Center
Hampton, Va. 23365

1. Report No. NASA TM X-2748	2. Government Accession No.	3. Recipient's Catalog No.
4. Title and Subtitle AERODYNAMIC CHARACTERISTICS OF A 55° CLIPPED-DELTA-WING ORBITER MODEL AT MACH NUMBERS FROM 1.60 TO 4.63		5. Report Date May 1973
		6. Performing Organization Code
7. Author(s) A. B. Blair, Jr., and Josephine Grow		8. Performing Organization Report No. L-8732
		10. Work Unit No. 502-37-01-01
9. Performing Organization Name and Address NASA Langley Research Center Hampton, Va. 23665		11. Contract or Grant No.
		13. Type of Report and Period Covered Technical Memorandum
12. Sponsoring Agency Name and Address National Aeronautics and Space Administration Washington, D.C. 20546		14. Sponsoring Agency Code

15. Supplementary Notes

16. Abstract

An investigation has been conducted in the Langley Unitary Plan wind tunnel to determine the supersonic aerodynamic characteristics of a delta-wing orbiter model. The model was tested at Mach numbers from 1.60 to 4.63, at nominal angles of attack from -2° to 30°, at nominal angles of sideslip from -4° to 10°, and at Reynolds numbers from 5.9×10^6 to 8.2×10^6 per meter (1.8×10^6 to 2.5×10^6 per ft).

17. Key Words (Suggested by Author(s)) Space-shuttle vehicle Delta-wing orbiter Entry vehicles	18. Distribution Statement Unclassified — Unlimited		
19. Security Classif. (of this report) Unclassified	20. Security Classif. (of this page) Unclassified	21. No. of Pages 94	22. Price* $3.00

AERODYNAMIC CHARACTERISTICS OF A 55° CLIPPED-DELTA-WING
ORBITER MODEL AT MACH NUMBERS FROM 1.60 TO 4.63

By A. B. Blair, Jr., and Josephine Grow
Langley Research Center

SUMMARY

A wind-tunnel investigation has been conducted at Mach numbers from 1.60 to 4.63, at nominal angles of attack from -2° to 30°, and at nominal angles of sideslip from -4° to 10° to determine the static aerodynamic characteristics of a 55° clipped-delta-wing orbiter model.

Results of this investigation indicated that the configuration had negative pitching moment at zero lift despite a significant positive increment provided by the flared rudder. The elevons were effective in producing positive pitch control throughout the angle-of-attack (α) range and Mach number range. The aerodynamic-center location varied about 10 percent of the fuselage length with change in Mach number from 1.60 to 4.63. The configuration is longitudinally stable at trimmed conditions for a flight α-schedule of a high-cross-range mission.

The configuration is directionally stable at all Mach numbers for $\alpha \approx 0°$. For the flight α-schedule, the model is directionally stable at low Mach numbers but becomes unstable at the higher Mach numbers. The model has positive effective dihedral across the Mach number range for either $\alpha \approx 0°$ or for the flight α-case. The rudder flare provided a large increase in directional stability and positive effective dihedral.

Differential elevon deflection is effective in producing rolling moment with resulting favorable yawing moments. The flared rudder provided directional control throughout the angle-of-attack range and Mach number range; however, an adverse rolling moment accompanied the yaw control.

INTRODUCTION

The National Aeronautics and Space Administration is currently engaged in a study directed toward the development of a reusable space-shuttle system capable of economically placing large payloads in near-earth orbit. As part of this study, the Langley Research Center has conducted investigations of various concepts in wind tunnels encompassing the Mach number range from subsonic to hypersonic speeds. One of the shuttle-

orbiter configurations investigated was the Grumman Aerospace Corporation H-33 design which had a low-fineness-ratio body with a large base, a 55° clipped-delta wing, and a center-line vertical tail. The summary aerodynamic characteristics of this design across its operational speed range have been published in reference 1. The objective of the present paper is to provide more detailed information for the H-33 configuration at supersonic speeds. The investigation was conducted in the Langley Unitary Plan wind tunnel at Mach numbers from 1.60 to 4.63 over a nominal angle-of-attack range from -2° to 30° and at nominal angles of sideslip from -4° to 10°. The Reynolds numbers of the tests varied from 5.9×10^6 to 8.2×10^6 per meter (1.8×10^6 to 2.5×10^6 per ft). The basic model had a 30° flared rudder. The tests include the effect of the flared rudder, the effects of rudder deflection, and the effect of elevon deflection for both pitch and roll control.

SYMBOLS

The results of this investigation are presented as force and moment coefficients with the longitudinal characteristics referred to the stability-axis system and the lateral characteristics referred to the body-axis system.

Measurements and calculations were made in U.S. Customary Units. They are presented herein in the International System of Units (SI) with the equivalent values in the U.S. Customary Units given parenthetically.

The moment reference point is located at 66.3 percent fuselage length.

b wing span, 43.576 cm (17.156 in.)

C_D drag coefficient, $\dfrac{\text{Drag}}{qS}$

$C_{D,b}$ base drag coefficient, $\dfrac{\text{Base drag}}{qS}$

C_L lift coefficient, $\dfrac{\text{Lift}}{qS}$

C_{L_α} lift-curve slope near $\alpha = 0°$, per deg

C_l rolling-moment coefficient, $\dfrac{\text{Rolling moment}}{qSb}$

C_{l_β} effective-dihedral parameter, $\left(\Delta C_l / \Delta \beta\right)_{\beta=0°,4°}$

2

C_m pitching-moment coefficient, $\dfrac{\text{Pitching moment}}{qSl}$

C_{m_α} slope of pitching-moment curve, $\dfrac{C_m}{\alpha} = \left(\dfrac{C_L}{\alpha}\right)\left(\dfrac{C_m}{C_L}\right)$, at trimmed conditions for the flight α-schedule

$C_{m_{\delta_e}}$ pitch control effectiveness of elevons at $\alpha = 0^O$, per deg

C_n yawing-moment coefficient, $\dfrac{\text{Yawing moment}}{qSb}$

C_{n_β} directional-stability parameter, $\left(\Delta C_n / \Delta \beta\right)_{\beta=0^O, 4^O}$

C_Y side-force coefficient, $\dfrac{\text{Side force}}{qS}$

C_{Y_β} side-force parameter, $\left(\Delta C_Y / \Delta \beta\right)_{\beta=0^O, 4^O}$

L/D lift-drag ratio

l reference fuselage length, 60.96 cm (24 in.)

M Mach number

q free-stream dynamic pressure, N/m^2 (psf)

S wing area, 0.09869 m^2 (1.06228 ft^2)

t/c thickness-chord ratio

x_{ac}/l aerodynamic-center location in percent fuselage length from model nose ($\alpha \approx 0^O$)

α angle of attack, deg

β angle of sideslip, deg

δ_e pitch-control deflection of elevons (symmetric), $\dfrac{\delta_{e_L} + \delta_{e_R}}{2}$, negative with trailing edge up, deg

δ_{e_L} left-elevon surface deflection angle (negative deflection, trailing edge up), deg

3

δ_{e_R} right-elevon surface deflection angle (negative deflection, trailing edge up), deg

δ_r full-span flared rudder deflection, $\dfrac{\delta_r(\text{left panel}) + \delta_r(\text{right panel})}{2}$, positive deflection is trailing edge left, deg

δ_{rf} rudder flare angle, split rudder deflection with left split rudder trailing edge left and right split rudder trailing edge right, $\dfrac{\delta_r(\text{left panel}) - \delta_r(\text{right panel})}{2}$, deg

Abbreviations:

BL   buttock line

MS   model station

WL   water line

Model components:

B_5 body

V_5 center-line vertical tail

W_4 wing

Subscripts:

max   maximum

o   at zero lift

APPARATUS AND METHODS

Tunnel

The tests were conducted in both the low and high Mach number test sections of the Langley Unitary Plan wind tunnel, which is a variable-pressure continuous-flow facility. The test sections are approximately 2.13 meters (7 ft) long and 1.22 meters (4 ft) square. The nozzles leading to the test sections are of the asymmetric sliding-block

4

type which permits a continuous variation in Mach number from about 1.5 to 2.9 in the low Mach number test section and from about 2.3 to 4.7 in the high Mach number test section.

Model

Details of the 0.0148-scale orbiter model are shown in figure 1 and tables I to V. A photograph of the model is shown as figure 2. The model had a 55° clipped-delta wing and a center-line vertical tail. Symmetric deflections of the wing-mounted elevons produced pitch control whereas differential deflections provided roll control. A full-span 30° flared rudder was provided for yaw control. Three simulated rocket nozzles protruded from the base of the model in a retracted position with the inner portion removed for sting clearance.

Unless otherwise indicated all configurations in the present report had a full-span flared rudder $\left(\delta_{rf} = 30^\circ\right)$.

Test Conditions

Tests were performed at the following tunnel conditions:

Mach number	Stagnation temperature		Stagnation pressure		Reynolds number	
	K	°F	kN/m²	psfa	per meter	per foot
1.60	325	125	46.49	971	5.9×10^6	1.8×10^6
1.90	325	125	57.50	1201	6.6	2.0
2.16	325	125	75.89	1585	7.9	2.4
2.86	339	150	123.05	2570	8.2	2.5
3.95	352	175	231.21	4829	8.2	2.5
4.63	352	175	315.72	6594	8.2	2.5

The dewpoint temperature measured at stagnation pressure was maintained below 239 K (-30° F) to assure negligible condensation effects. All tests were performed with boundary-layer transition strips on the fuselage 3.05 cm (1.20 in.) aft of the nose, and on both sides of the wing and vertical tail 1.02 cm (0.40 in.) aft of the leading edges, measured streamwise. For M = 1.60, 1.90, 2.16, and 2.86 the transition strips were approximately 0.159 cm wide (0.062 in.) and were composed of No. 60 sand grains sprinkled in acrylic plastic. For M = 3.95 and 4.63, the transition strips were composed of a single line of No. 45 sand grains.

Measurements

Aerodynamic forces and moments were measured by means of a six-component electrical strain-gage balance housed within the model. The balance was rigidly fastened to a sting support system. Balance-chamber pressure was measured by means of a single static-pressure orifice located in the vicinity of the balance. In addition, pressure measurements were made at the bases of the fuselage and engine nozzles.

Corrections

Angles of attack have been corrected for tunnel-flow misalinement. Angles of attack and sideslip have been corrected for deflection of the sting and balance due to aerodynamic loads. The drag results have not been adjusted to correspond to free-stream static-pressure conditions at the base. However, typical values of base drag coefficient that include balance chamber, nozzle, and fuselage base drag coefficients are presented in figure 3.

PRESENTATION OF RESULTS

RESULTS AND DISCUSSION

Flight Regimes

The proposed return-from-orbit flight plan calls for entry into the earth's atmosphere at high angles of attack much like a ballistic spacecraft. An attitude-control propulsion system is used for pitch, yaw, and roll control during the high-altitude hypersonic flight where dynamic pressures are low. At lower altitudes when dynamic pressures

become sufficiently high, a mixed-mode control is possible (i.e., both aerodynamic and reaction control systems). In the supersonic and transonic phase of the flight the vehicle is in a transition maneuver from high to lower angles of attack where aerodynamic controls alone are to be used. At subsonic speeds, an aircraft-mode glide to a horizontal landing is made. A typical flight trajectory (from ref. 1) for a high cross range ($\approx$1000 nautical miles) is presented in figure 4. As may be seen, the angle of attack of the orbiter in the speed range of the present investigation (M = 1.60 to 4.63) varies from about 7° to 27°; however, vehicle angles of attack at supersonic speeds for other missions such as a minimum-cross-range quick-return-to-earth case may be as high as 45°. The angle-of-attack range of greatest interest for the shuttle, therefore, is considerably higher and broader than that of conventional supersonic aircraft. For convenience of discussion, however, the trajectory of figure 4 will be considered as the nominal mission for the vehicle.

Longitudinal Characteristics

The longitudinal aerodynamic characteristics of the configuration including elevon pitch-control effectiveness are presented in figure 5. The variation in lift with angle of attack is reasonably linear throughout the Mach number range and angle-of-attack range. At Mach numbers to 2.16 a pitch-up tendency is indicated that limits the trim angles of attack available. The stable trim range is sufficient, however, for the low angles of attack expected for flight in this Mach range (see fig. 4). At the higher Mach numbers a pitch-down tendency occurs so that the high trim angles of attack which are required are attainable. The trim-control deflections required are somewhat large due to the negative $C_{m,o}$ that exists throughout the test Mach number range. The elevons are effective in producing pitching moment with an increase in elevon effectiveness indicated with increase in lift particularly at the higher Mach numbers (see fig. 5(f), for example). The results shown in figures 6(d) to 6(f) indicate that combining $\pm$10° of roll deflection with elevon pitch deflections of -10° and -20° has only a slight effect on the pitch characteristics.

Flaring the rudder of the H-33 configuration was done primarily to increase directional stability; there were also effects on the longitudinal characteristics. For example, there is a significant positive increment in $C_{m,o}$ for the configuration with the flared rudder when compared with that for the unflared rudder (fig. 7). The data indicate that the increase in $C_{m,o}$ is caused primarily by the higher drag of the flared configuration since the drag increment is above the moment center. A similar increment in $C_{m,o}$ due to rudder flare is also seen in figure 8 where, for δ_e = -20°, the complete configuration (vertical tail with rudder flare) is compared with the configuration with the vertical tail removed. Except for a slight increase in C_D and $C_{m,o}$, a rudder deflection of 5° has little effect on the longitudinal characteristics of the model (fig. 9).

A summary of the longitudinal aerodynamic characteristics at low angles of attack ($\alpha \approx 0^{\circ}$) and at trimmed conditions for the flight α-schedule (fig. 4) may be found in figures 10(a) and 10(b), respectively. In figure 10(a) the data show the usual decrease in $C_{L_{\alpha}}$, $C_{D,o}$, $(L/D)_{max}$, and elevon effectiveness with increase in Mach number. These data also show a change in aerodynamic-center location of almost 10 percent of the fuselage length with change in Mach number from 1.60 to 4.63. In figure 10(b) the longitudinal aerodynamic characteristics that are shown were taken from figure 5 at trimmed conditions for the flight α-schedule. These data show that the configuration is longitudinally stable $\left(-C_{m_{\alpha}}\right)$ at trimmed conditions for the given flight α-schedule. The maximum trimmed lift-drag value for the configuration was about 1.80 at M = 2.86.

<center>Lateral Characteristics</center>

The lateral aerodynamic characteristics in sideslip for the model at several angles of attack are presented in figure 11. These data are shown primarily to indicate the linearity of the coefficients with sideslip angles since all lateral parameters were obtained from incremental results of tests made through the angle-of-attack range at $\beta = 0^{\circ}$ and 4°. The results were generally linear for the lower angles of attack to $\beta = 4^{\circ}$ and indicated that the comparative results shown for the lateral parameters at these angles of attack are valid. It should be noted that the data shown in figure 11 at Mach numbers up to 2.16 are for the configuration with the unflared rudder rather than for the basic configuration which is shown for the higher Mach numbers. Although the stability level for these lower Mach number data will be considerably different, the linearity of the data should not be materially affected.

Figure 12 shows the effect of elevon deflections (symmetric for pitch) on the lateral parameters. Tests were made only for Mach numbers of 2.86 and above and indicate there is little effect on $C_{n_{\beta}}$ and some reduction in positive effective dihedral $\left(-C_{l_{\beta}}\right)$ due to pitch-control deflection.

The effect of the rudder flare (see fig. 13) is to increase the side-force parameter with an attendant increase in directional stability and in positive effective dihedral. Removal of the entire vertical tail, of course, leads to a directionally unstable model at all test Mach numbers.

A summary of the lateral and directional stability parameters at $\alpha \approx 0^{\circ}$ and for the flight α-schedule is presented in figures 14(a) and 14(b), respectively. At $\alpha \approx 0^{\circ}$ the configuration is directionally stable at all Mach numbers. For the flight α-schedule, the model is directionally stable at low Mach numbers but becomes unstable at the two highest Mach numbers. The model has positive effective dihedral across the Mach range for either $\alpha \approx 0^{\circ}$ or for the flight α-case.

8

Elevon and rudder effectiveness is shown in figures 15 and 16, respectively. Differential elevon deflection is effective in producing rolling moment with resulting favorable yawing moments. The flared rudder provided directional control that generally decreased with increase in α and Mach number. An adverse rolling moment accompanied the yaw control, however.

CONCLUSIONS

A wind-tunnel investigation has been conducted at Mach numbers from 1.60 to 4.63, at nominal angles of attack from -2° to 30°, and at nominal angles of sideslip from -4° to 10° to determine the static aerodynamic characteristics of a 55° clipped-delta-wing orbiter model. Results of this investigation indicated the following conclusions:

1. The configuration had negative pitching moment at zero lift $(-C_{m,o})$ despite a significant positive increment in $C_{m,o}$ provided by the flared rudder. The elevons were effective in producing positive pitch control throughout the angle-of-attack (α) range and Mach number range.

2. The aerodynamic-center location varied about 10 percent of the fuselage length with change in Mach number from 1.60 to 4.63.

3. The configuration is longitudinally stable at trimmed conditions for the flight α-schedule of a high-cross-range mission.

4. The configuration is directionally stable at all Mach numbers for $\alpha \approx 0^{\circ}$. For the flight α-schedule, the model is directionally stable at low Mach numbers but becomes unstable at the higher Mach numbers. The model has positive effective dihedral across the Mach number range for either $\alpha \approx 0^{\circ}$ or for the flight α-case.

5. The flared rudder provided a large increase in directional stability and positive effective dihedral.

6. Differential elevon deflection is effective in producing rolling moment with resulting favorable yawing moments. The flared rudder provided directional control throughout the angle-of-attack range and Mach number range; however, an adverse rolling moment accompanied the yaw control.

Langley Research Center,
    National Aeronautics and Space Administration,
        Hampton, Va., March 29, 1973.

REFERENCE

1. Rainey, Robert W.; Ware, George M.; Powell, Richard W.; Brown, Lawrence W.; and Stone, David R.: Grumman H-33 Space Shuttle Orbiter Aerodynamic and Handling-Qualities Study. NASA TN D-6948, 1972.

TABLE I.- GEOMETRIC CHARACTERISTICS OF THE

BASIC H-33 ORBITER BODY $\left(B_5\right)$

	Full scale	Model (0.0148) scale
Length, cm (in.)	4114.8 (1620)	60.960 (24.000)
Maximum width, cm (in.)	762.0 (300)	11.288 (4.444)
Maximum depth, cm (in.)	838.2 (330)	12.418 (4.889)
Fineness ratio	4.92	4.92
Area:		
Maximum cross-sectional, m^2 (ft^2) . . .	49.24 (530.0)	0.0108 (0.1163)
Planform, m^2 (ft^2)	289.86 (3120.0)	0.0636 (0.6848)
Wetted, m^2 (ft^2)	0.97 (10.4)	0.2109 (2.2705)
Base, m^2 (ft^2)	42.83 (461.0)	0.0094 (0.1012)

TABLE II.- GEOMETRIC CHARACTERISTICS OF THE
BASIC H-33 ORBITER WING $\left(W_4\right)$

	Full scale	Model (0.0148) scale
Area:[a]		
Planform, m^2 (ft^2)	449.64 (4840.0)	0.0987 (1.0623)
Wetted, m^2 (ft^2)	551.83 (5940.0)	0.1211 (1.3037)
Span[a] (equivalent), cm (in.)	2880.36 (1134.00)	42.67 (16.800)
Aspect ratio[a]	1.845	1.845
Taper ratio[a]	0.178	0.178
Dihedral angle, deg	5	5
Incidence angle, deg	2 at body, -3 at tip	2 at body, -3 at tip
Sweepback angles:		
Leading edge, deg	55	55
Trailing edge, deg	-5	-5
0.25 chord, deg	46.32	46.32
Chords:[a]		
Root (wing station 0.0), cm (in.)	2650.54 (1043.52)	39.268 (15.460)
Tip (equivalent), cm (in.)	471.83 (185.76)	6.990 (2.752)
Mean aerodynamic chord, cm (in.)	1813.56 (714.00)	26.868 (10.578)
Airfoil section:		
Root	t/c = 9.5 percent cambered section	t/c = 9.5 percent cambered section
Tip	t/c = 9.5 percent cambered section	t/c = 9.5 percent cambered section
Area,[b] m^2 (ft^2)	269.41 (2900.0)	0.0591 (0.6365)
Span,[b] (equivalent), cm (in.)	2118.36 (834.00)	31.384 (12.356)
Aspect ratio[b]	1.666	1.666
Taper ratio[b]	0.228	0.228
Chords:[b]		
Root, cm (in.)	2072.03 (815.76)	30.696 (12.085)
Tip, cm (in.)	471.83 (185.76)	6.990 (2.752)
Mean aerodynamic chord, cm (in.)	1438.66 (566.40)	21.313 (8.391)

[a] Data for total wing.

[b] Data for exposed wing only.

TABLE III.- GEOMETRIC CHARACTERISTICS OF THE

ELEVON FOR W_4 WING

	Full scale	Model (0.0148) scale
Area, m^2 (ft^2)	38.09 (410.0)	0.0084 (0.0900)
Span (equivalent), cm (in.)	1059.18 (417.0)	15.692 (6.178)
Chords (equivalent):		
Inboard, cm (in.)	414.53 (163.2)	6.142 (2.418)
Outboard, cm (in.)	304.80 (120.0)	4.516 (1.778)
Sweepback angles:		
Leading edge, deg	0	0
Trailing edge, deg	-5	-5
Hinge line, deg	0	0

TABLE IV.- GEOMETRIC CHARACTERISTICS OF THE
BASIC H-33 ORBITER VERTICAL TAIL $\left(V_5\right)$

	Full scale		Model (0.0148) scale	
Area, m^2 (ft^2)	79.43	(855.0)	0.0174	(0.1877)
Chords (equivalent):	1028.70	(405.0)	15.240	(6.000)
Inboard, cm (in.)	1117.40	(439.9)	16.553	(6.517)
Outboard, cm (in.)	426.72	(168.0)	6.322	(2.489)
Ratio elevator chord to horizontal tail chord:				
At inboard equivalent chord		0.348		0.348
At outboard equivalent chord.		0.351		0.351
Sweepback angles:				
Leading edge, deg		47		47
Trailing edge, deg		21.85		21.85
Hinge line, deg		32		32
Aspect ratio.		1.33		1.33
Taper ratio		0.38		0.38
Mean aerodynamic chord, cm (in.)	822.96	(324.0)	12.192	(4.800)
Airfoil section	NACA 64A010		NACA 64A010	

TABLE V.- GEOMETRIC CHARACTERISTICS OF THE
RUDDER FOR V_5 VERTICAL TAIL

	Full scale	Model (0.0148) scale
Area, m^2 (ft^2)	27.13 (292.0)	0.0060 (0.0641)
Span (equivalent), cm (in.)	1059.18 (417.0)	15.692 (6.178)
Chords (equivalent):		
Inboard, cm (in.)	388.87 (153.1)	5.761 (2.268)
Outboard, cm (in.)	149.86 (59.0)	2.223 (0.875)
Sweepback angles:		
Leading edge, deg	32	32
Trailing edge, deg	21.85	21.85
Hinge line, deg	32	32
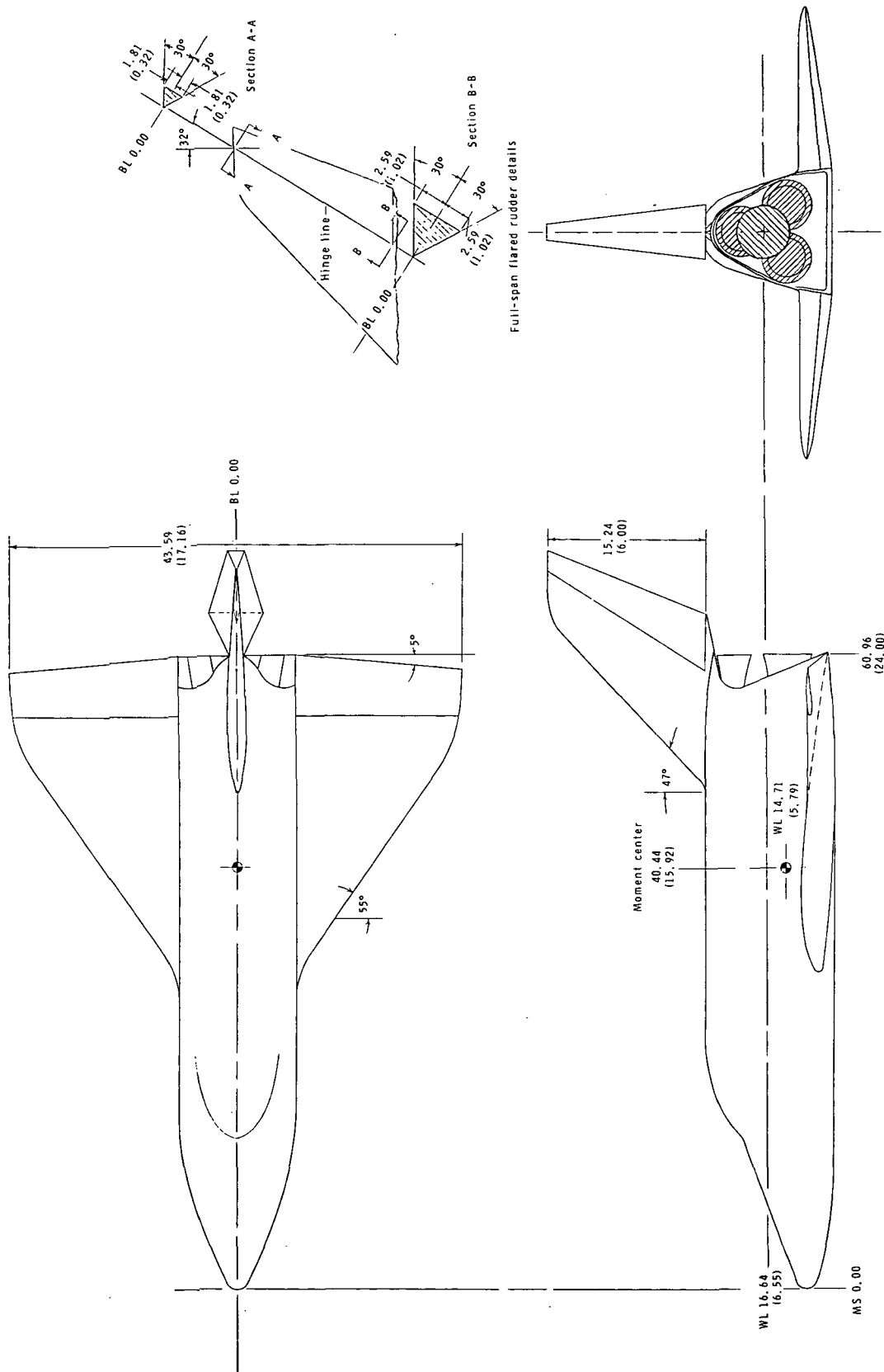
Figure 1.- Model details. All dimensions are given in centimeters (inches).
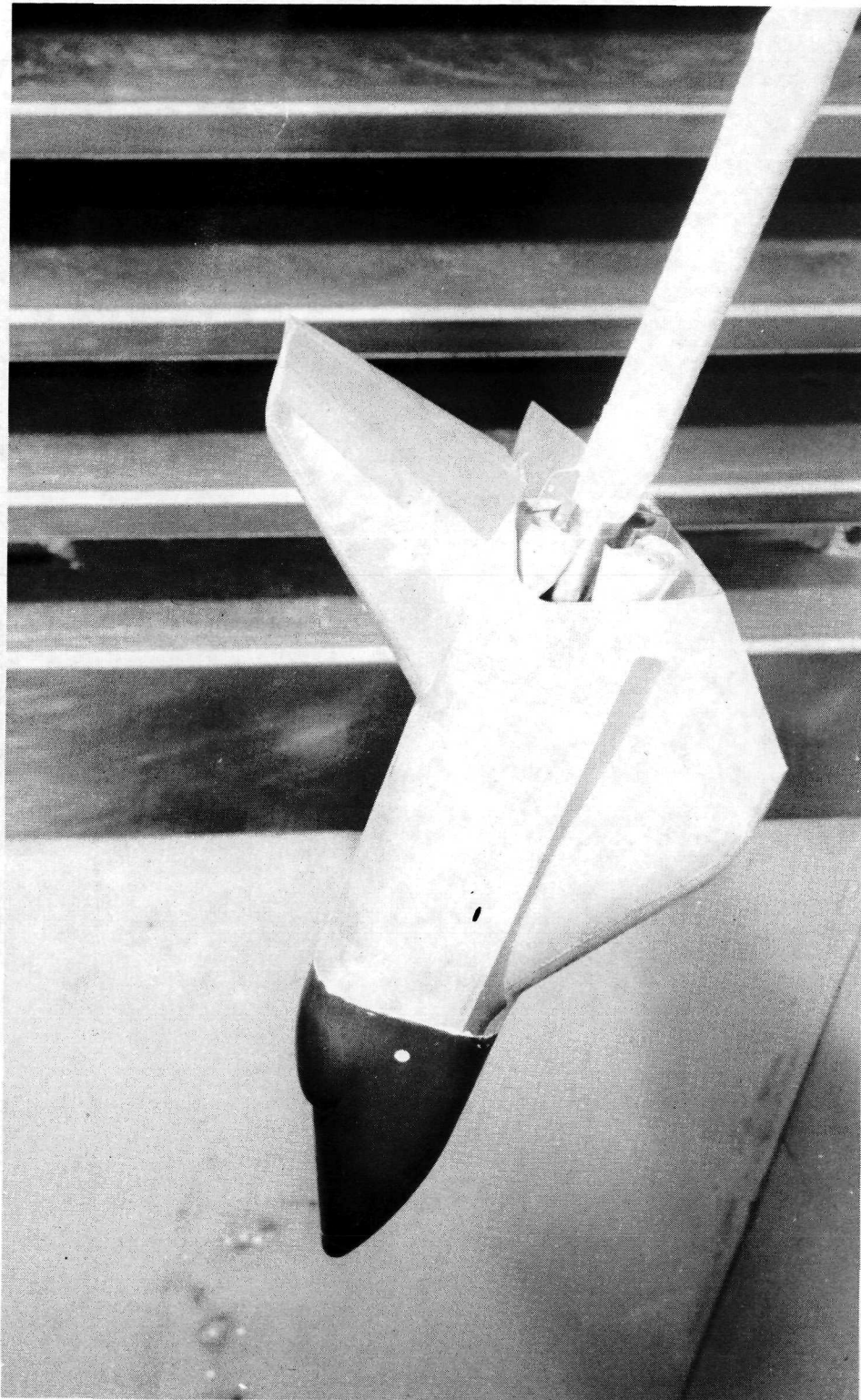
Figure 2.- Model photograph.
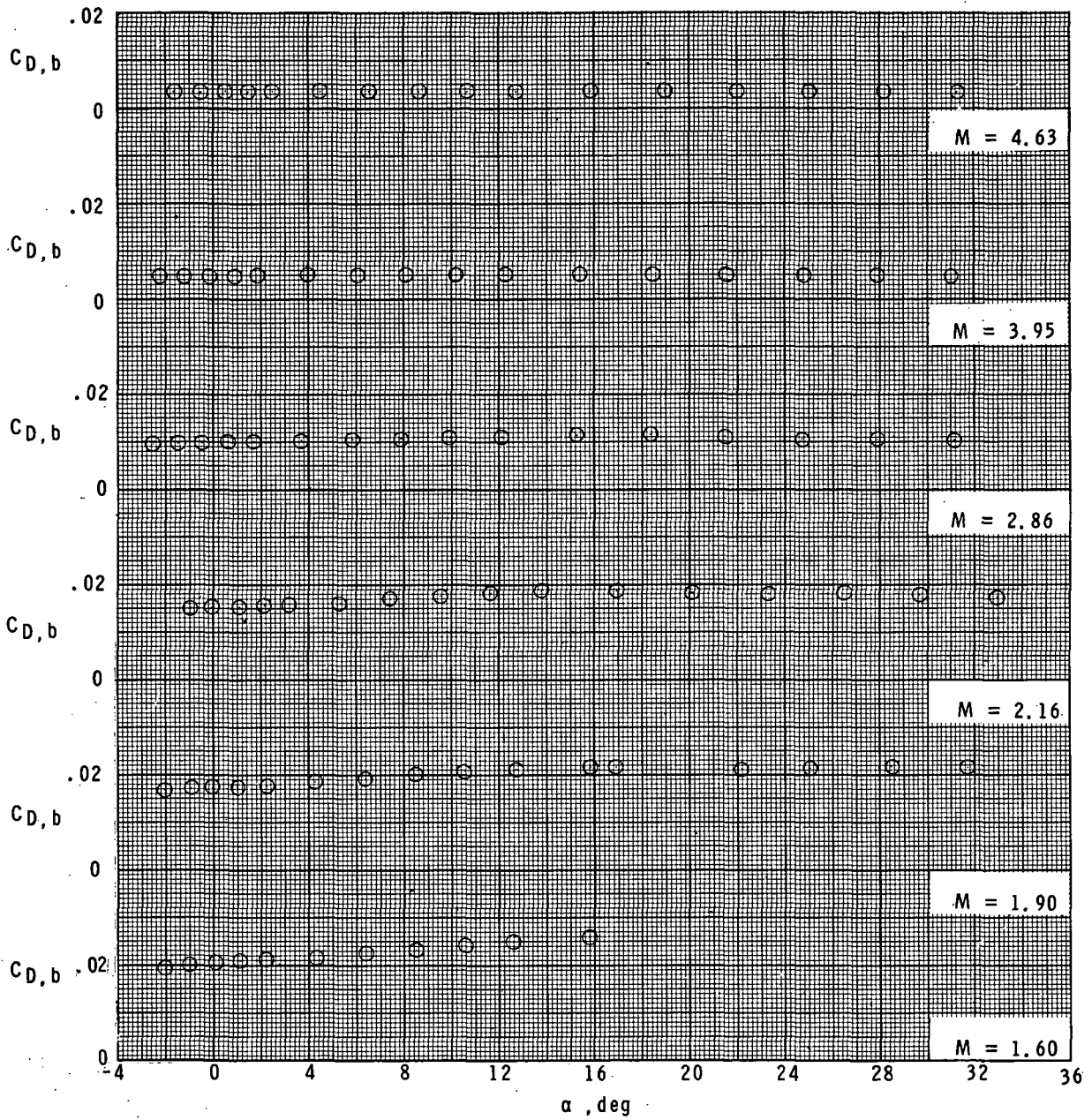
Figure 3.- Typical values of the base drag coefficients.
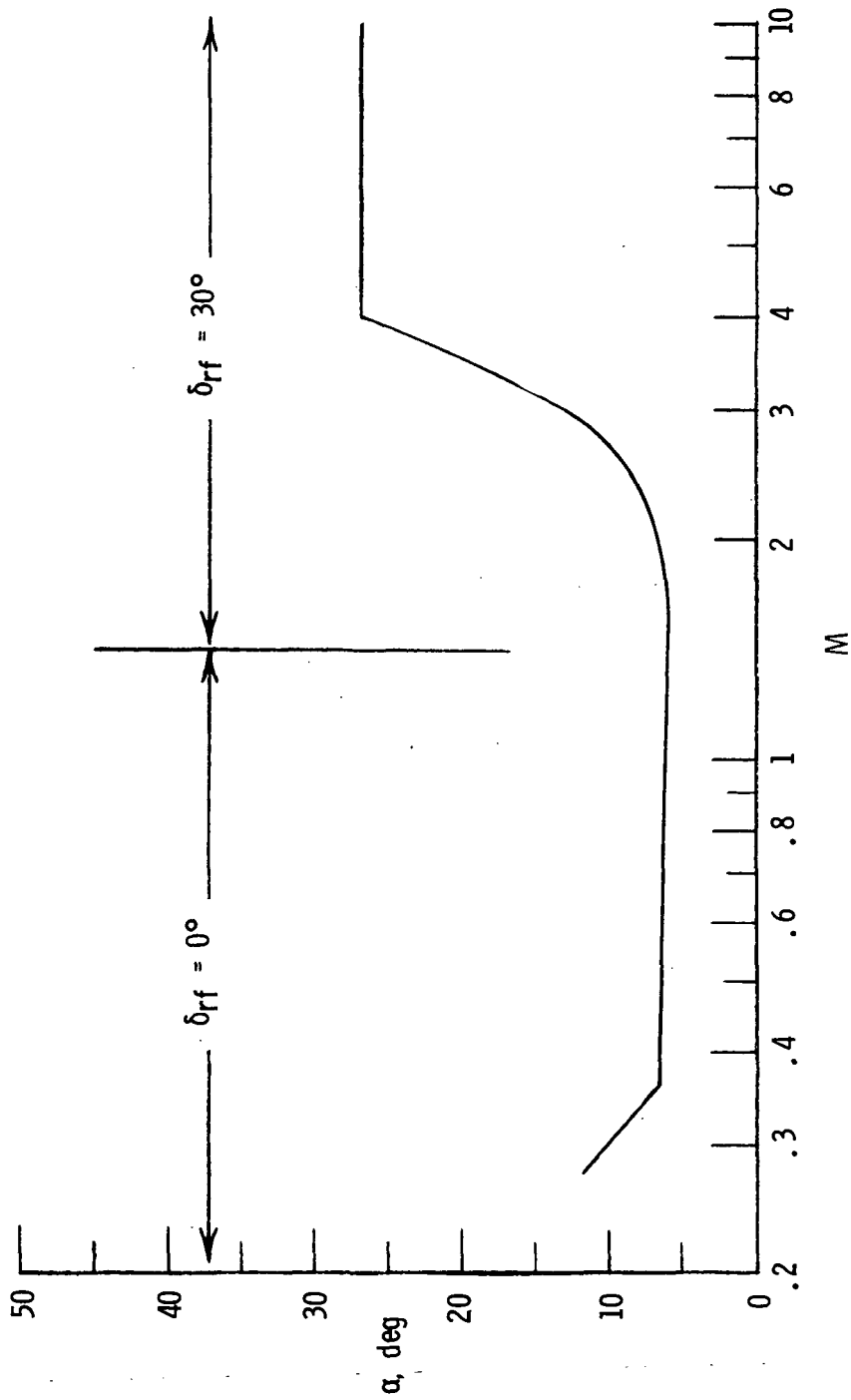
Figure 4.- Nominal operational α-schedule for high-cross-range mission (ref. 1).

18
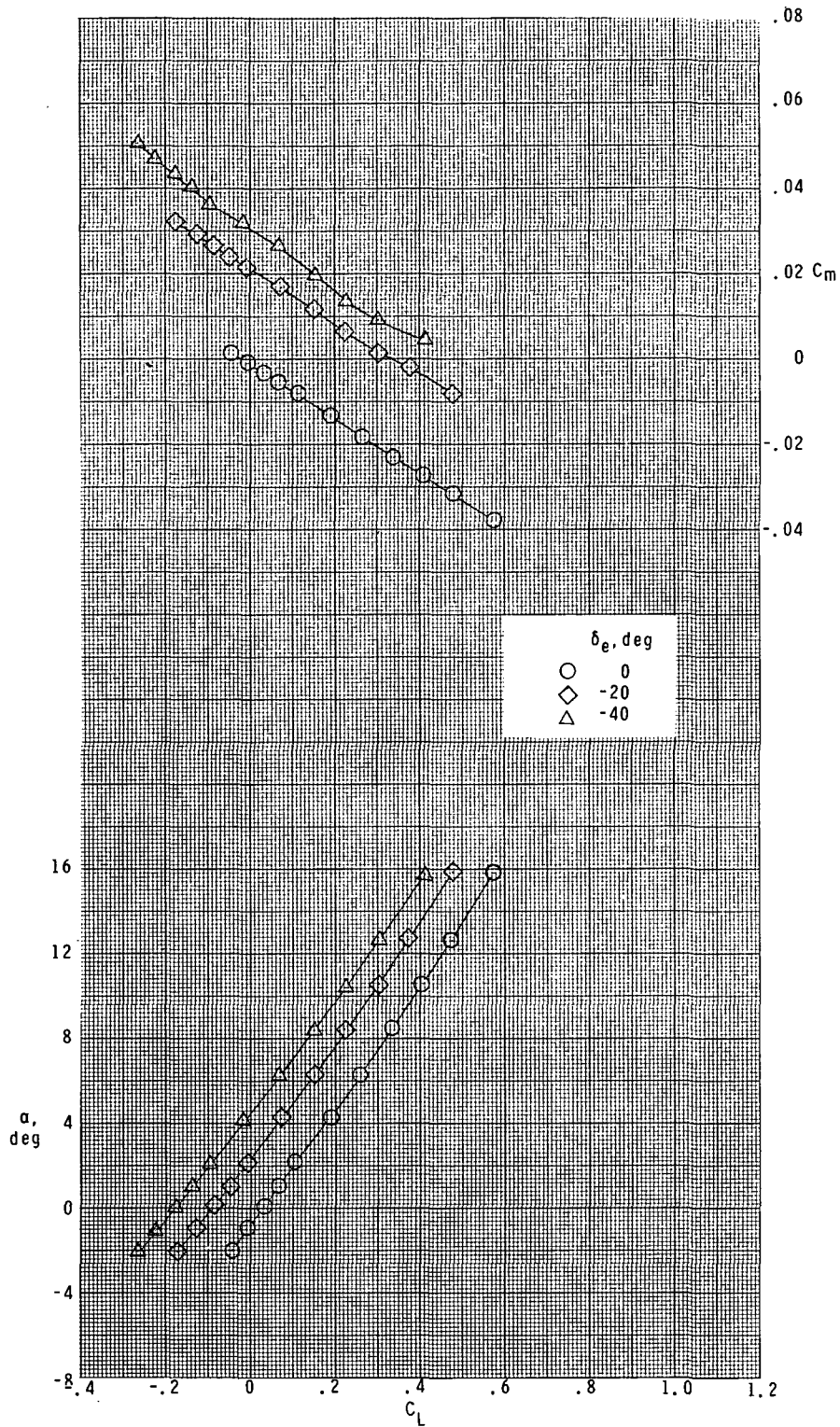
(a) M = 1.60.

Figure 5.- Elevon effectiveness in pitch. $\delta_{rf} = 30^O$.
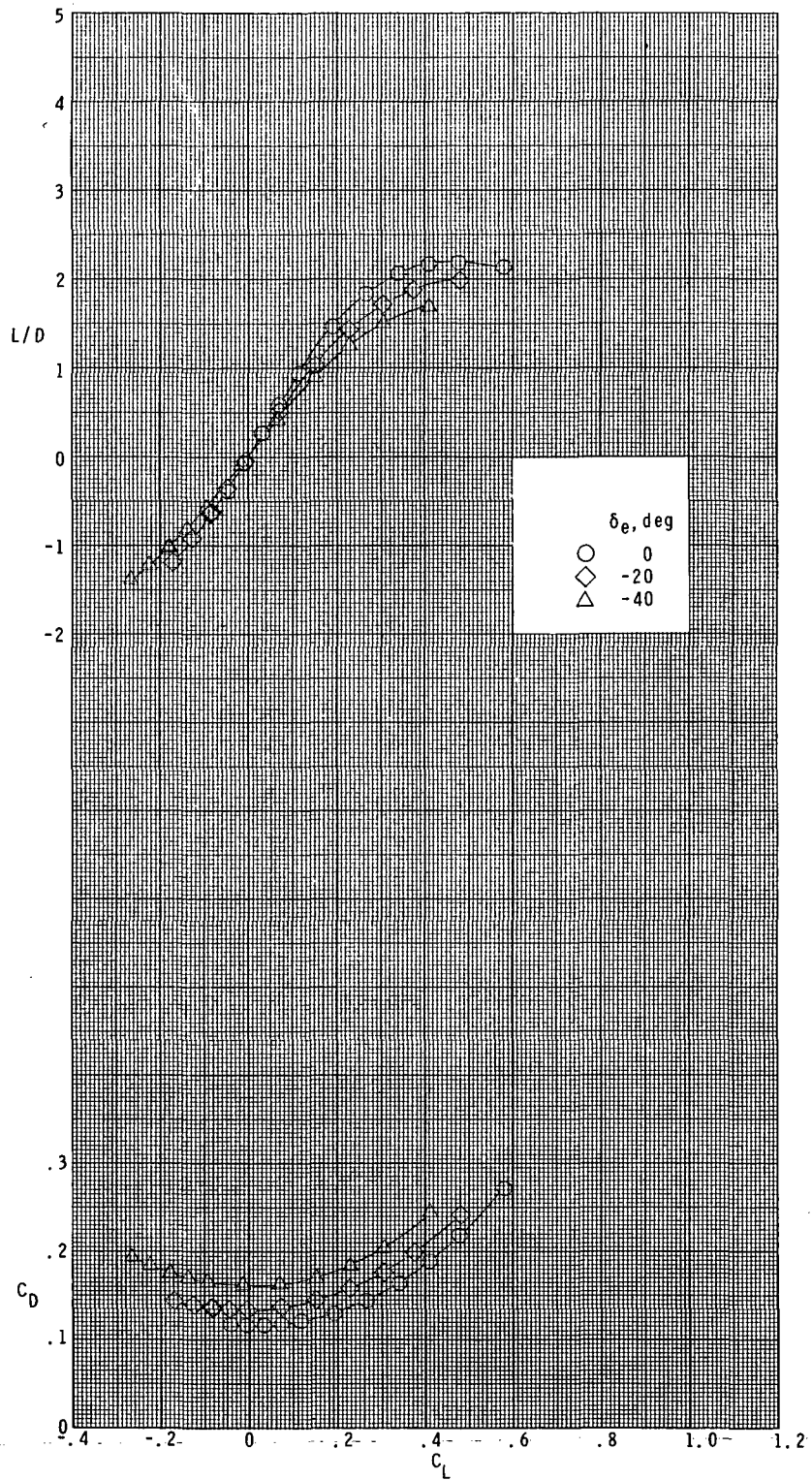
(a) Concluded.
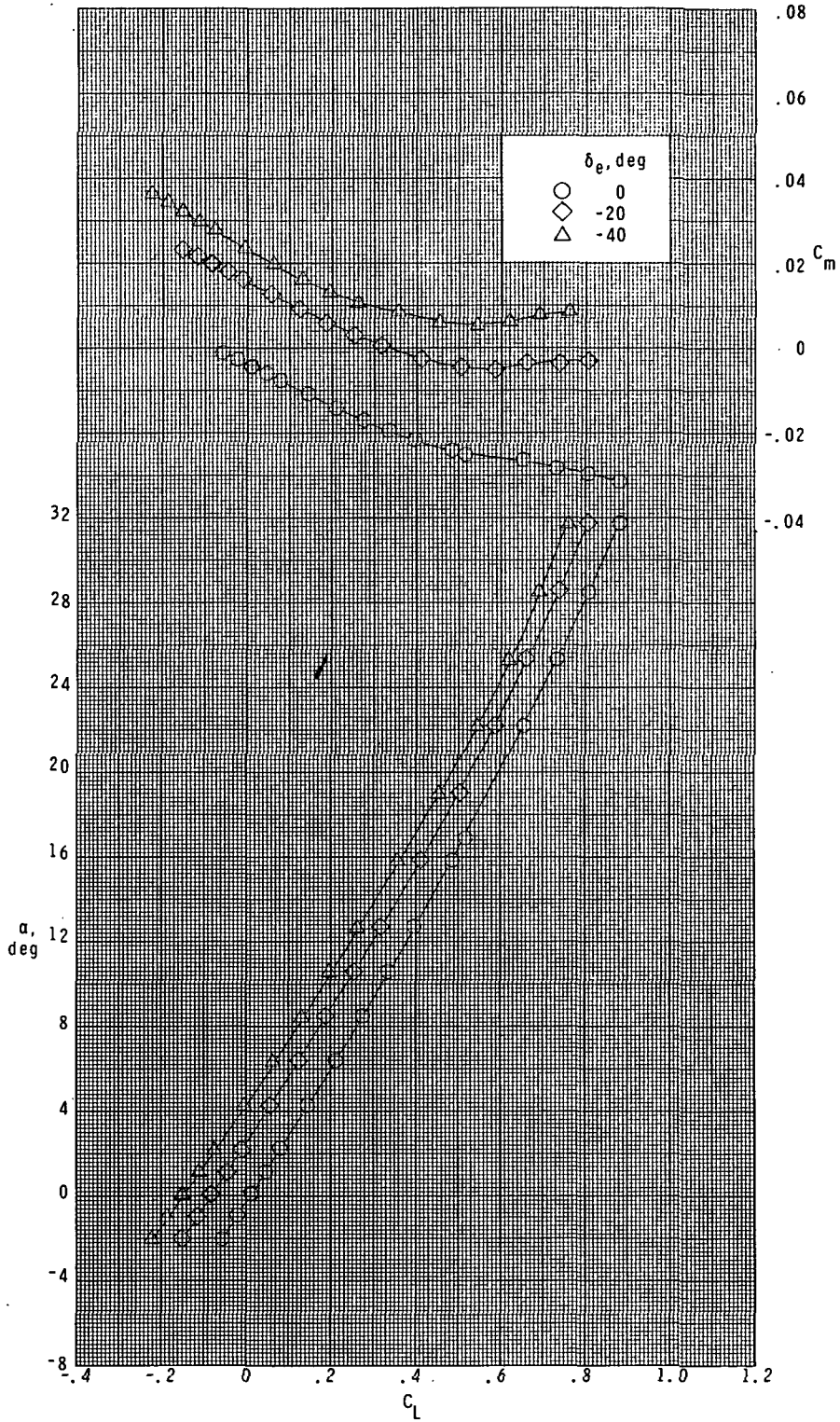
Figure 5.- Continued.

(b) M = 1.90.

Figure 5.- Continued.
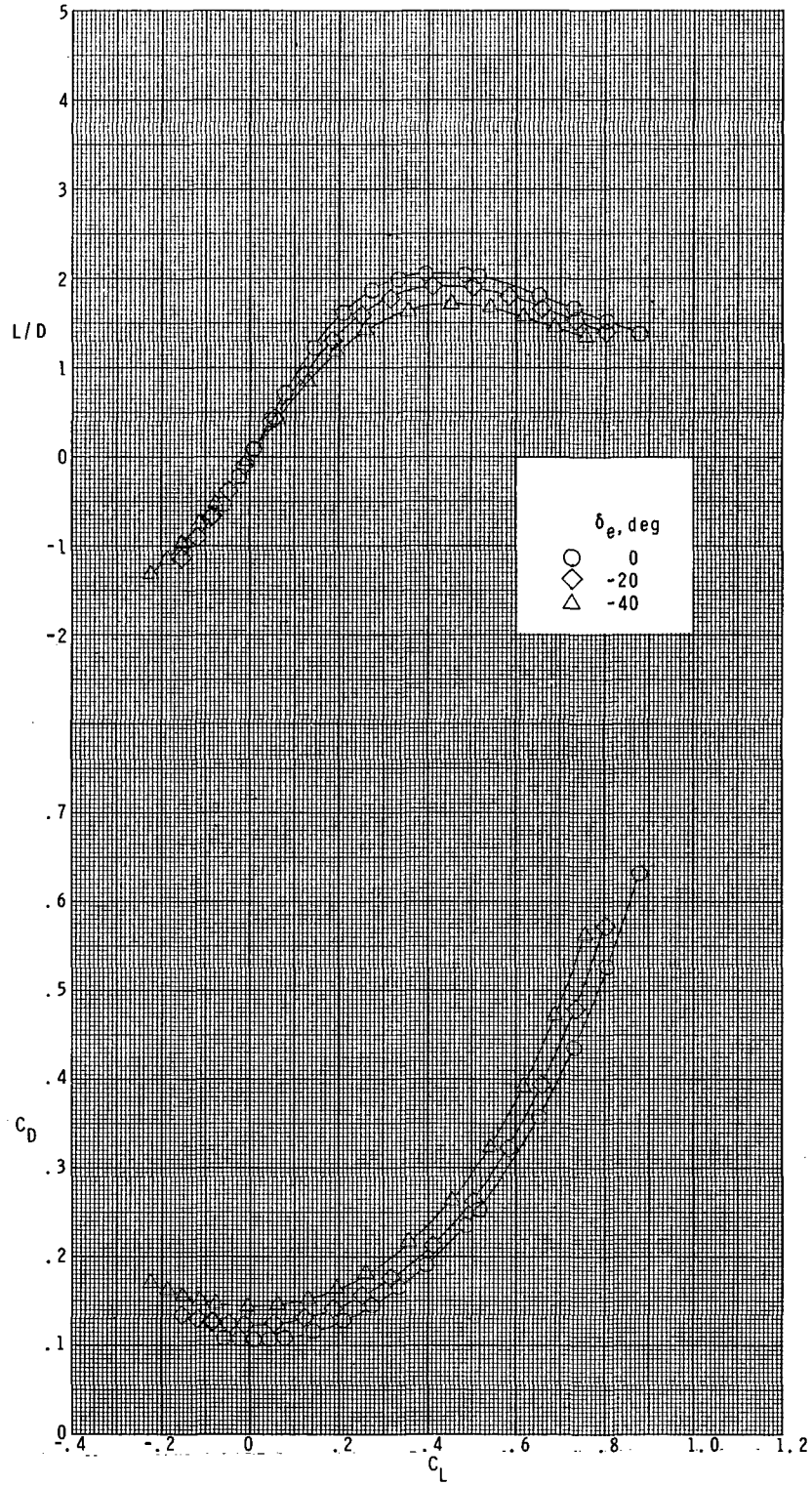
(b) Concluded.
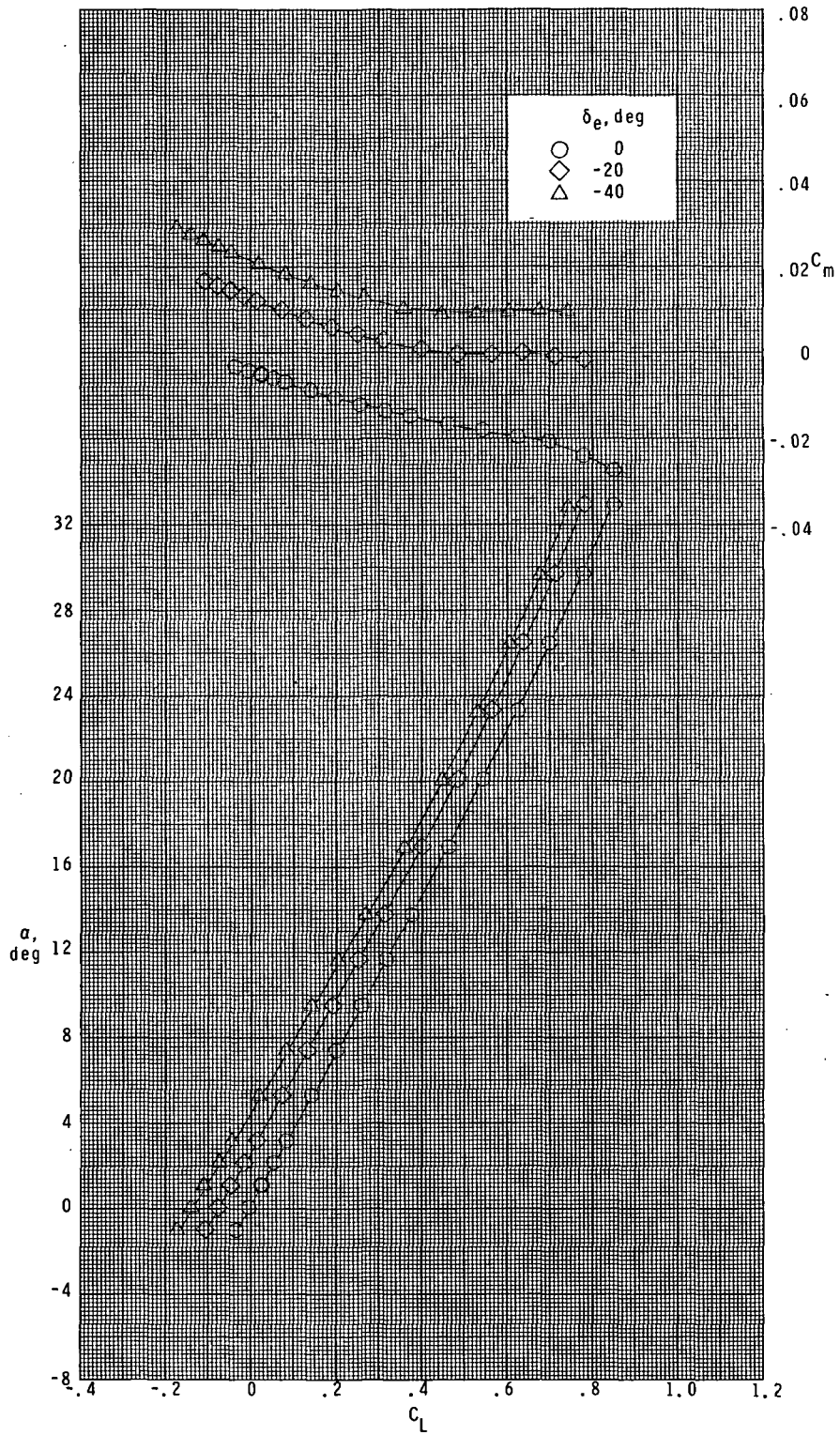
Figure 5.- Continued.

(c)   M = 2.16.

Figure 5.- Continued.
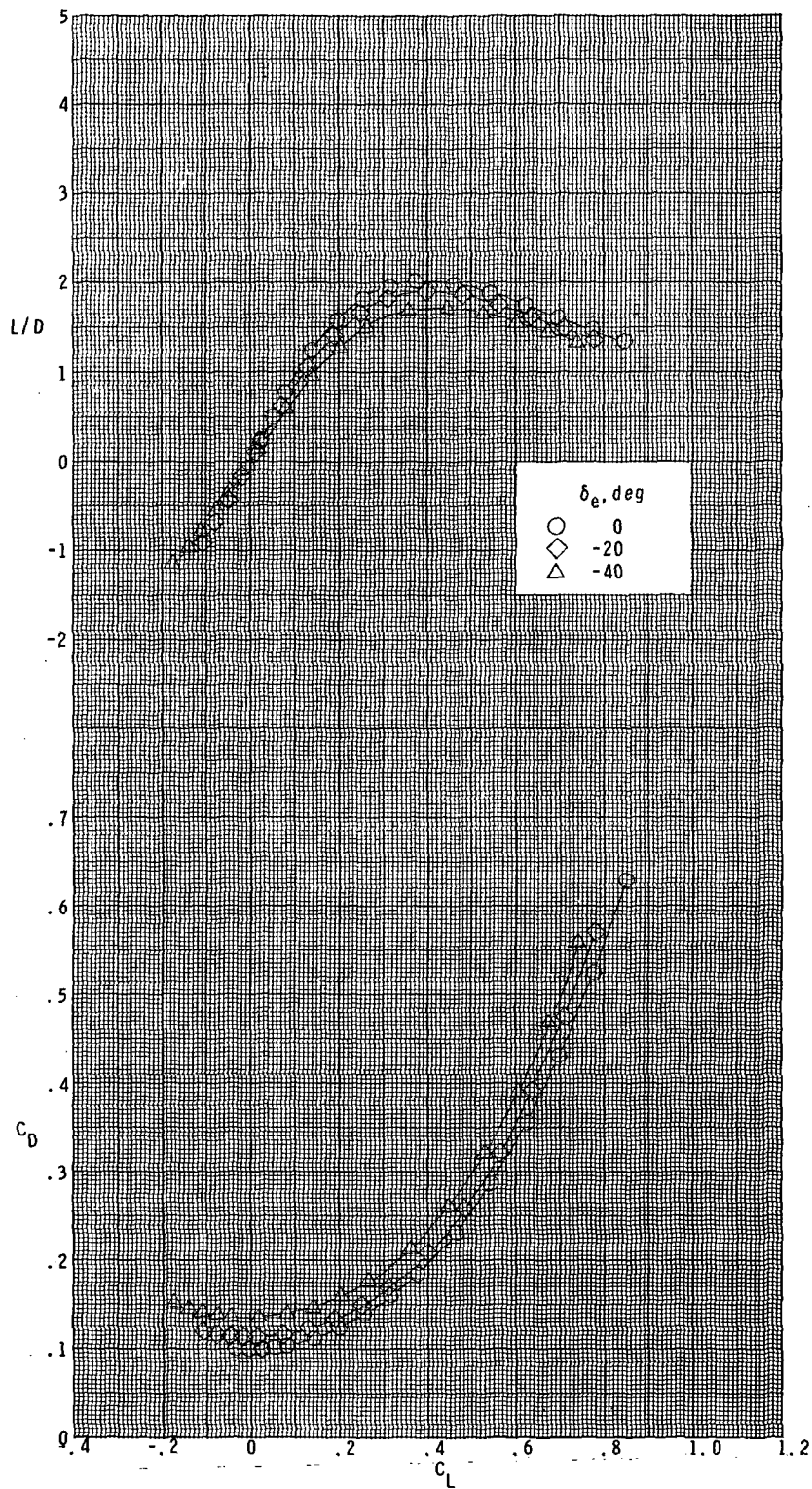
(c) Concluded.
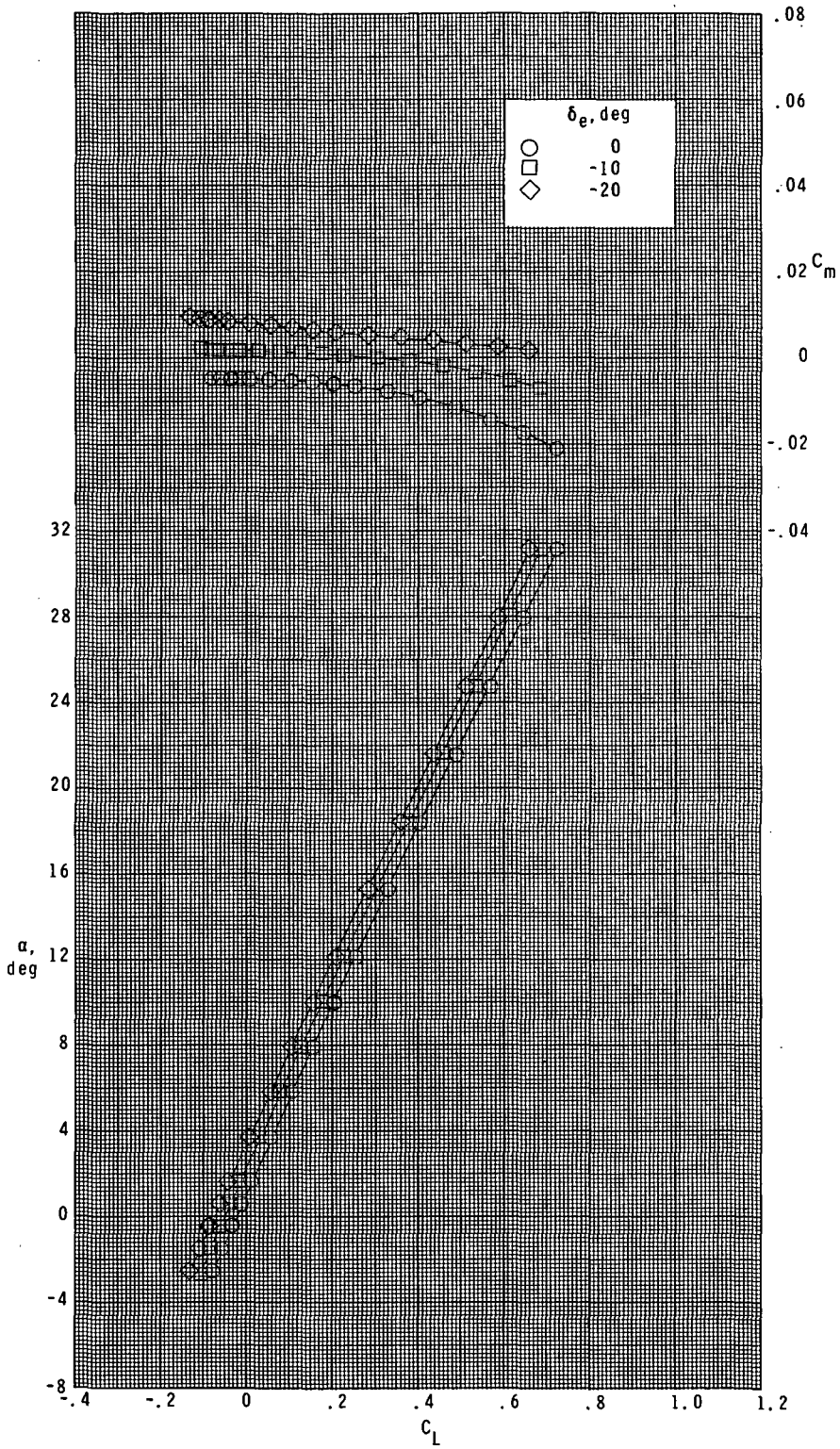
Figure 5.- Continued.

(d)   M = 2.86.

Figure 5.- Continued.
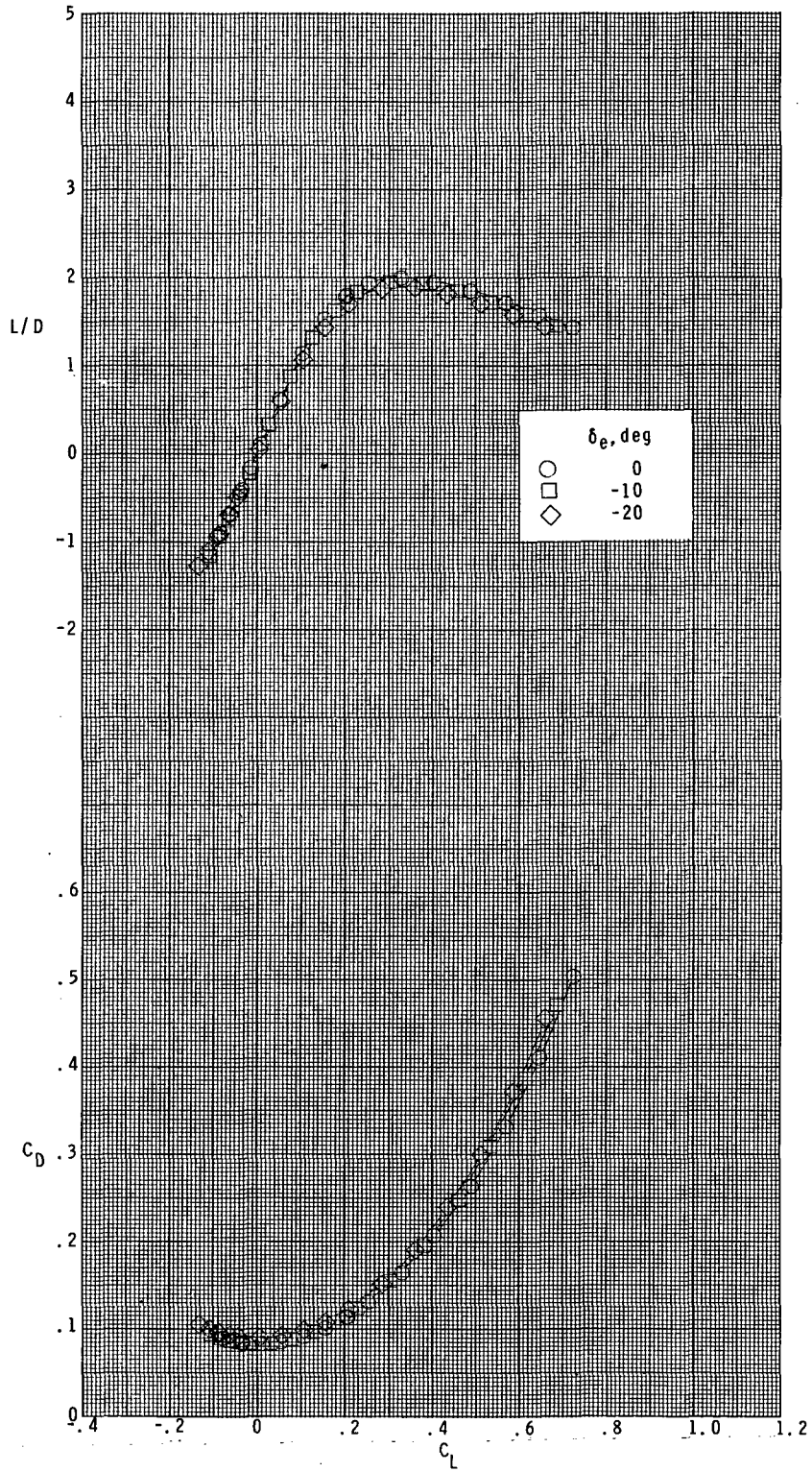
(d) Concluded.
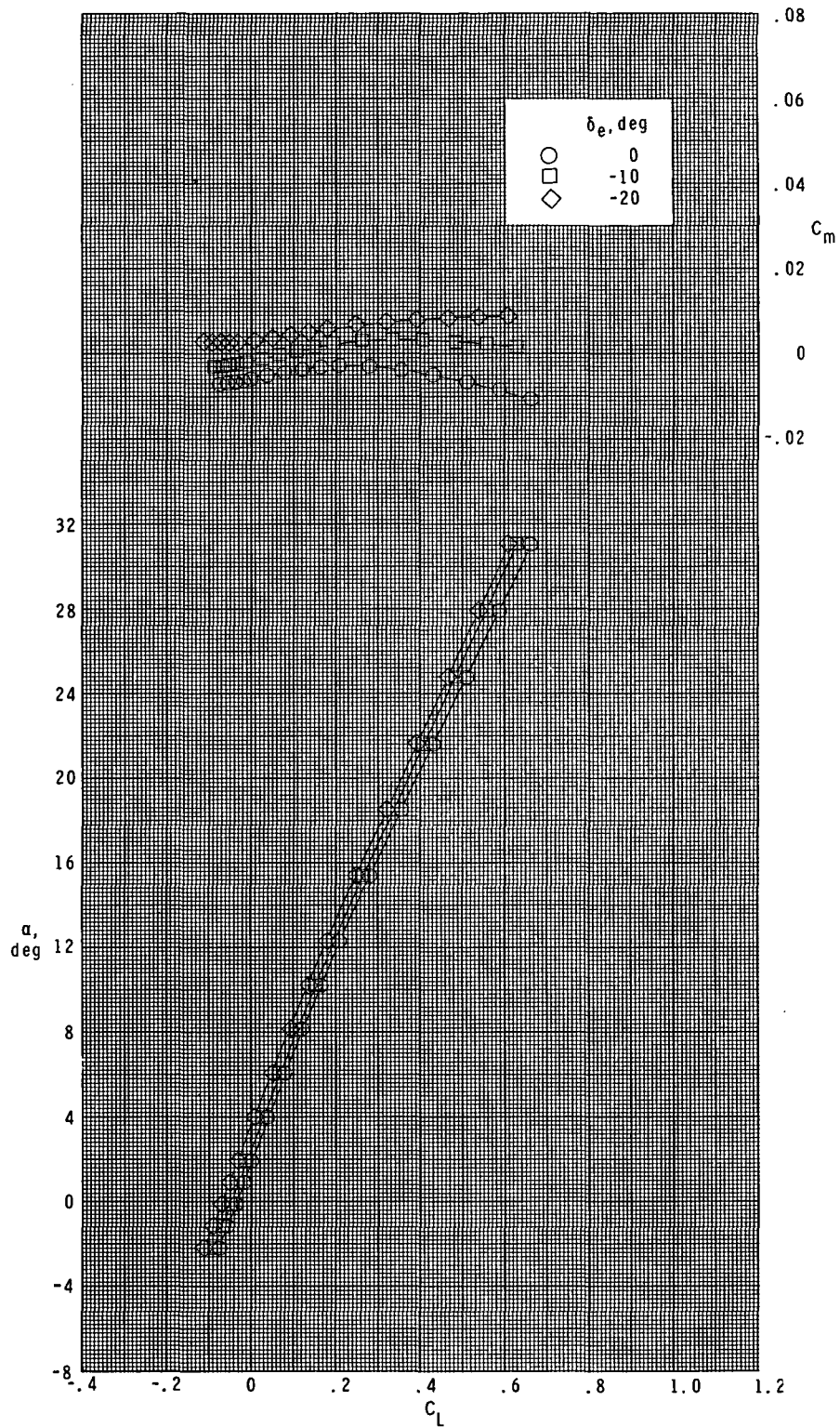
Figure 5.- Continued.

(e) M = 3.95.

Figure 5.- Continued.
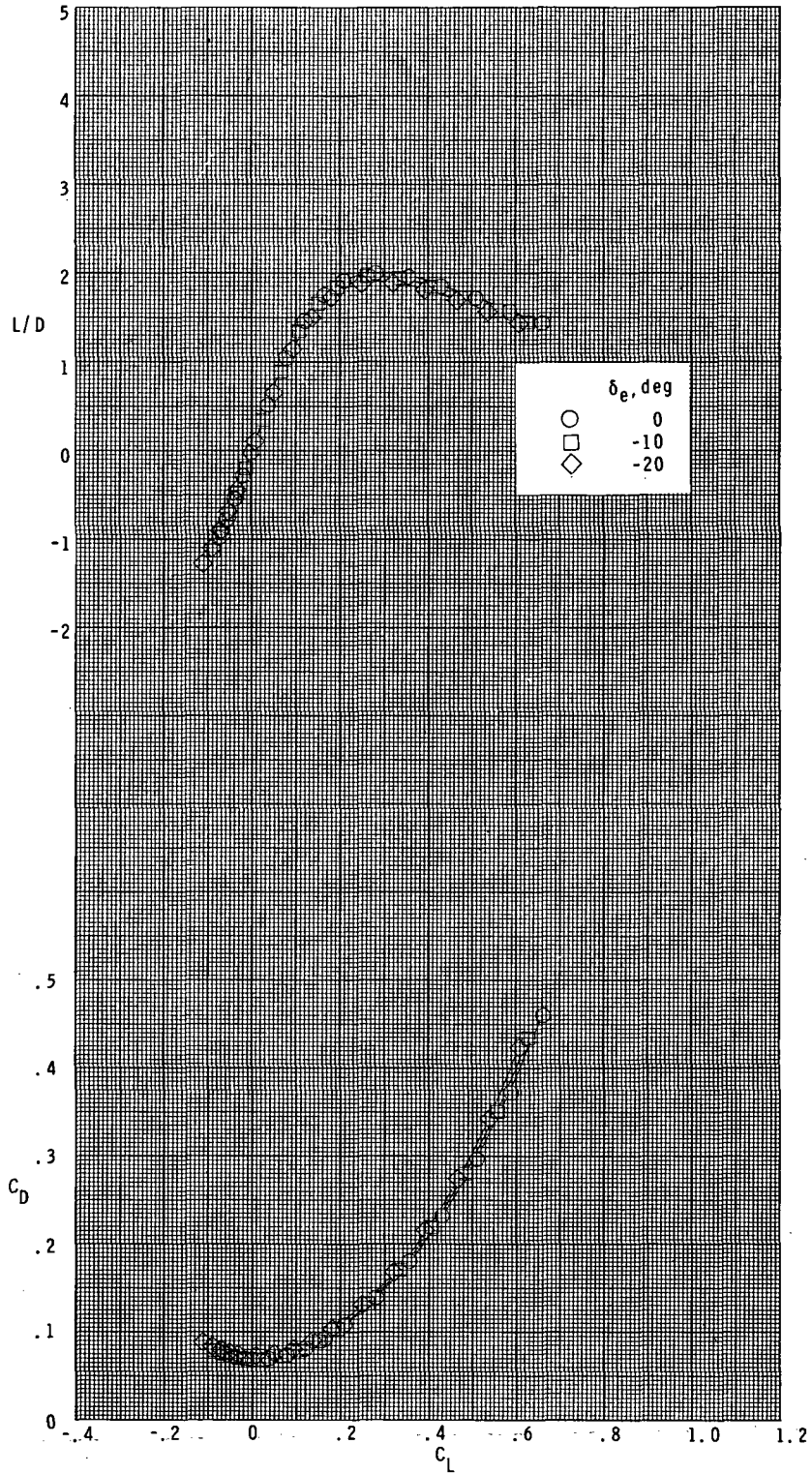
(e) Concluded.
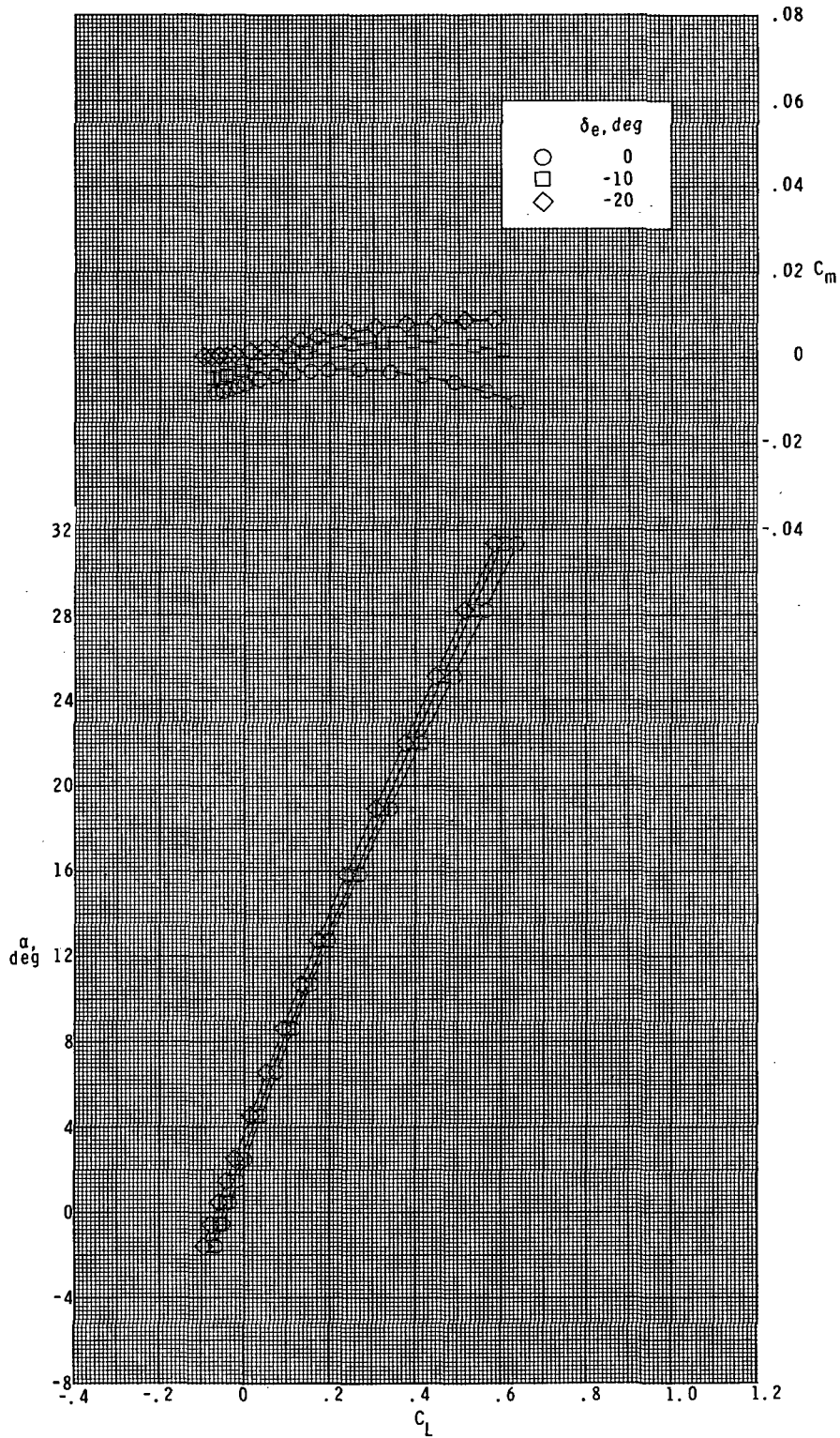
Figure 5.- Continued.

(f)   M = 4.63.

Figure 5.- Continued.
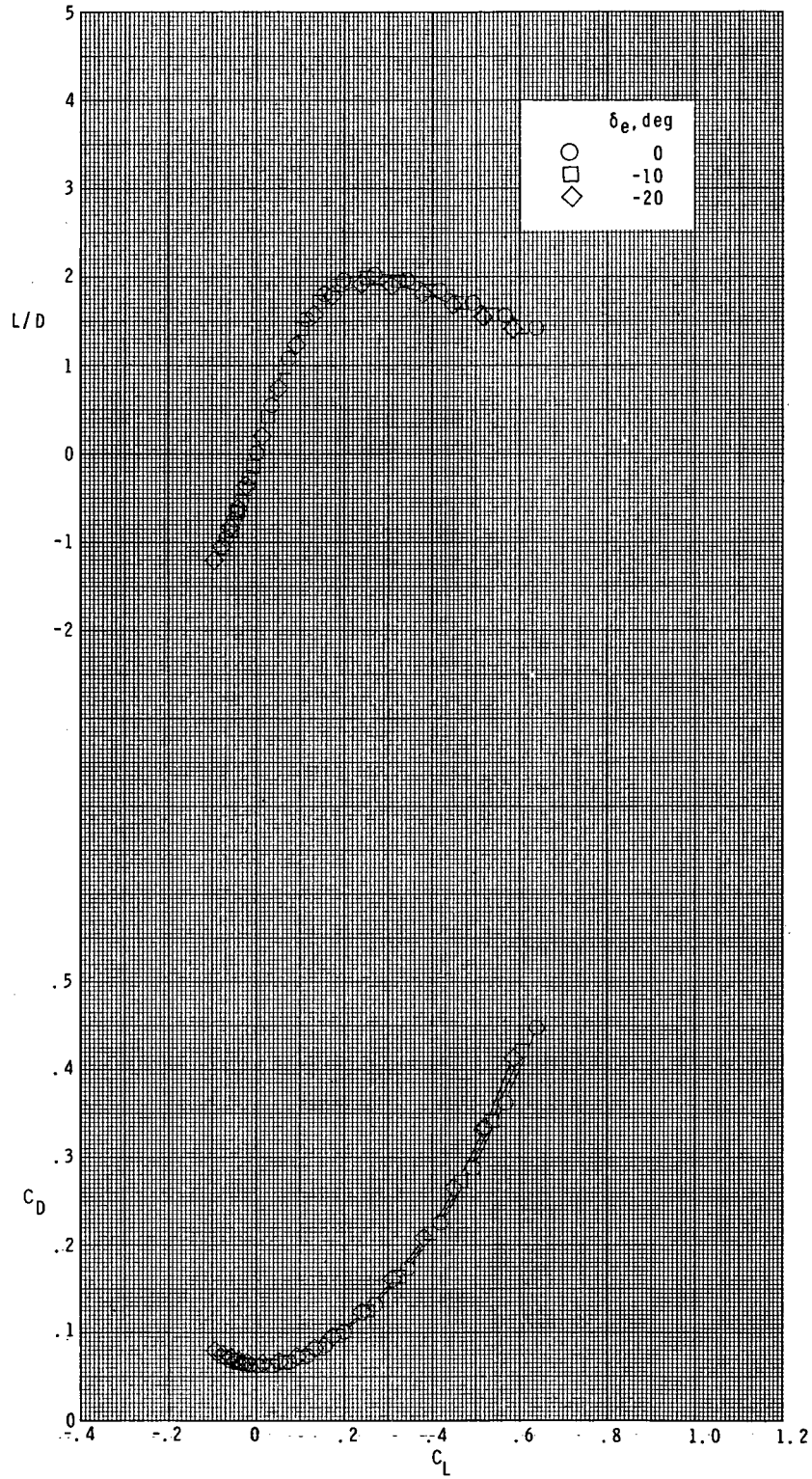
(f) Concluded.

Figure 5.- Concluded.
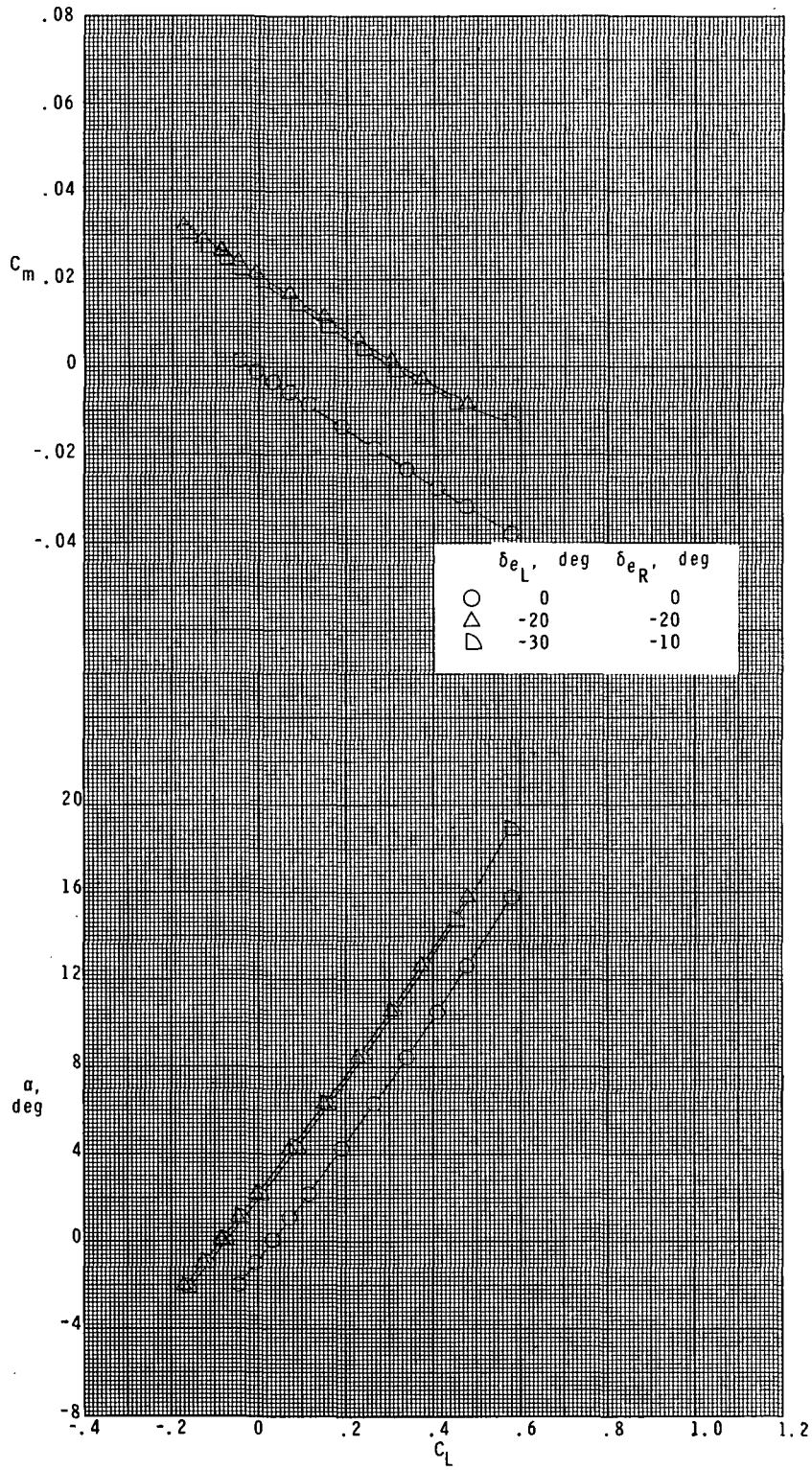
(a) M = 1.60.

Figure 6.- Effect of differential elevon deflections on pitch characteristics. δ_{rf} = 30°.
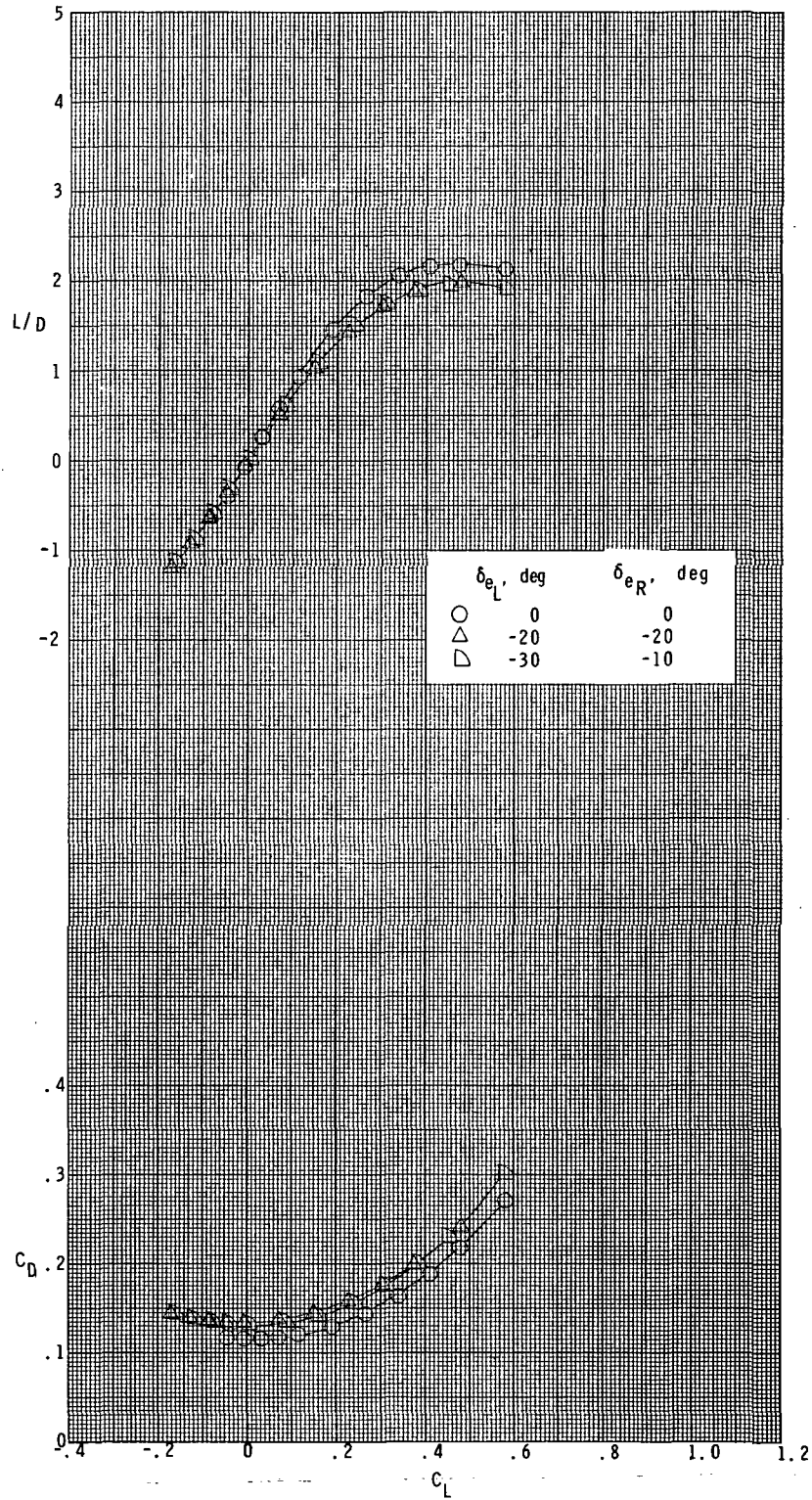
(a) Concluded.
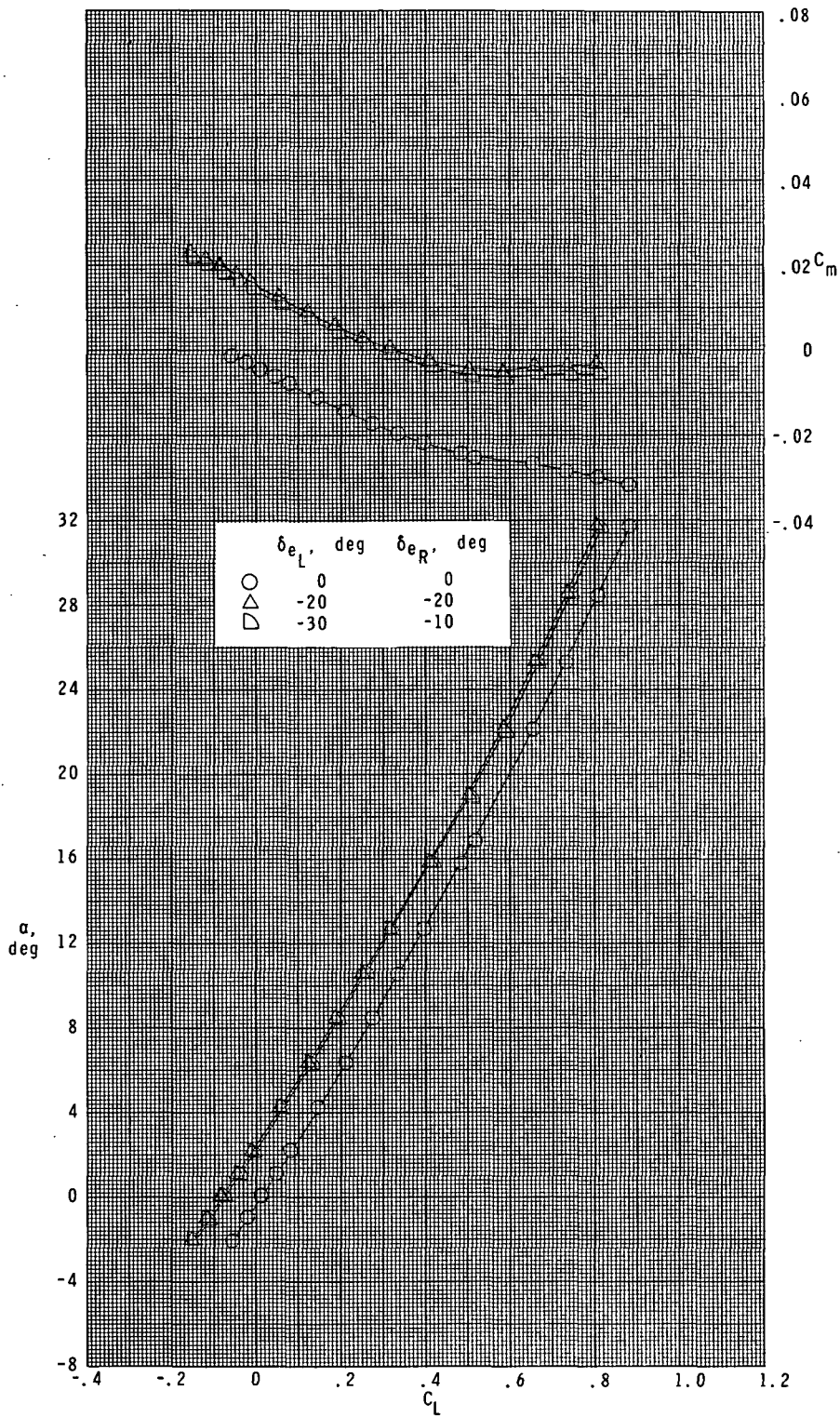
Figure 6.- Continued.

(b) M = 1.90.

Figure 6.- Continued.
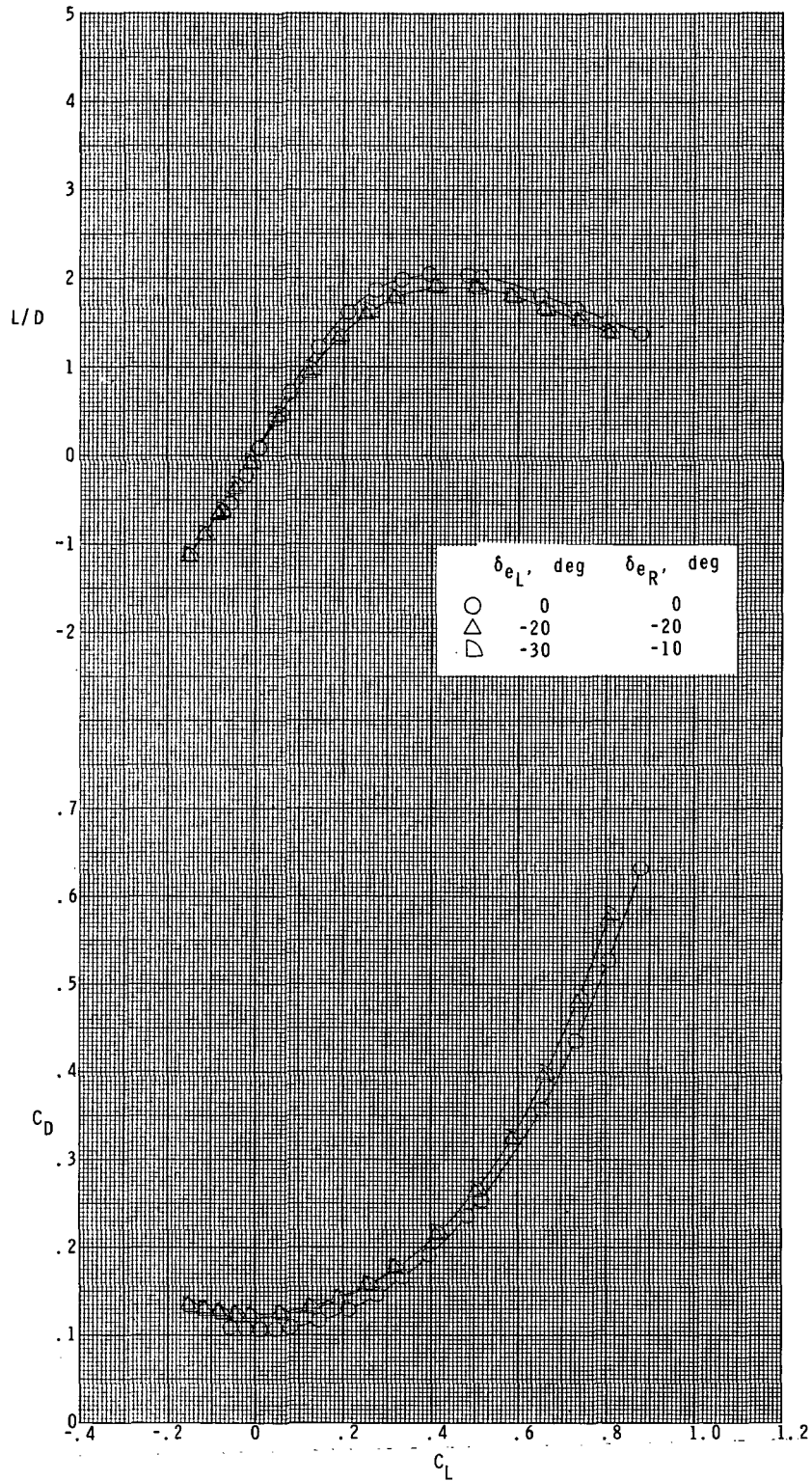
(b) Concluded.
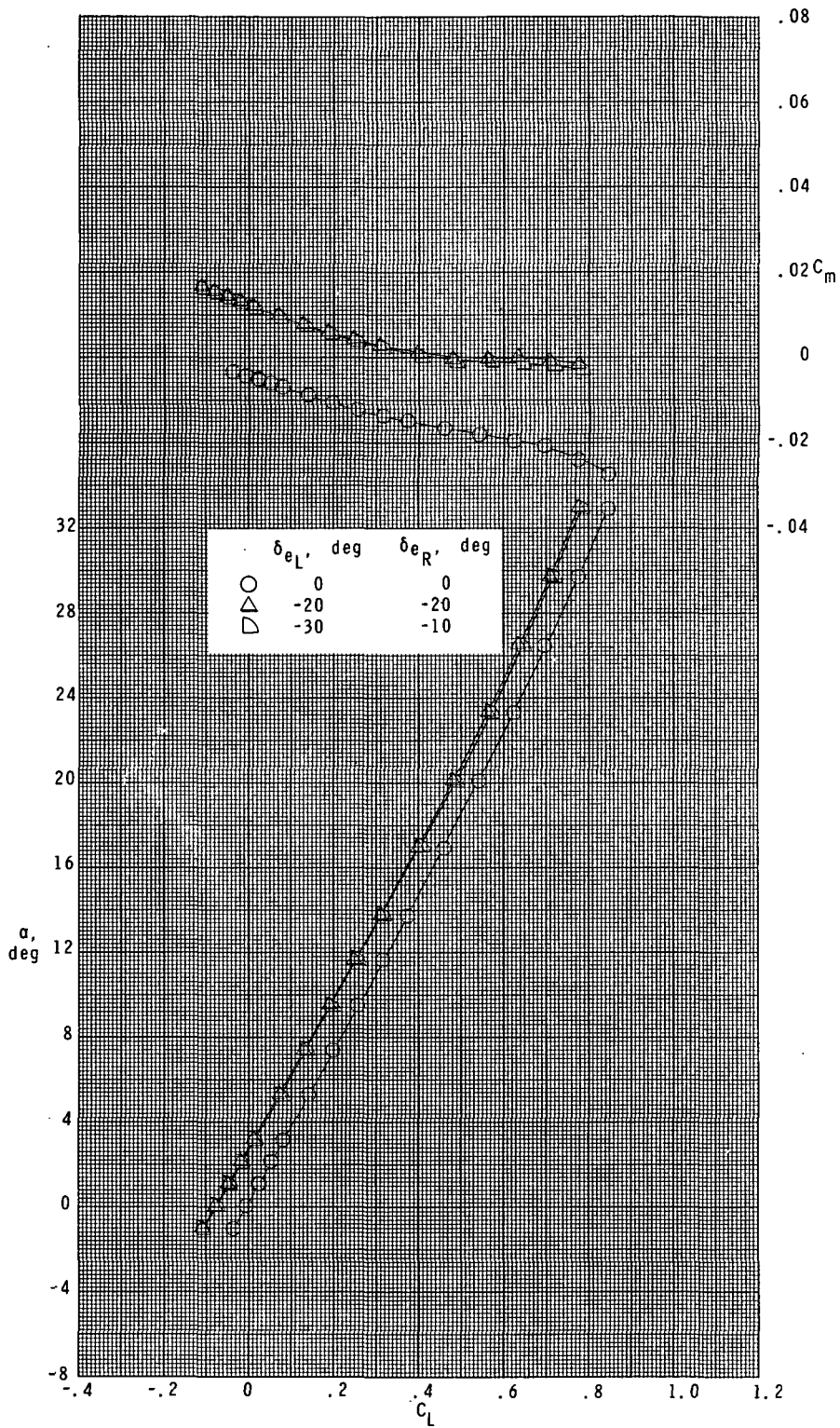
Figure 6.- Continued.

(c) M = 2.16.

Figure 6.- Continued.
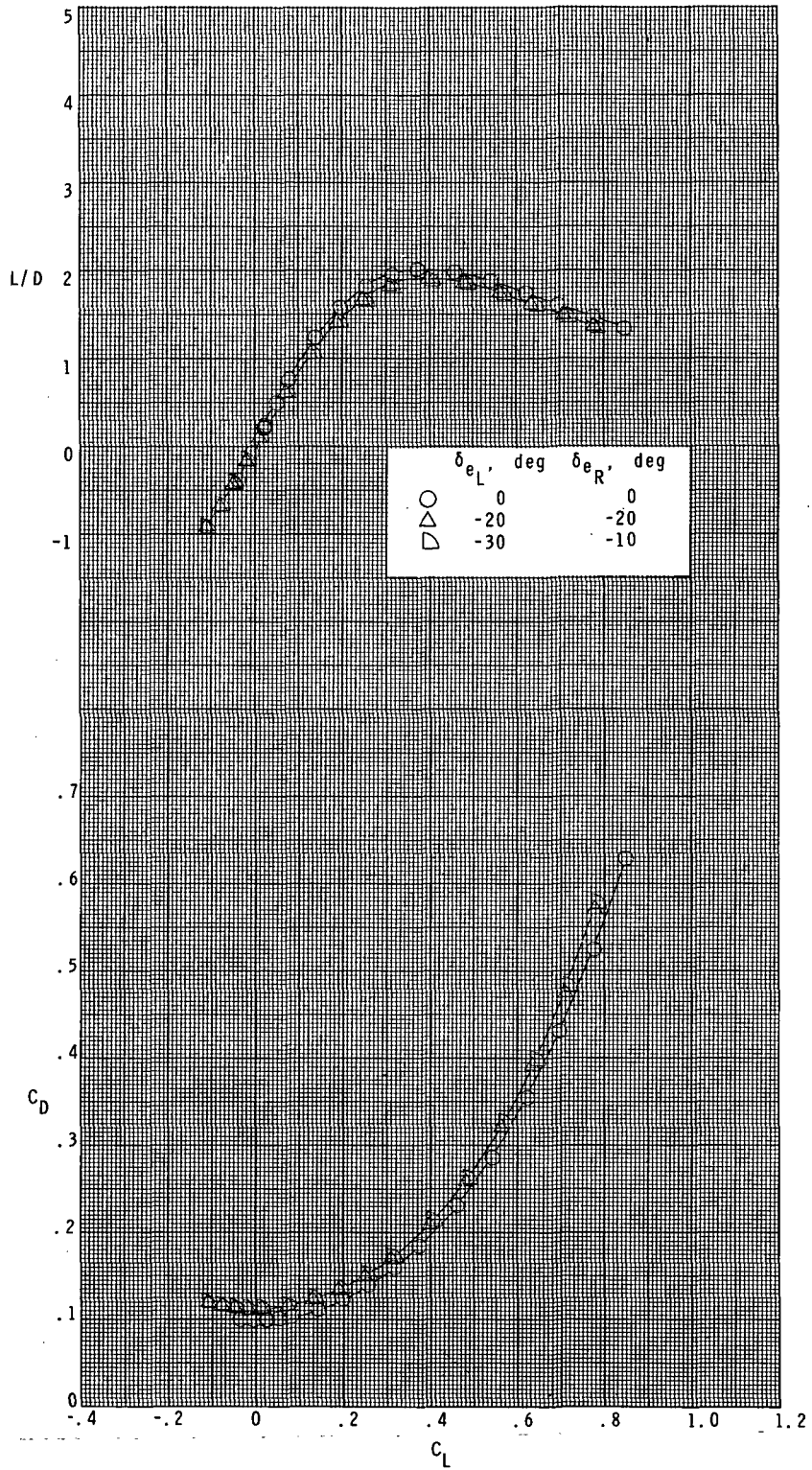
(c) Concluded.
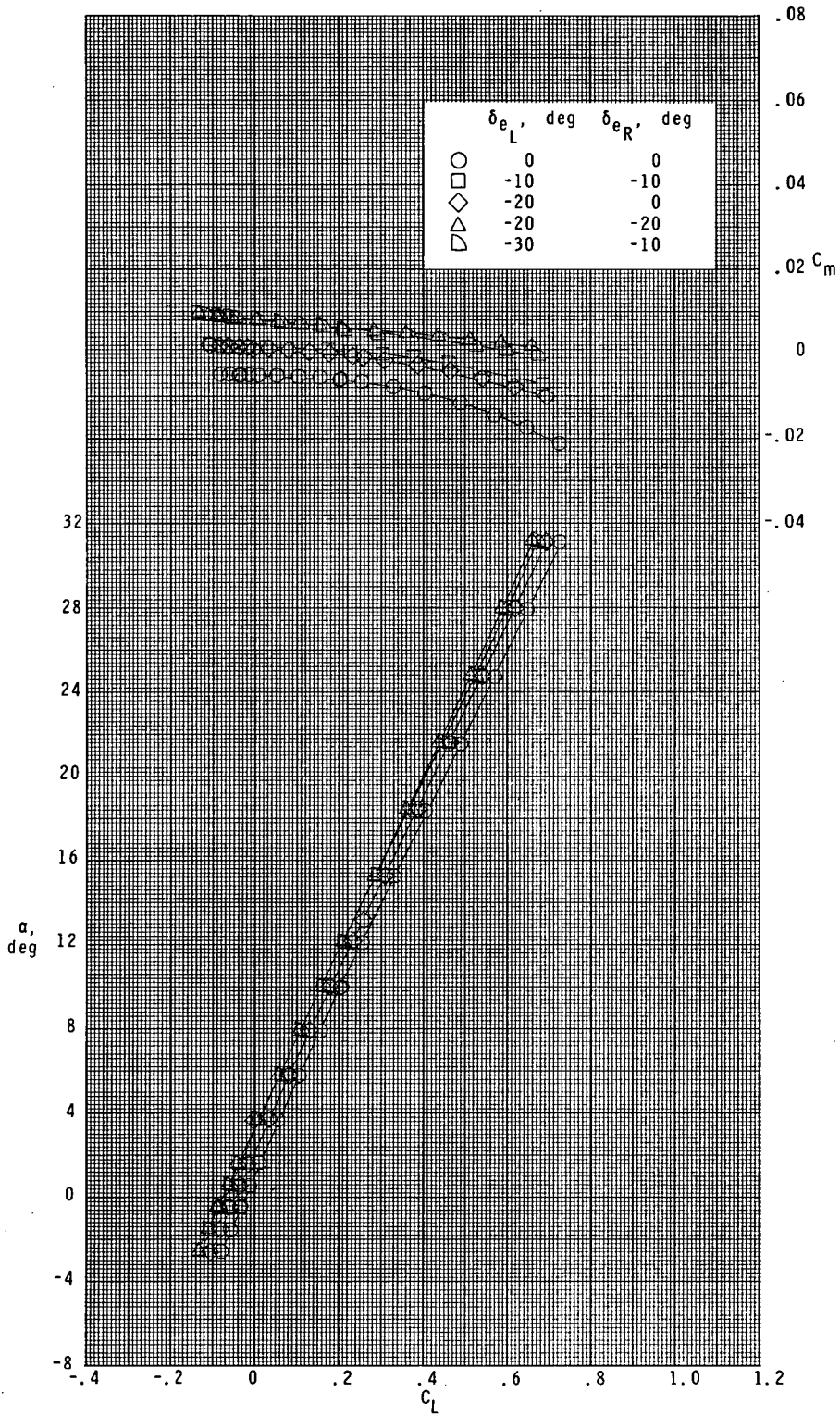
Figure 6.- Continued.

(d) M = 2.86.

Figure 6.- Continued.
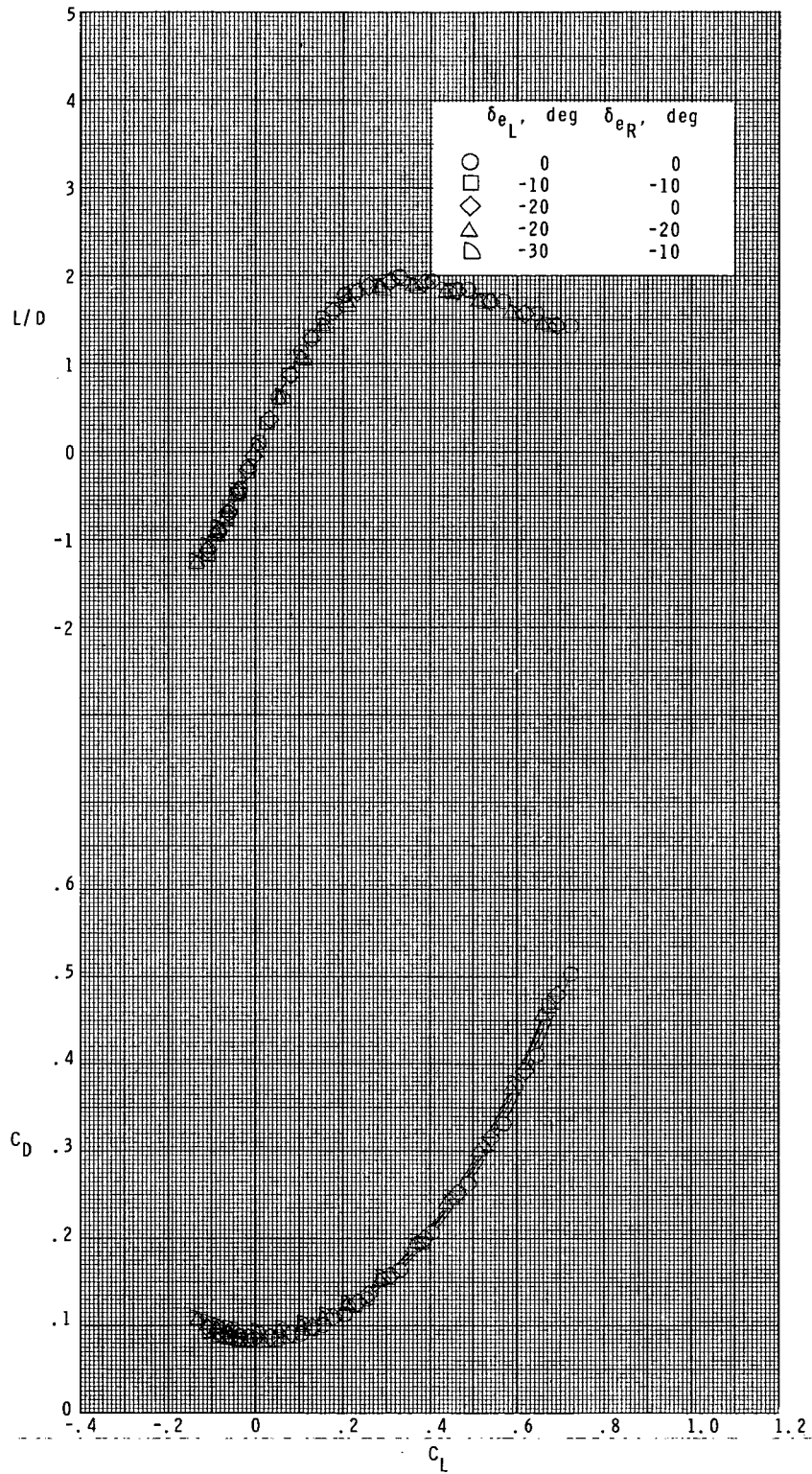
(d) Concluded.
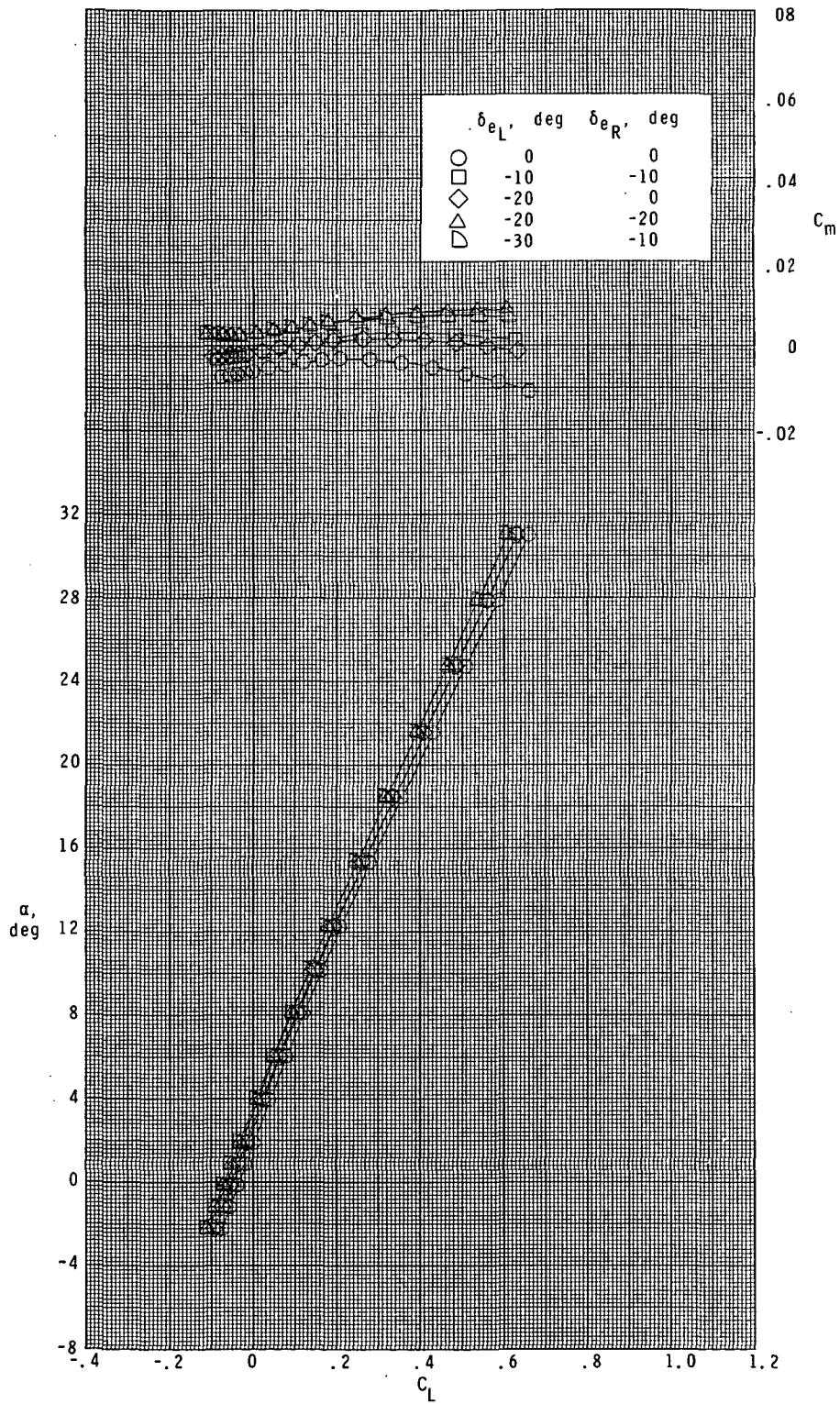
Figure 6.- Continued.

(e) M = 3.95.

Figure 6.- Continued.
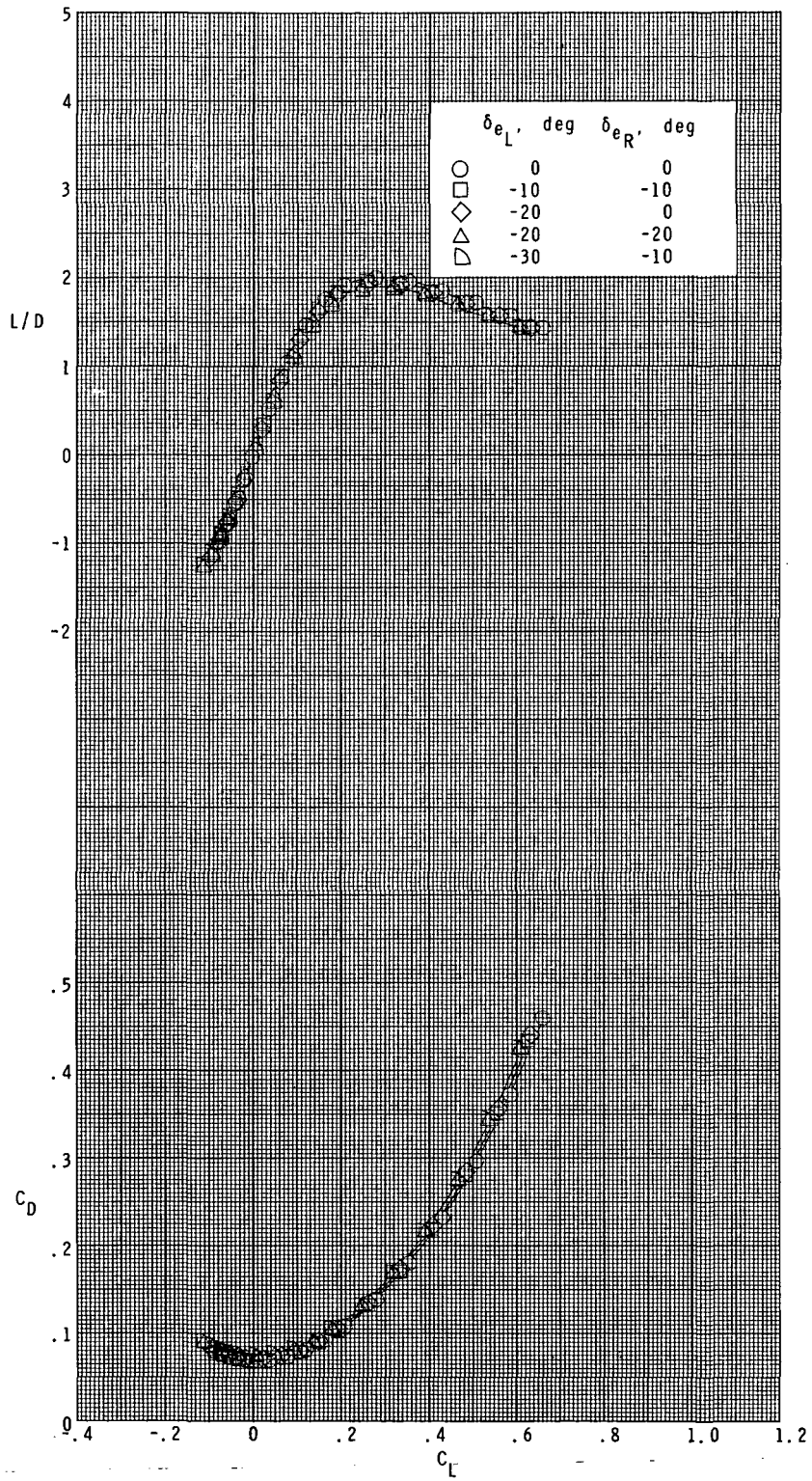
(e) Concluded.
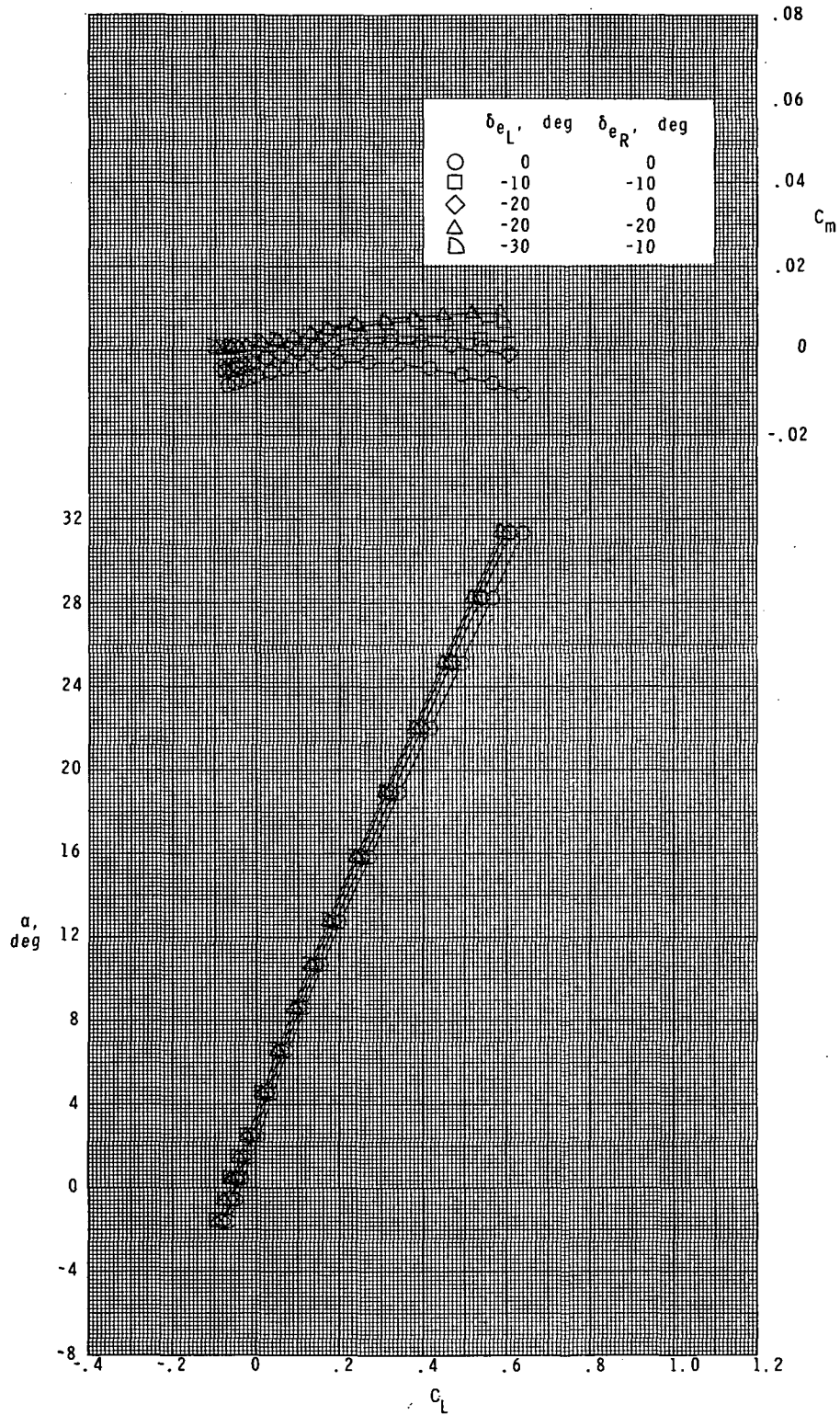
Figure 6.- Continued.

(f) M = 4.63.

Figure 6.- Continued.
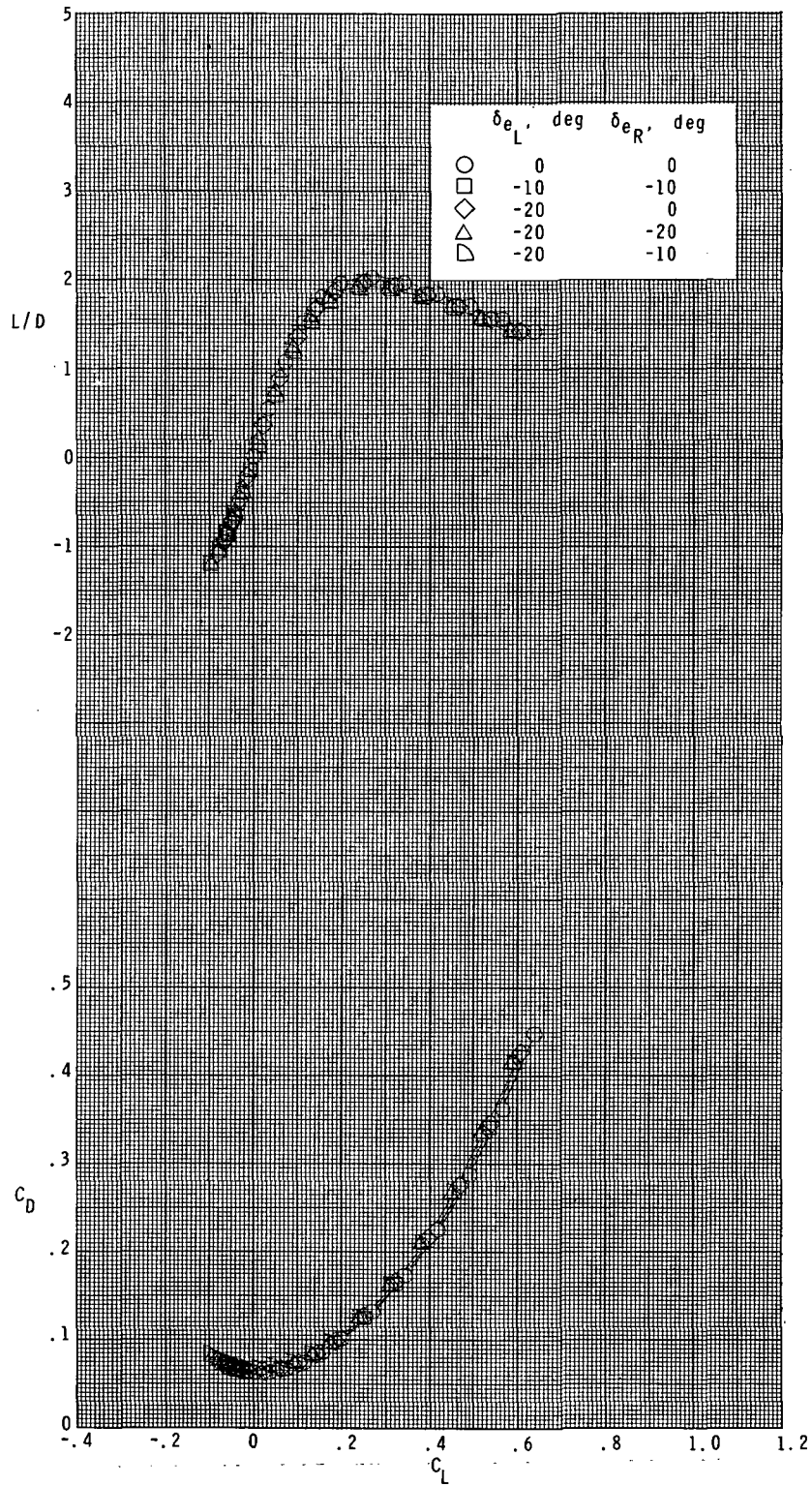
(f) Concluded.

Figure 6.- Concluded.
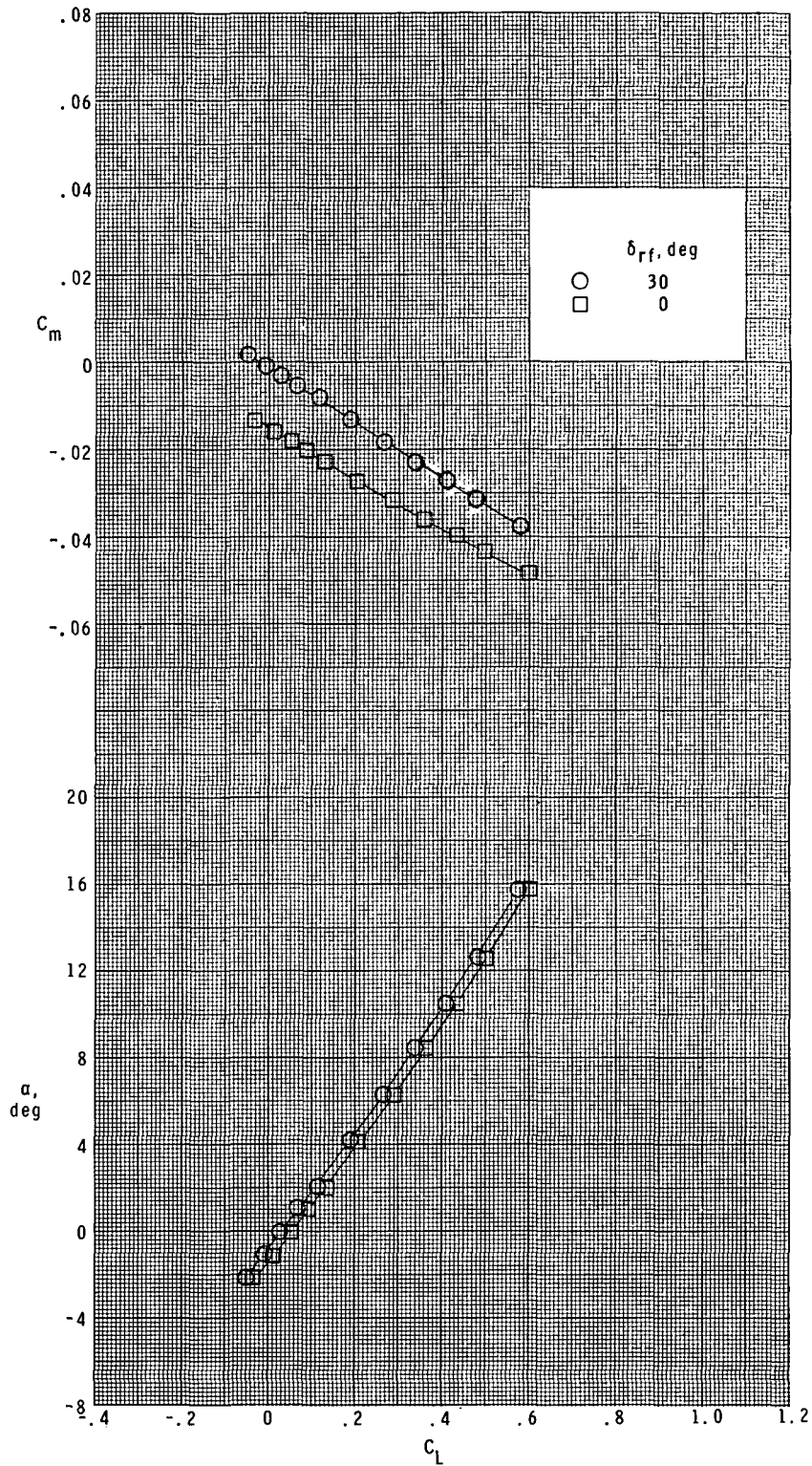
(a)   M = 1.60.

Figure 7.- Effect of rudder flare on longitudinal aerodynamic characteristics.
$\delta_{e_L} = \delta_{e_R} = 0^\circ$.
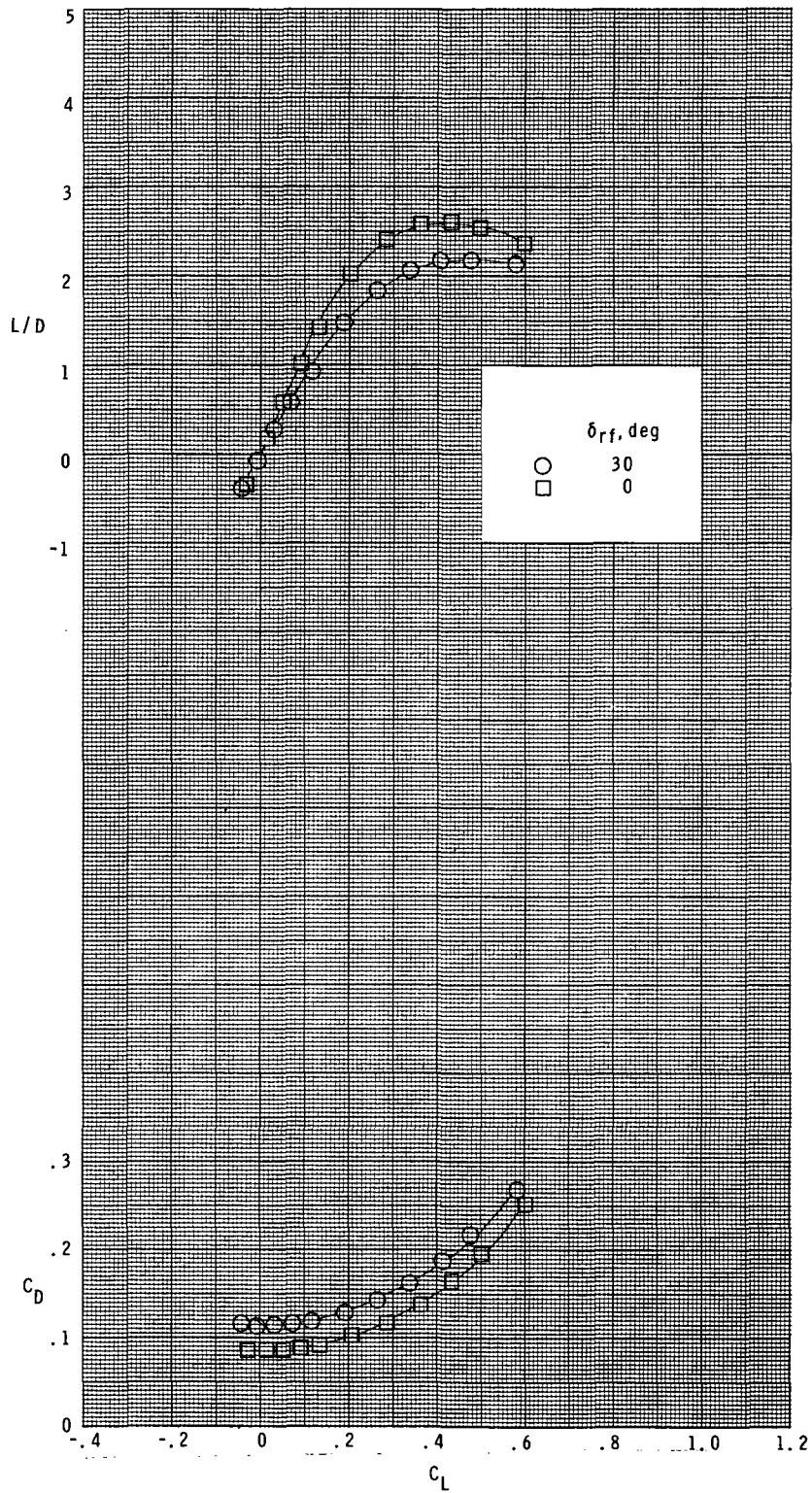
(a) Concluded.

Figure 7.- Continued.
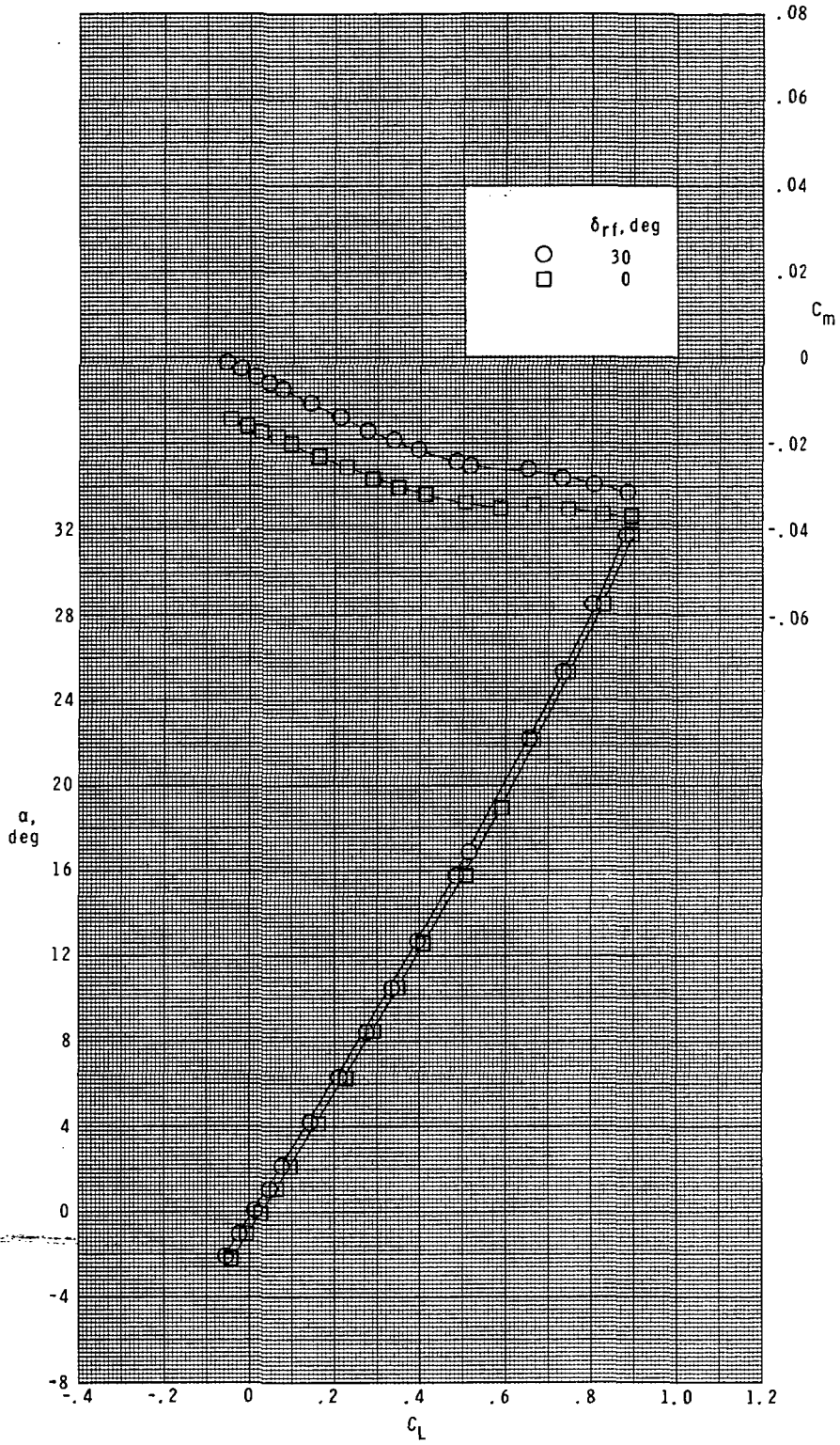
(b)   M = 1.90.

Figure 7.- Continued.
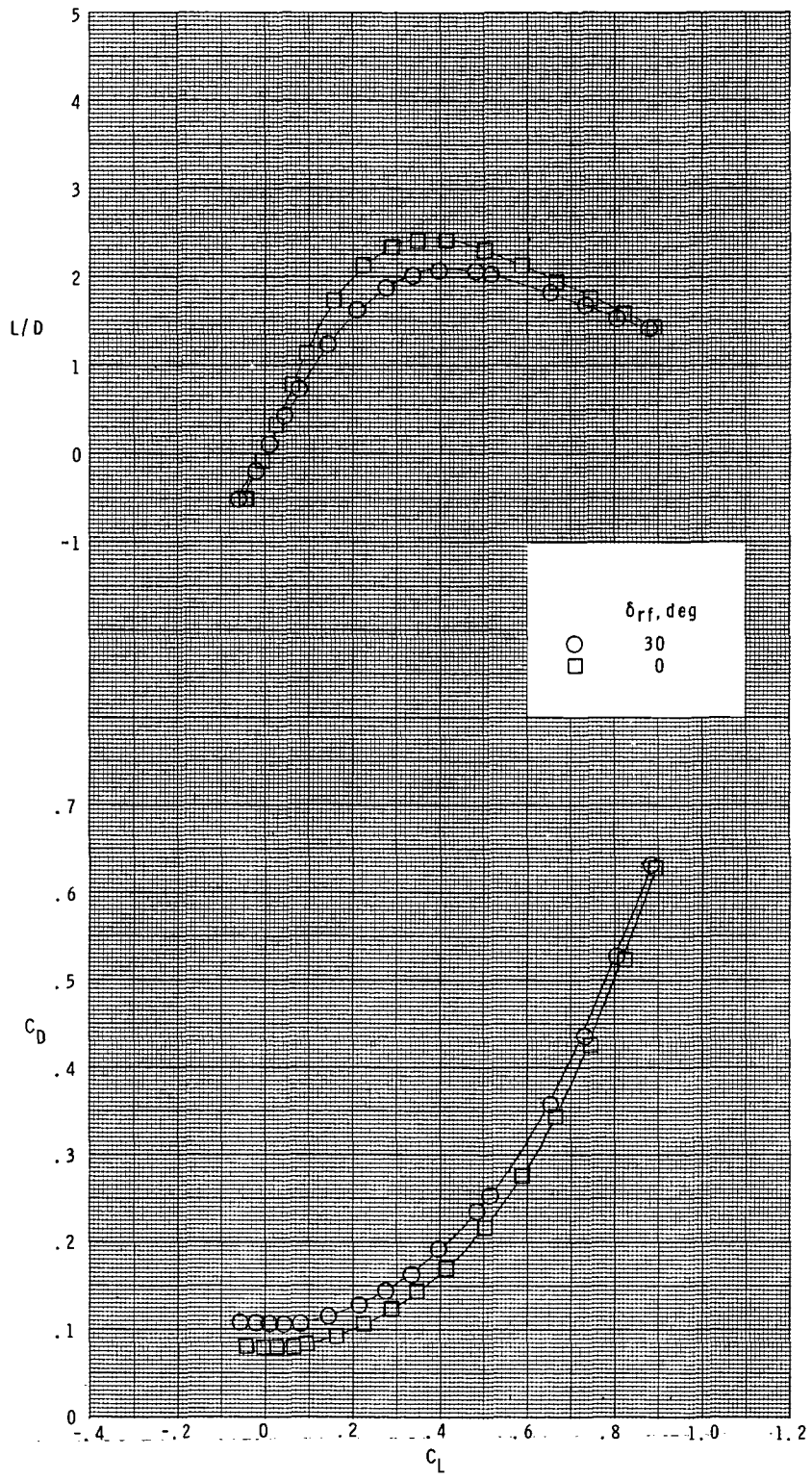
(b) Concluded.
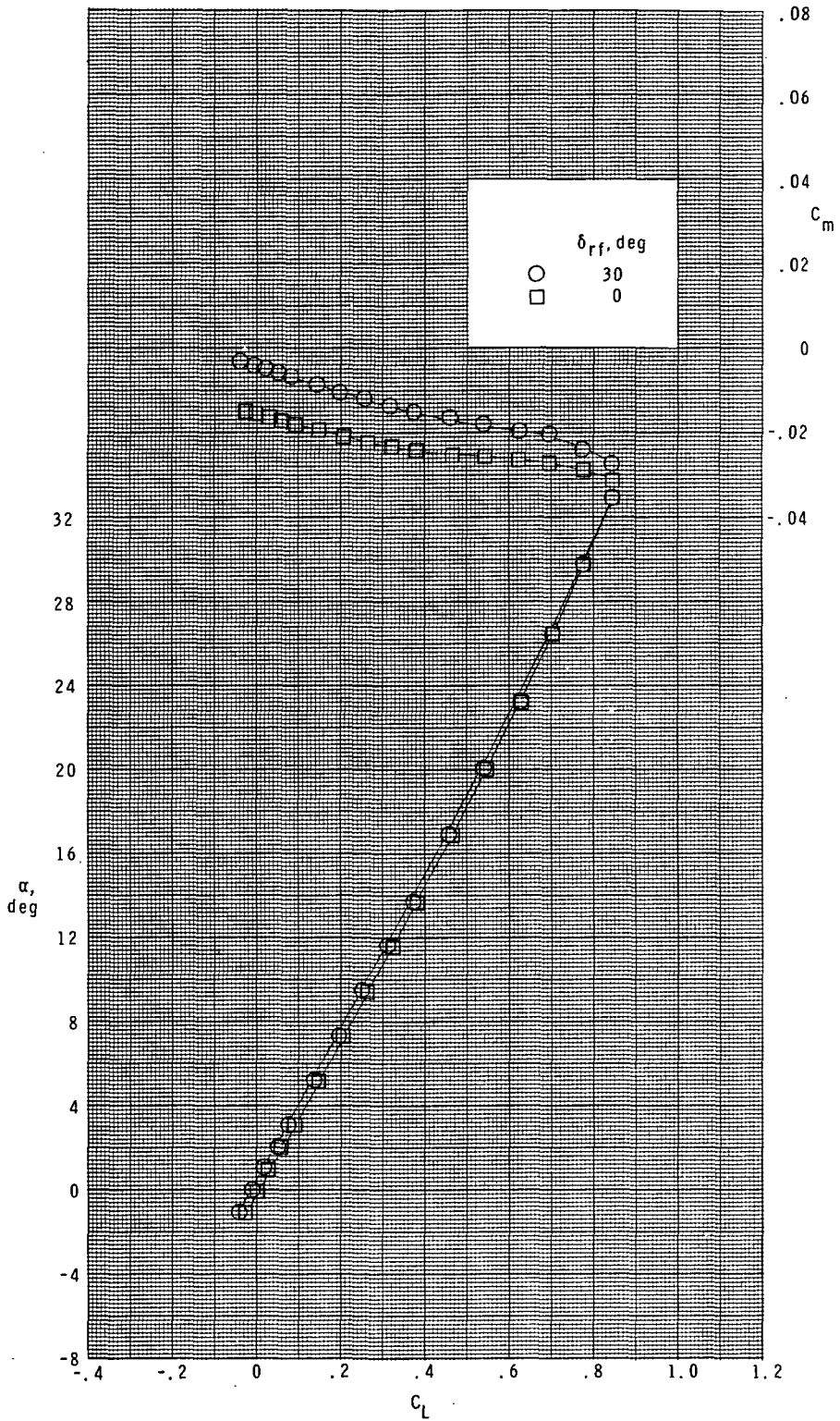
Figure 7.- Continued.

(c) M = 2.16.

Figure 7.- Continued.
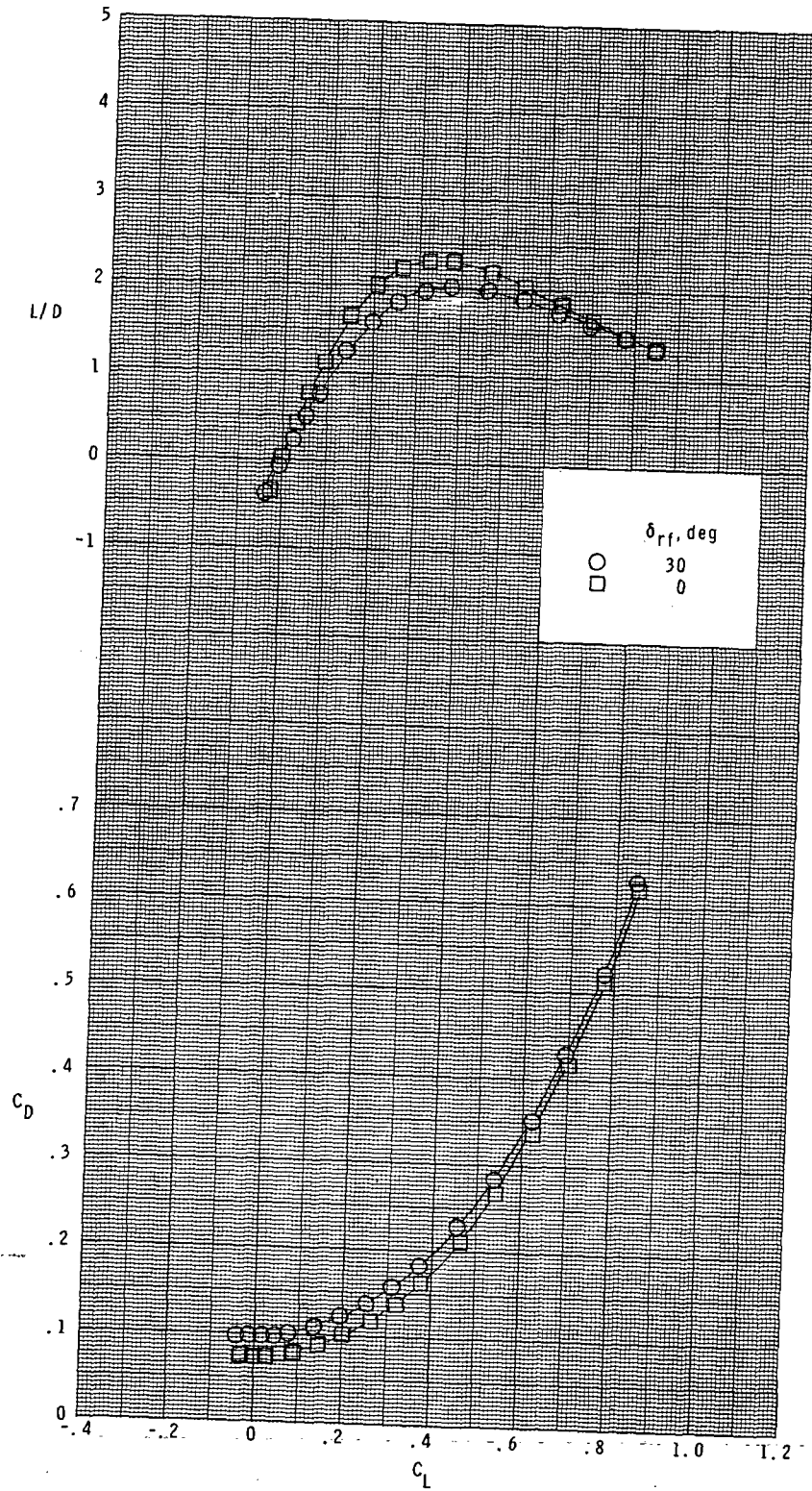
(c) Concluded.

Figure 7.- Concluded.
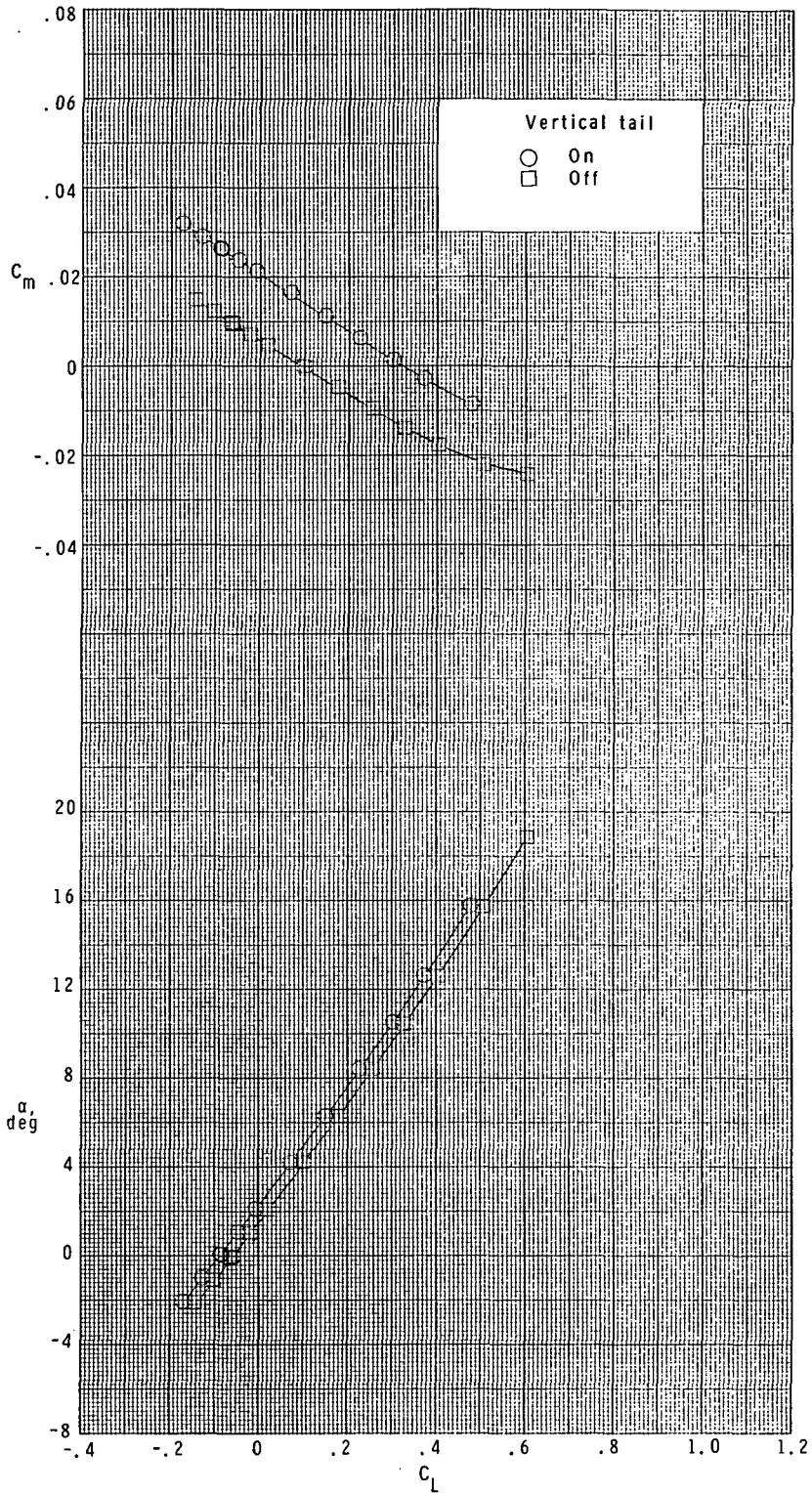
(a)   M = 1.60.

Figure 8.- Effect of vertical tail on longitudinal aerodynamic characteristics.

δ_e = -20°; δ_{rf} = 30°.
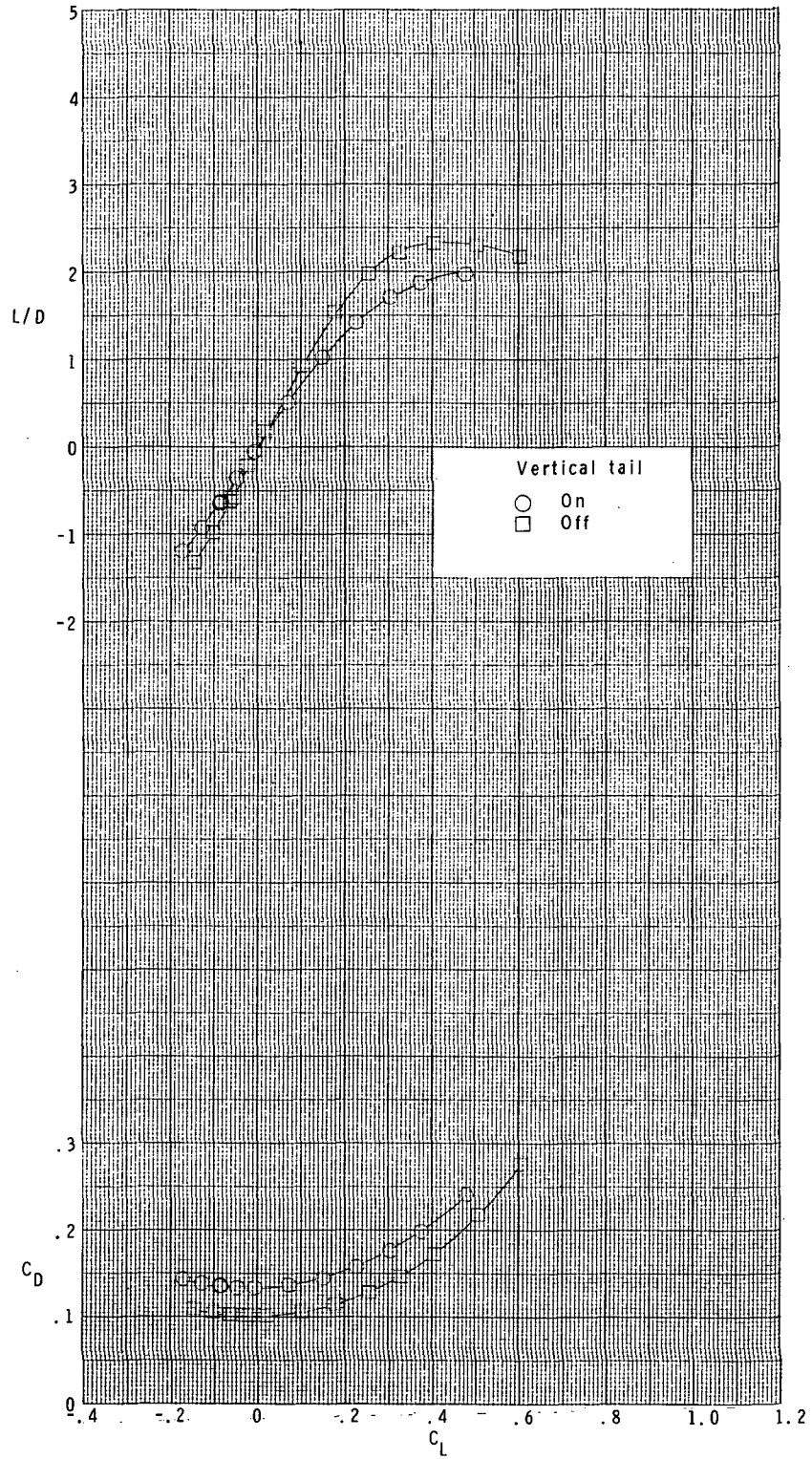
(a) Concluded.
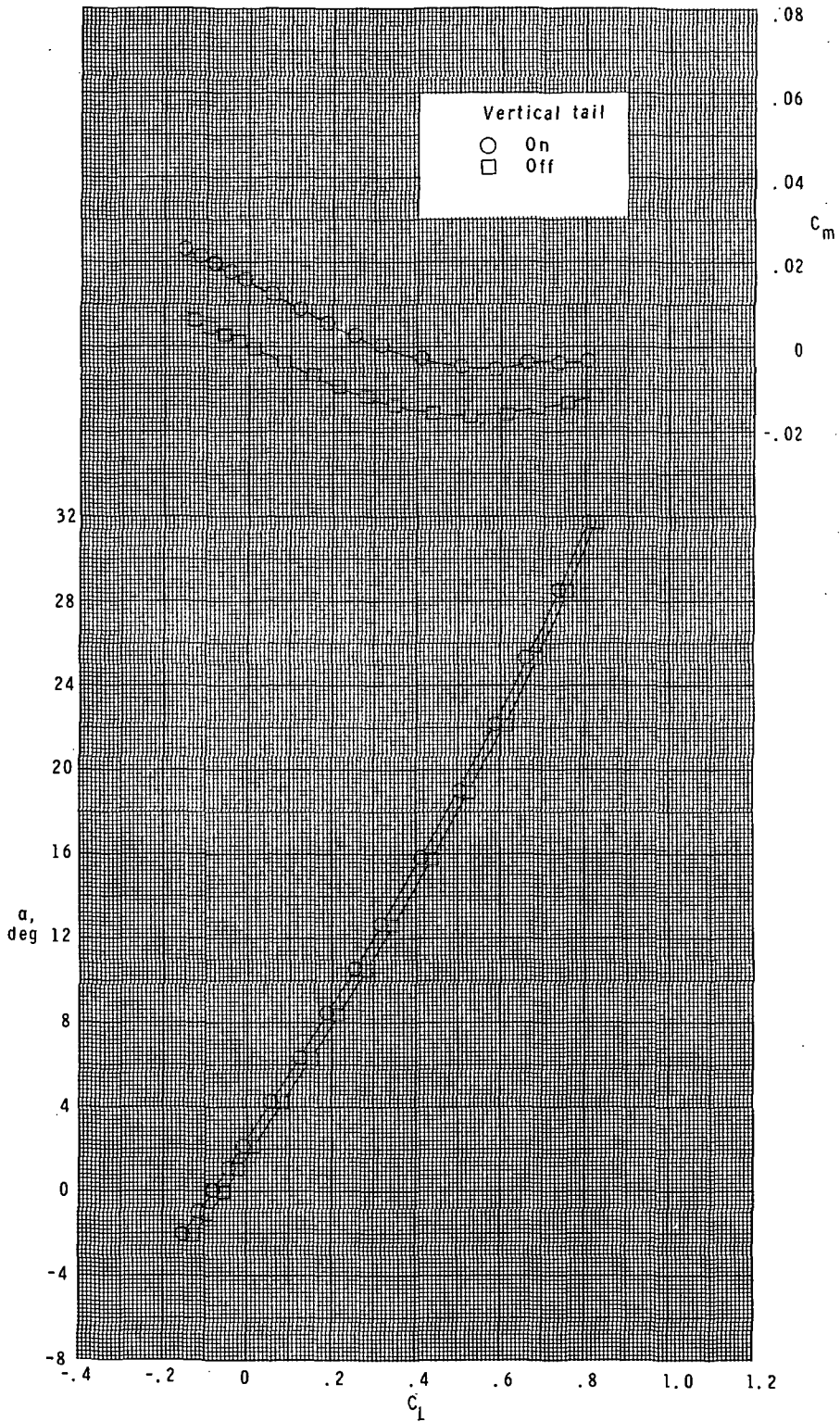
Figure 8.- Continued.

(b)   M = 1.90.

Figure 8.- Continued.
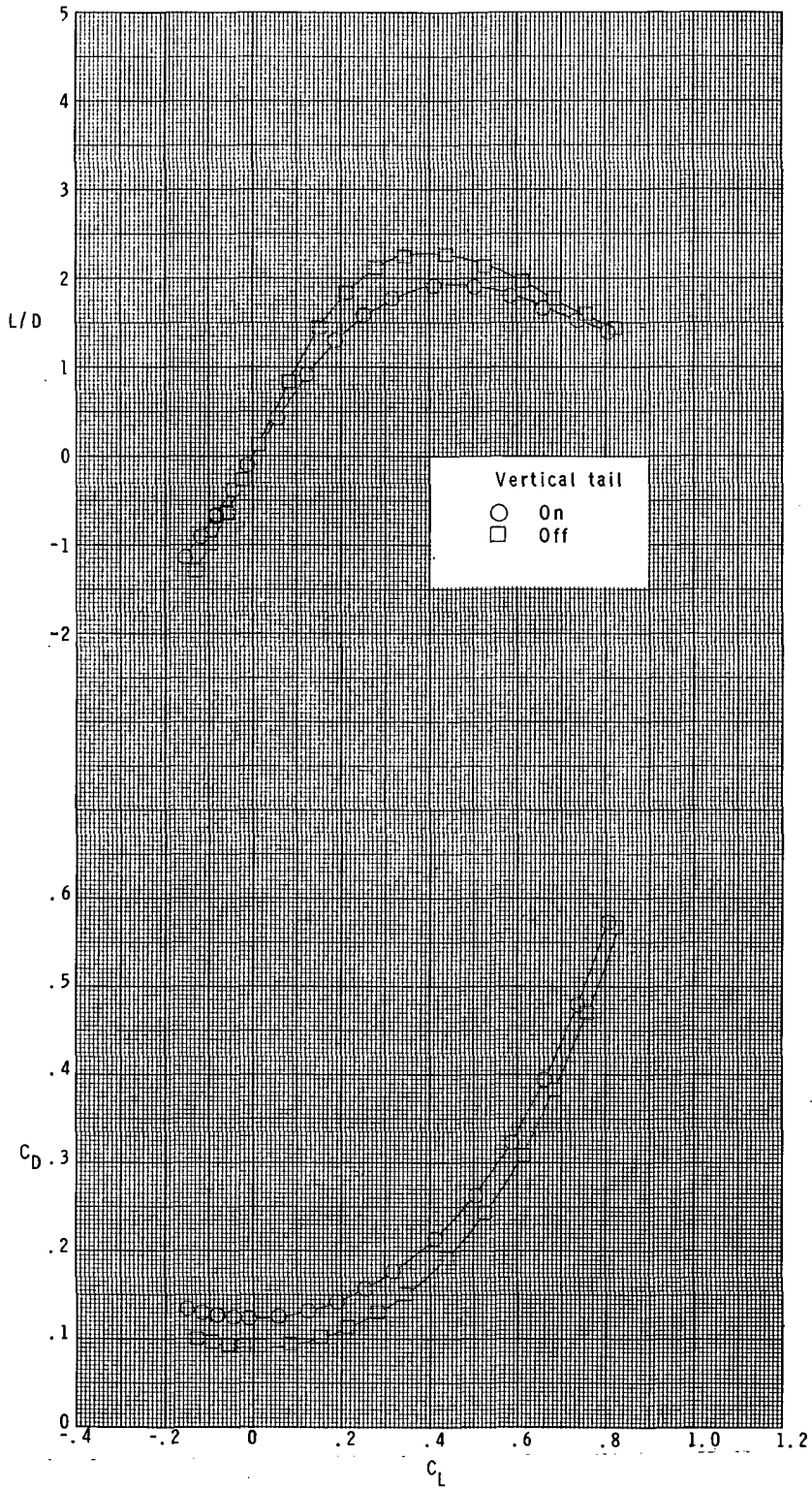
(b) Concluded.
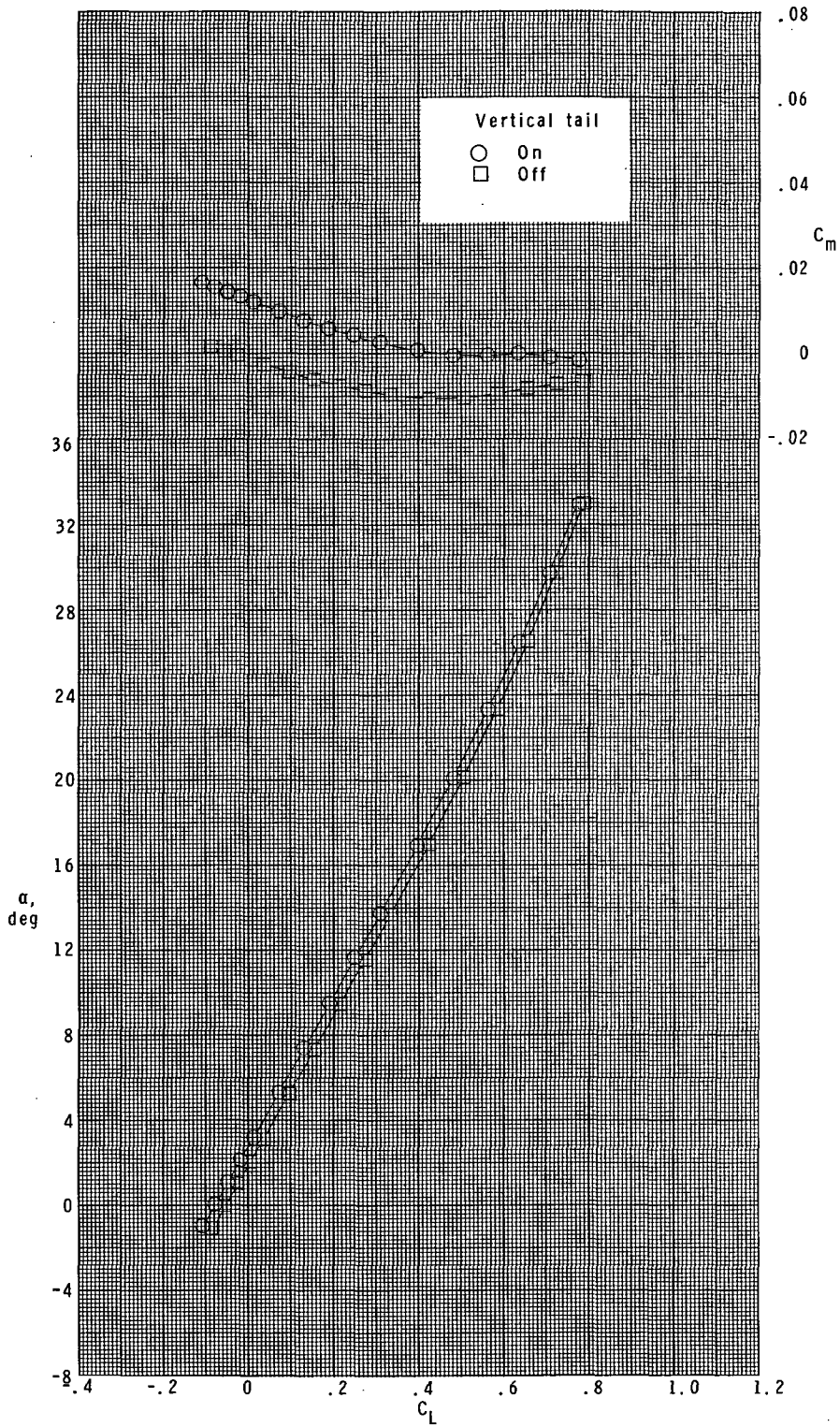
Figure 8.- Continued.

(c) M = 2.16.

Figure 8.- Continued.
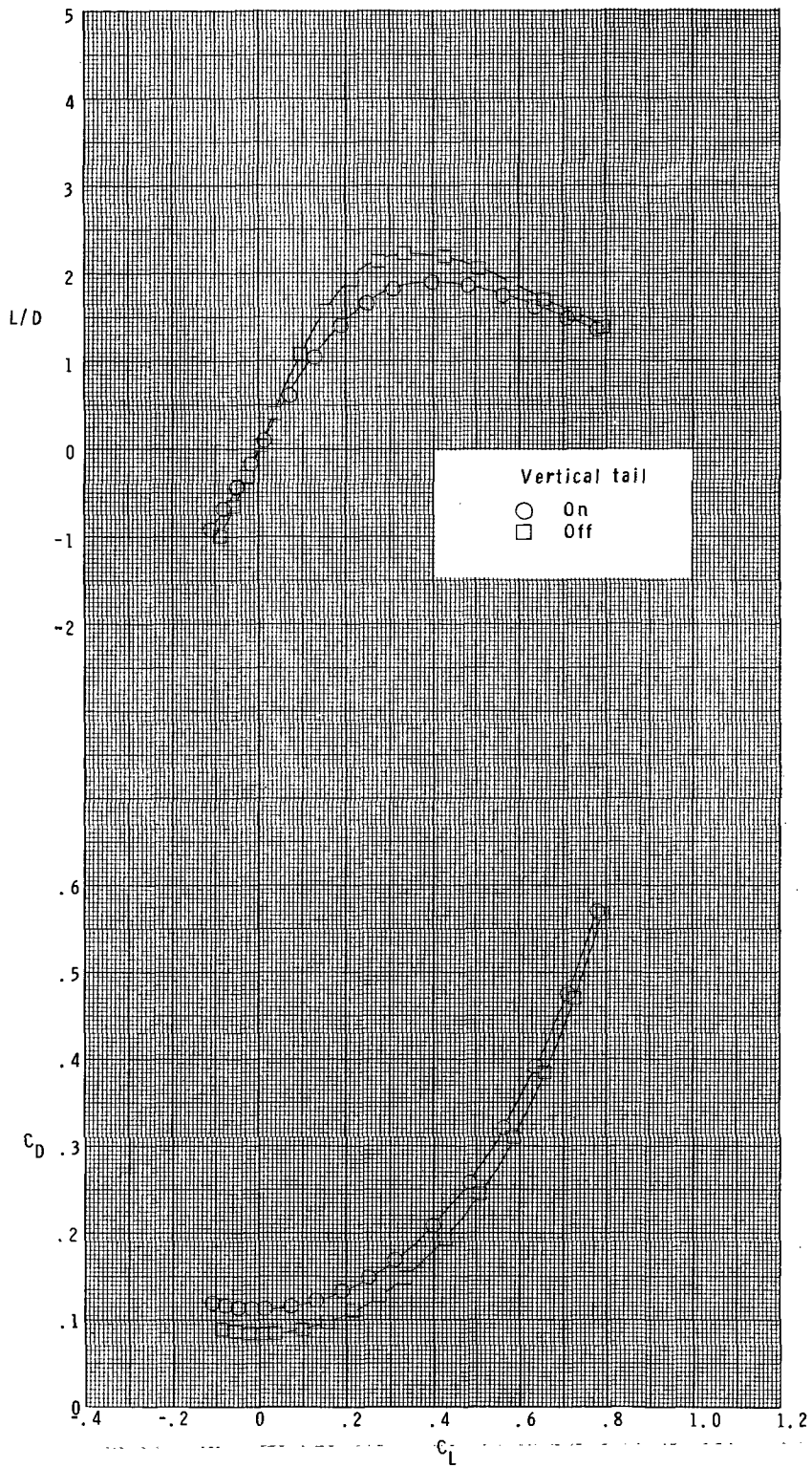
(c) Concluded.

Figure 8.- Concluded.
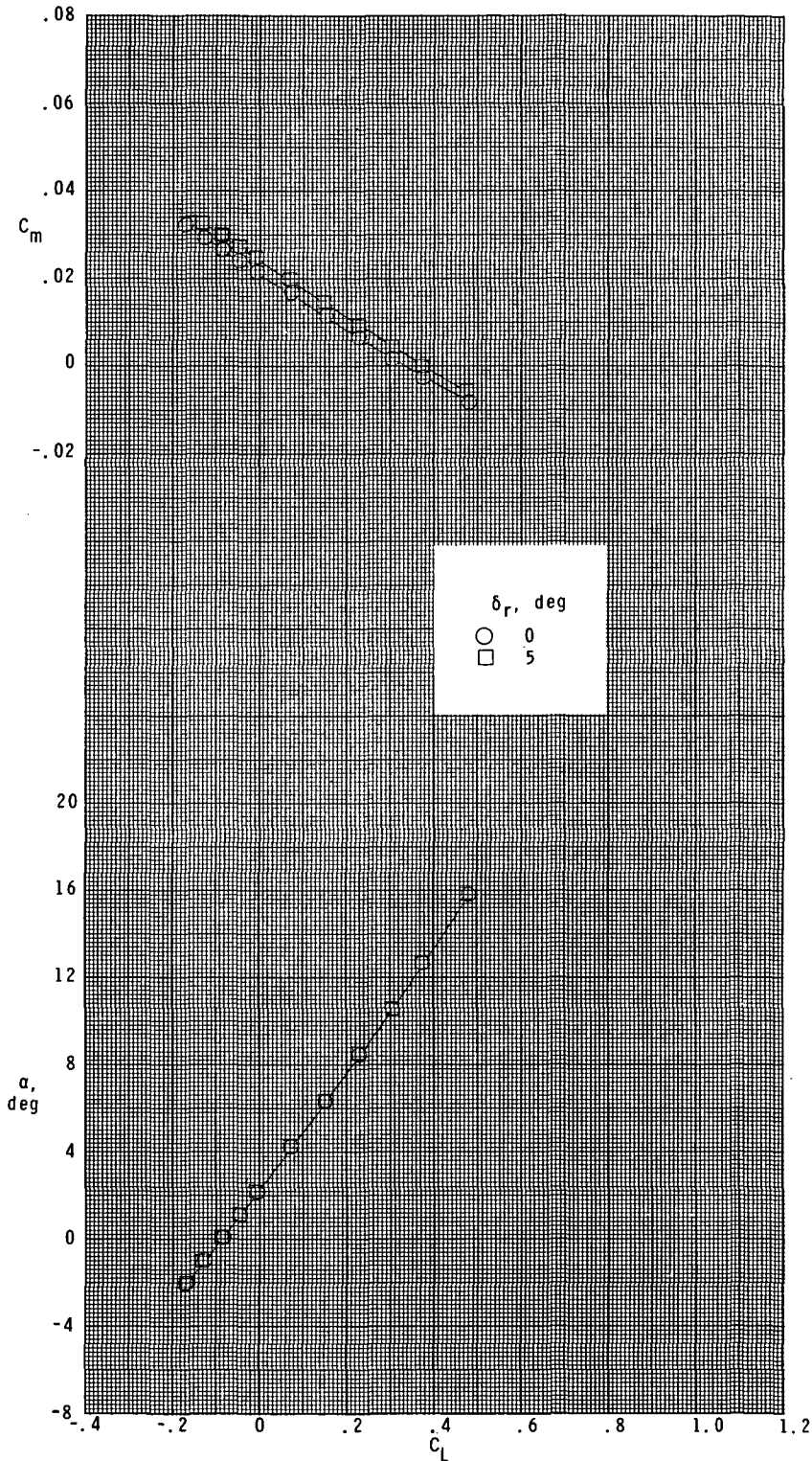
(a) M = 1.60; δ_e = -20°.

Figure 9.- Effect of rudder deflection on longitudinal aerodynamic characteristics. δ_{rf} = 30°.
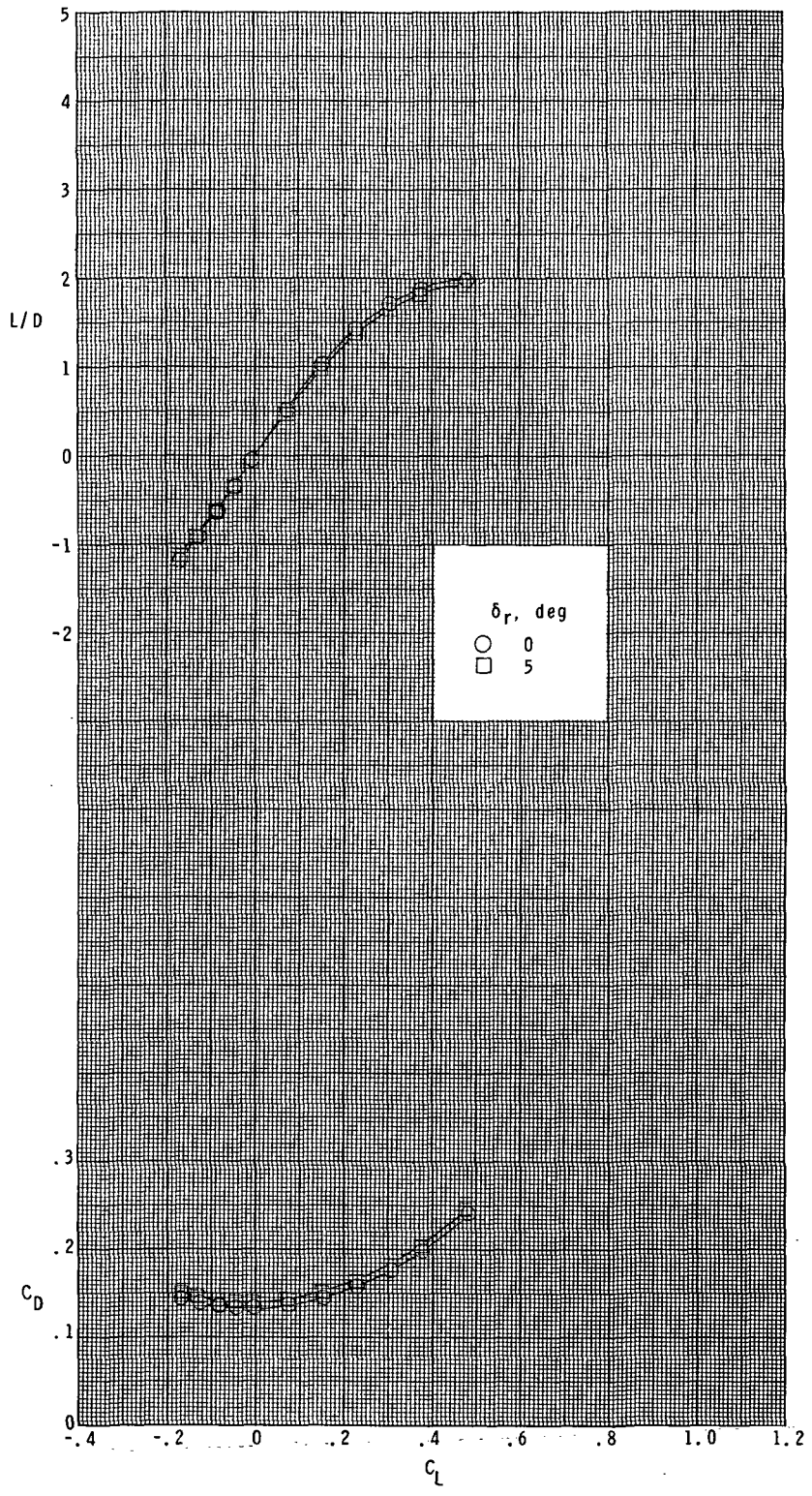
(a) Concluded.

Figure 9.- Continued.

(b)   M = 1.90; δ_e = -20°.
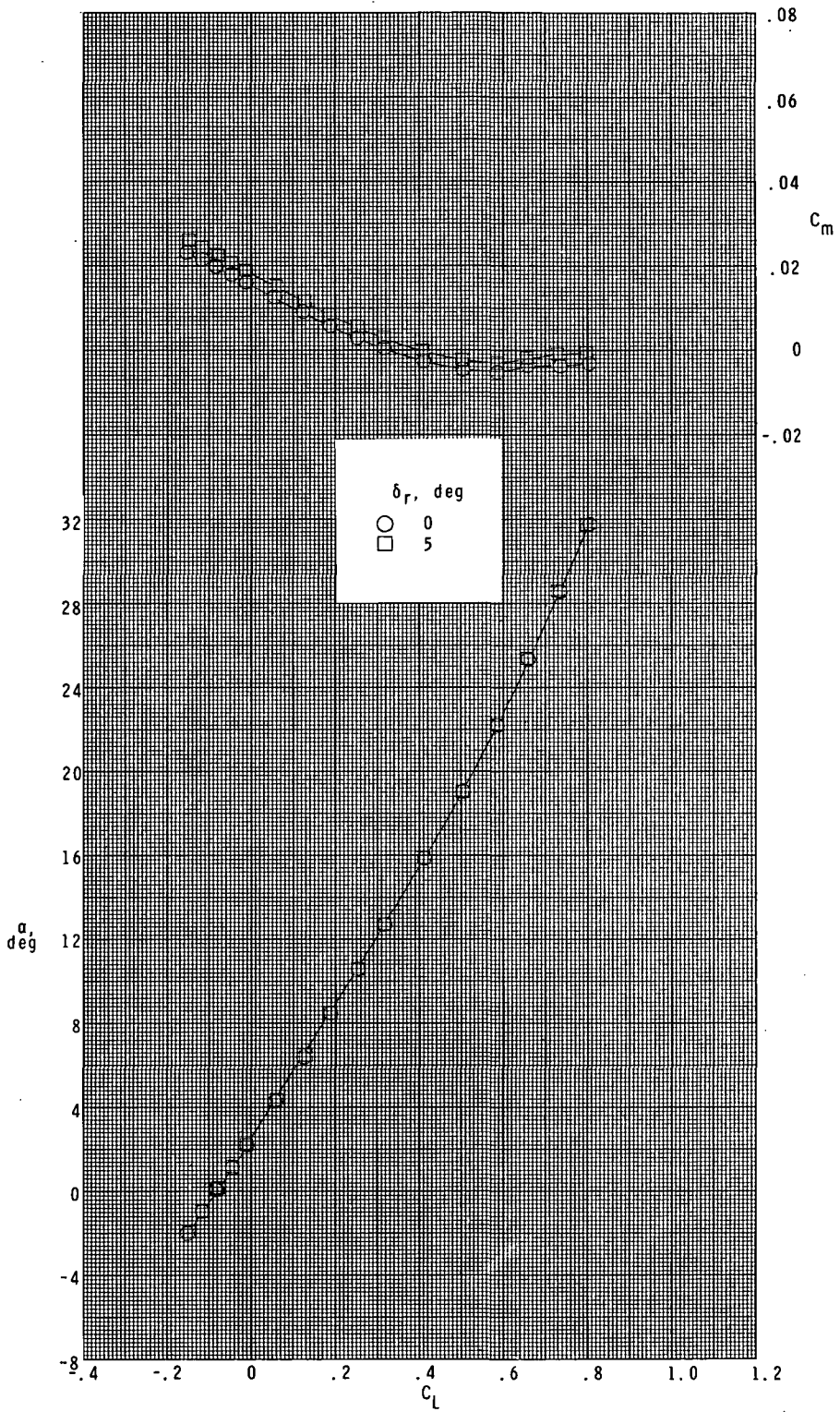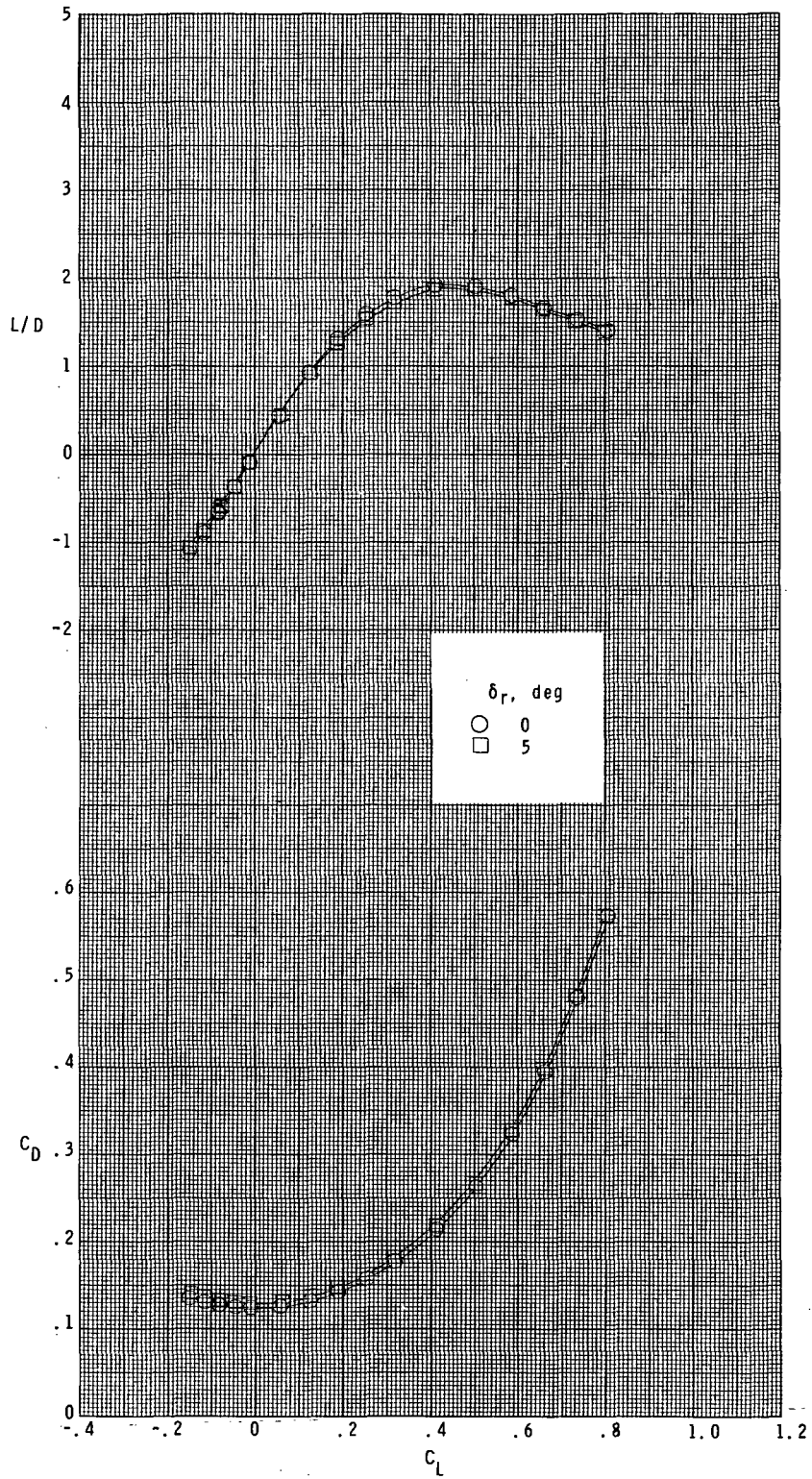
Figure 9.- Continued.

(b) Concluded.

Figure 9.- Continued.

(c) M = 2.16; δ_e = -20°.
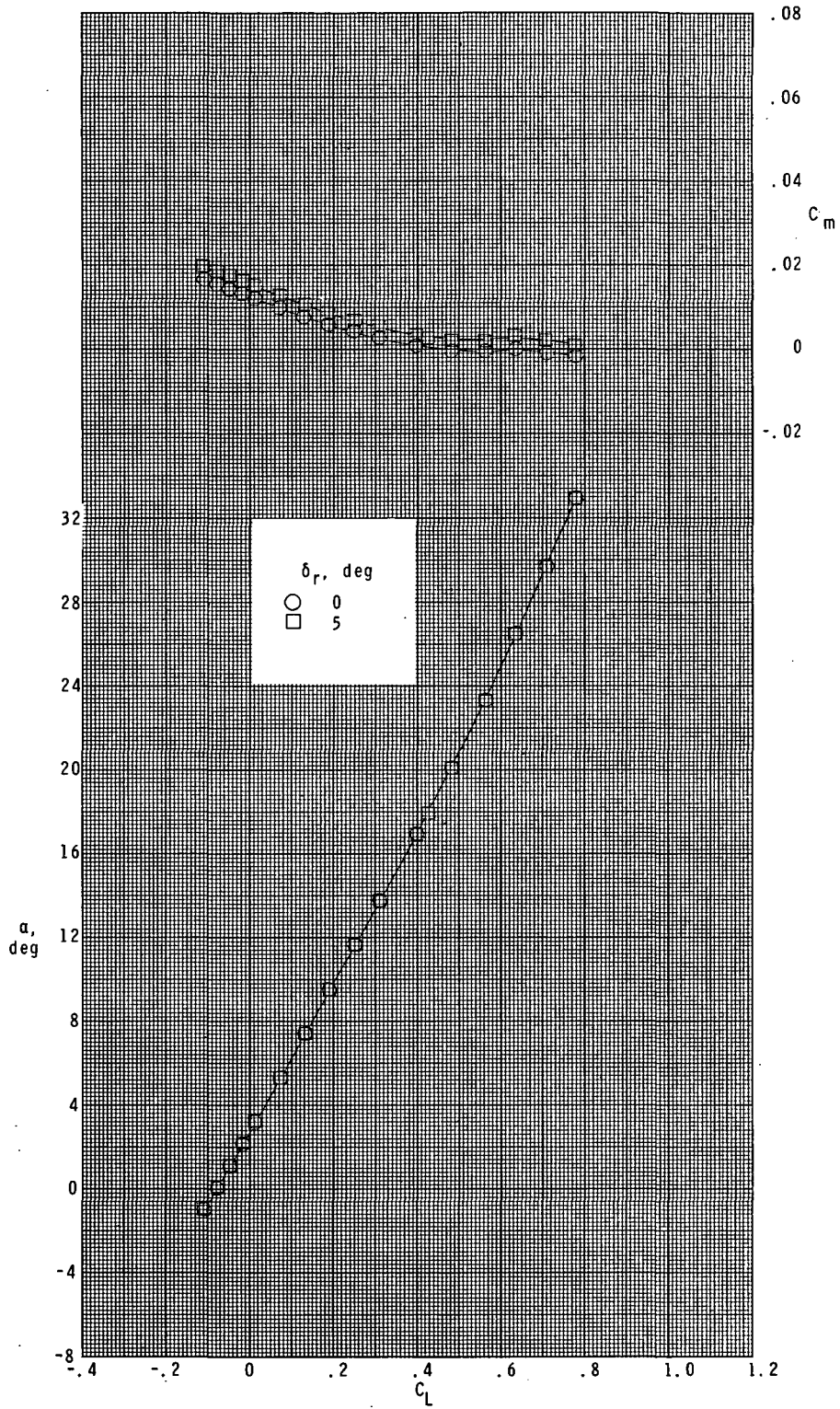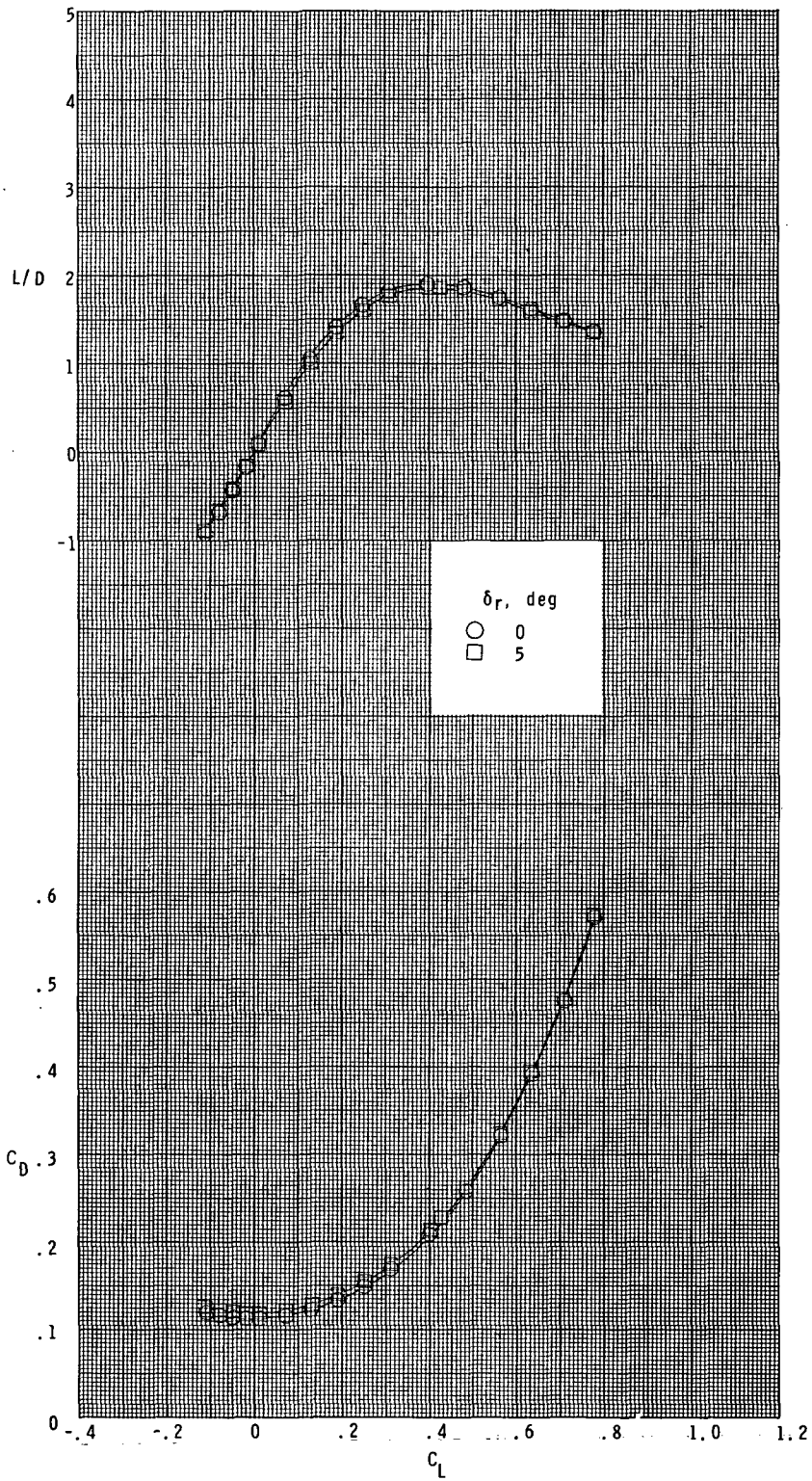
Figure 9.- Continued.

(c) Concluded.

Figure 9.- Continued.

(d)   M = 2.86; δ_e = -10°.
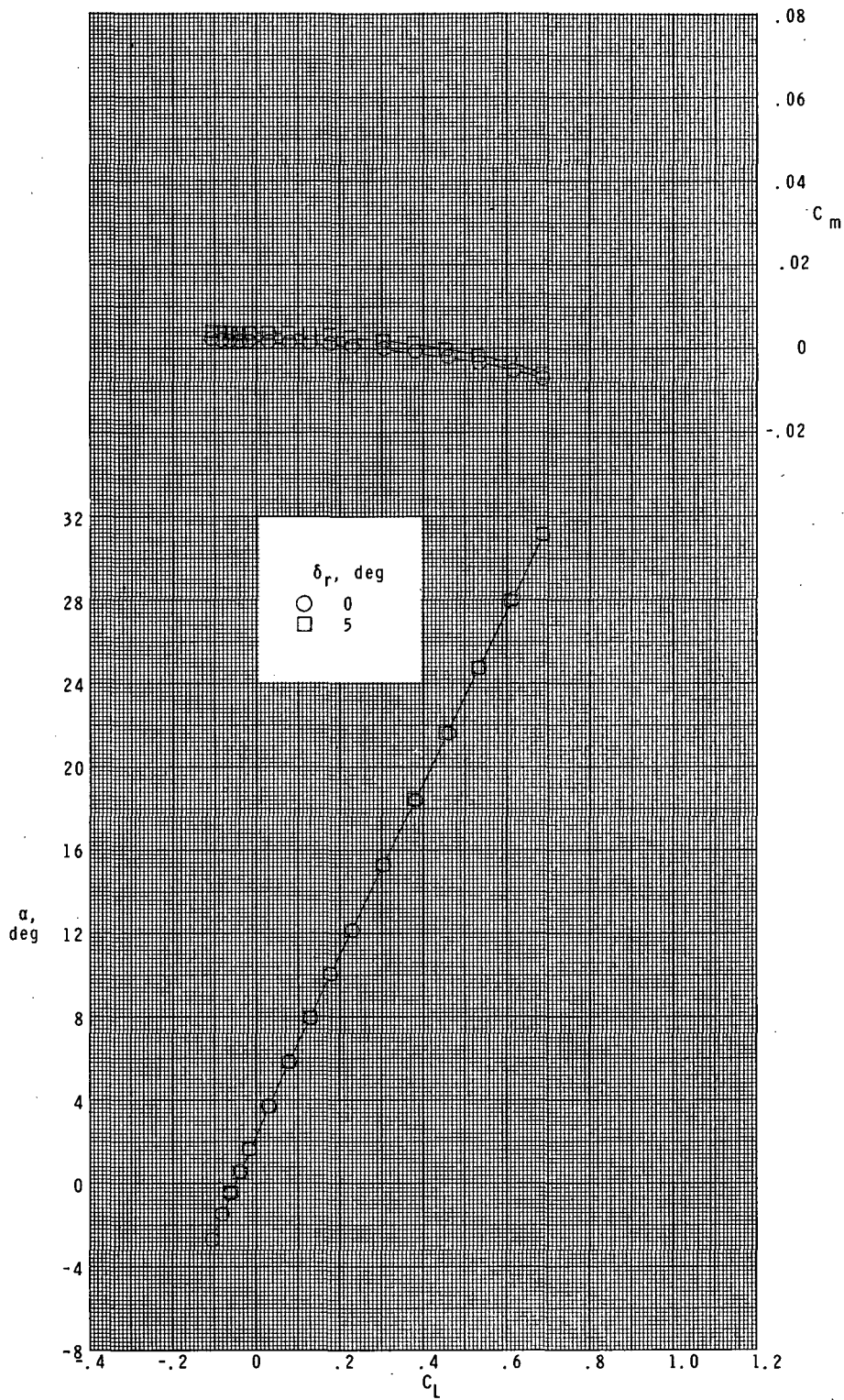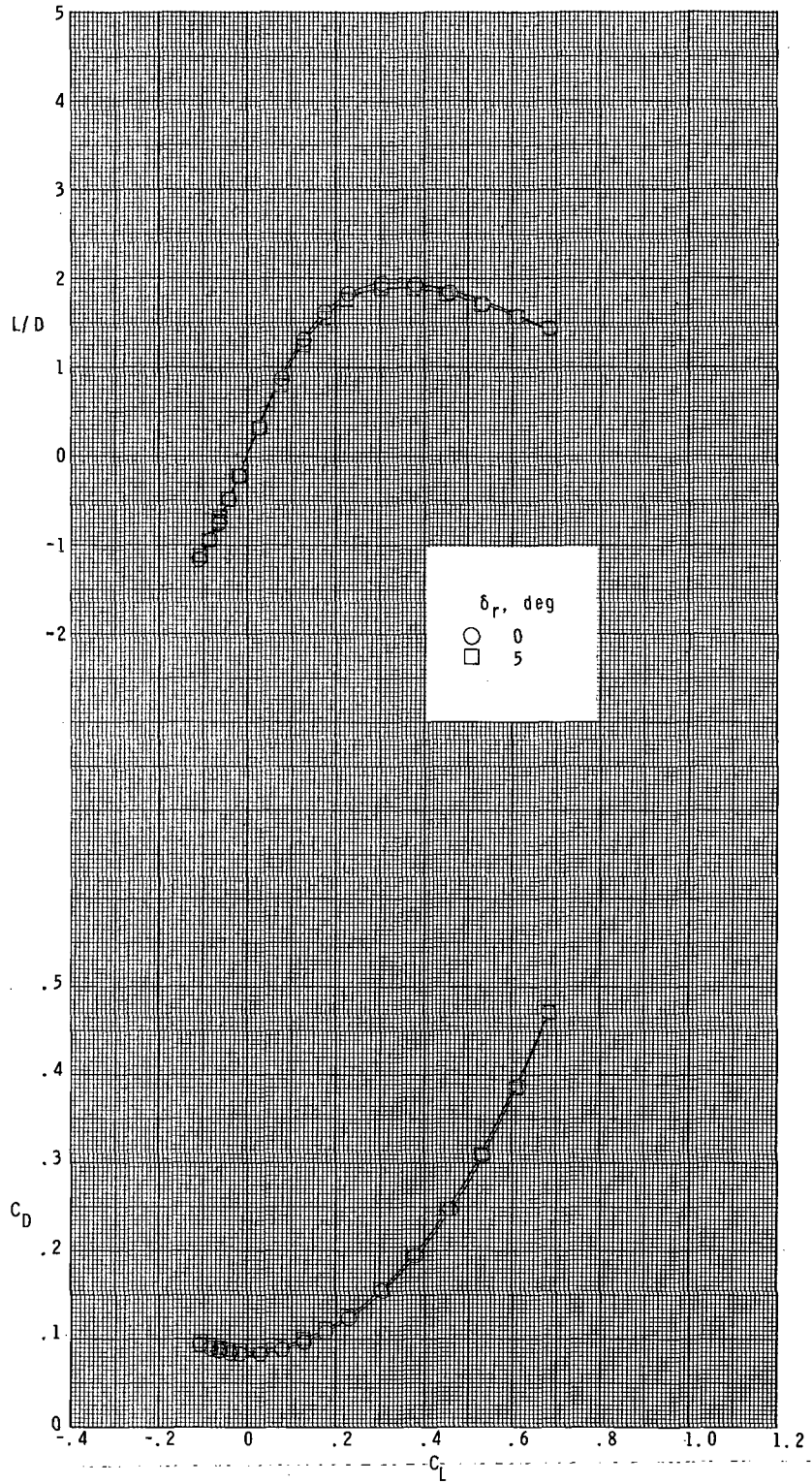
Figure 9.- Continued.

(d) Concluded.

Figure 9.- Continued.

(e) M = 3.95; δ_e = -10°.
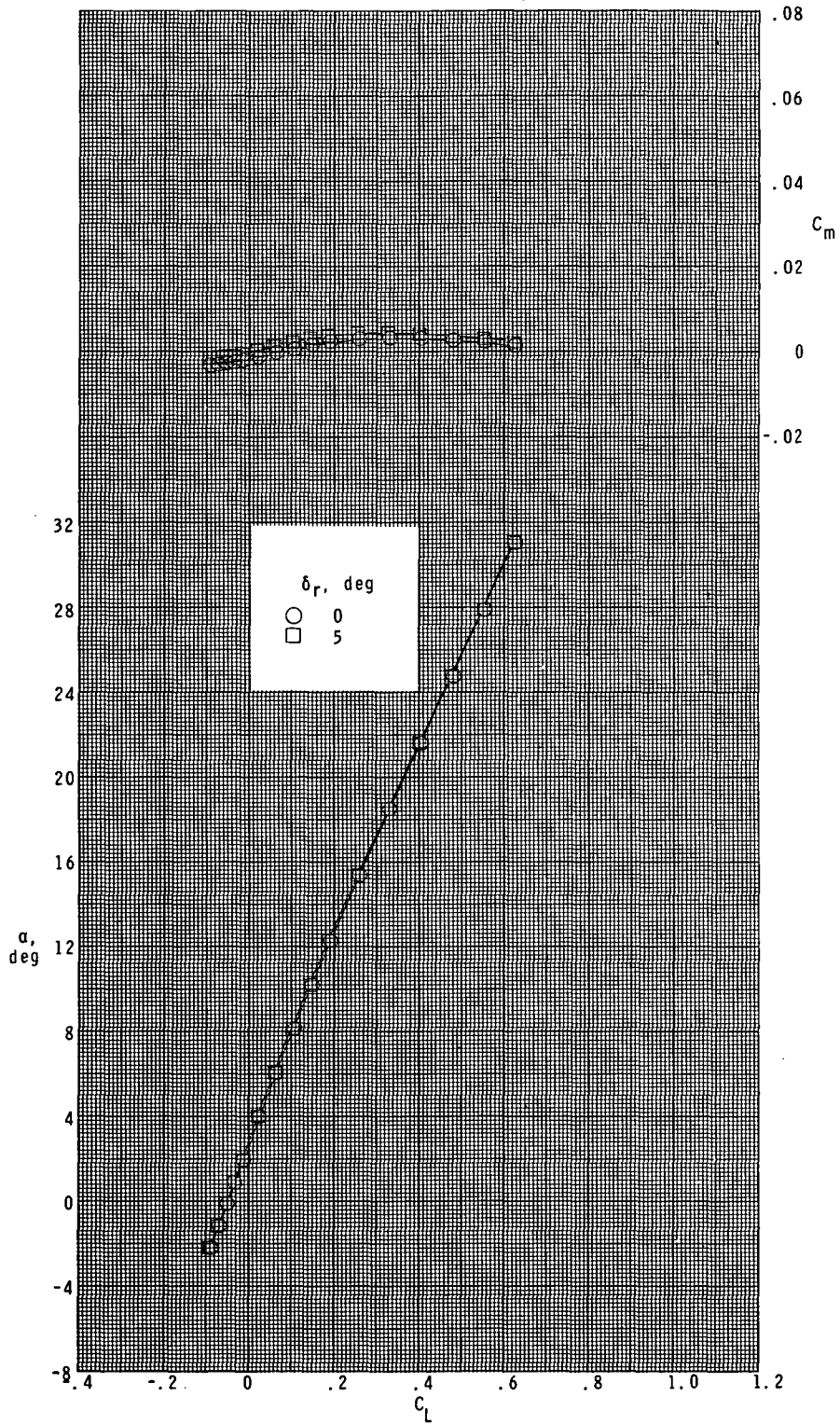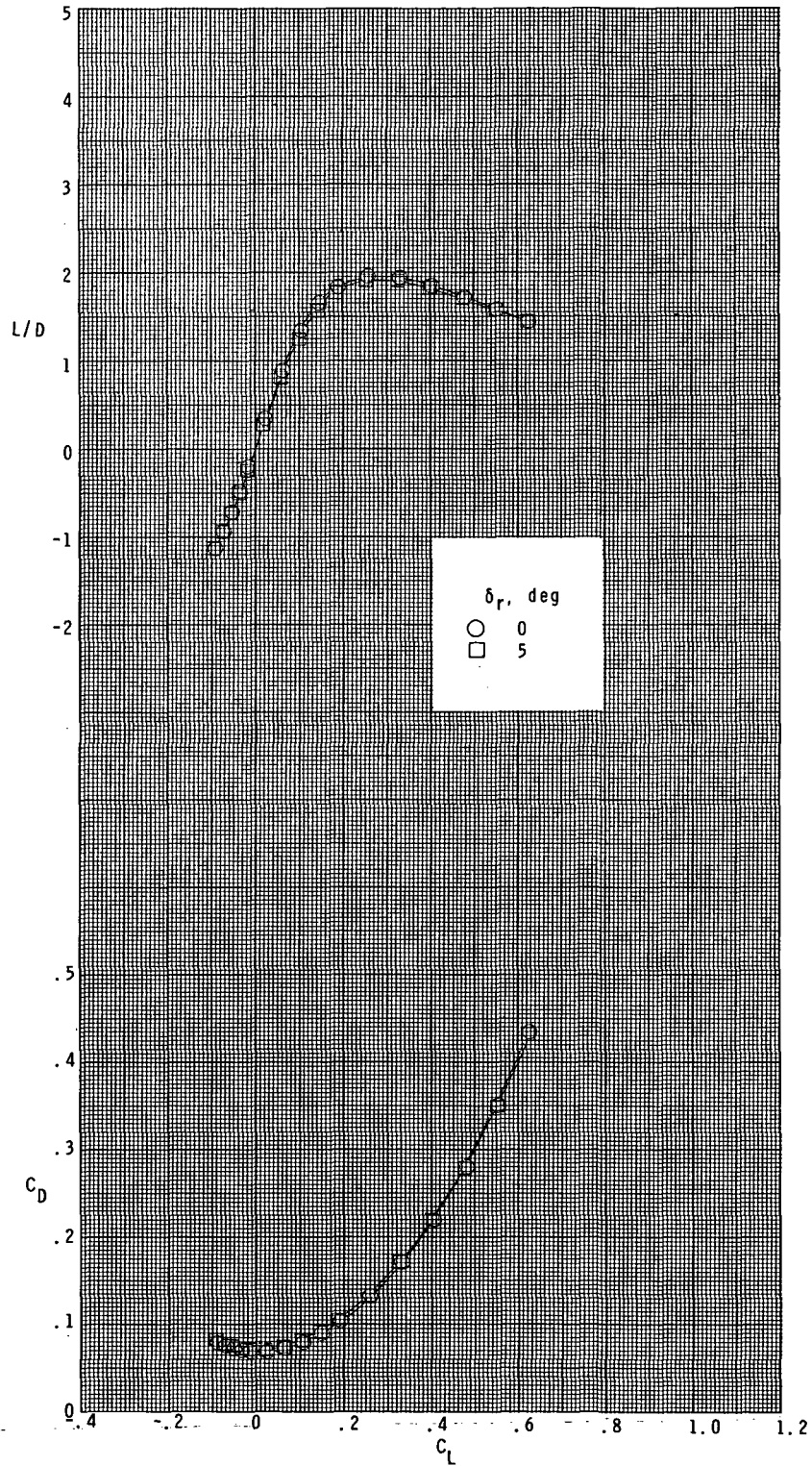
Figure 9.- Continued.

(e) Concluded.

Figure 9.- Continued.

(f) M = 4.63; δ_e = -10°.
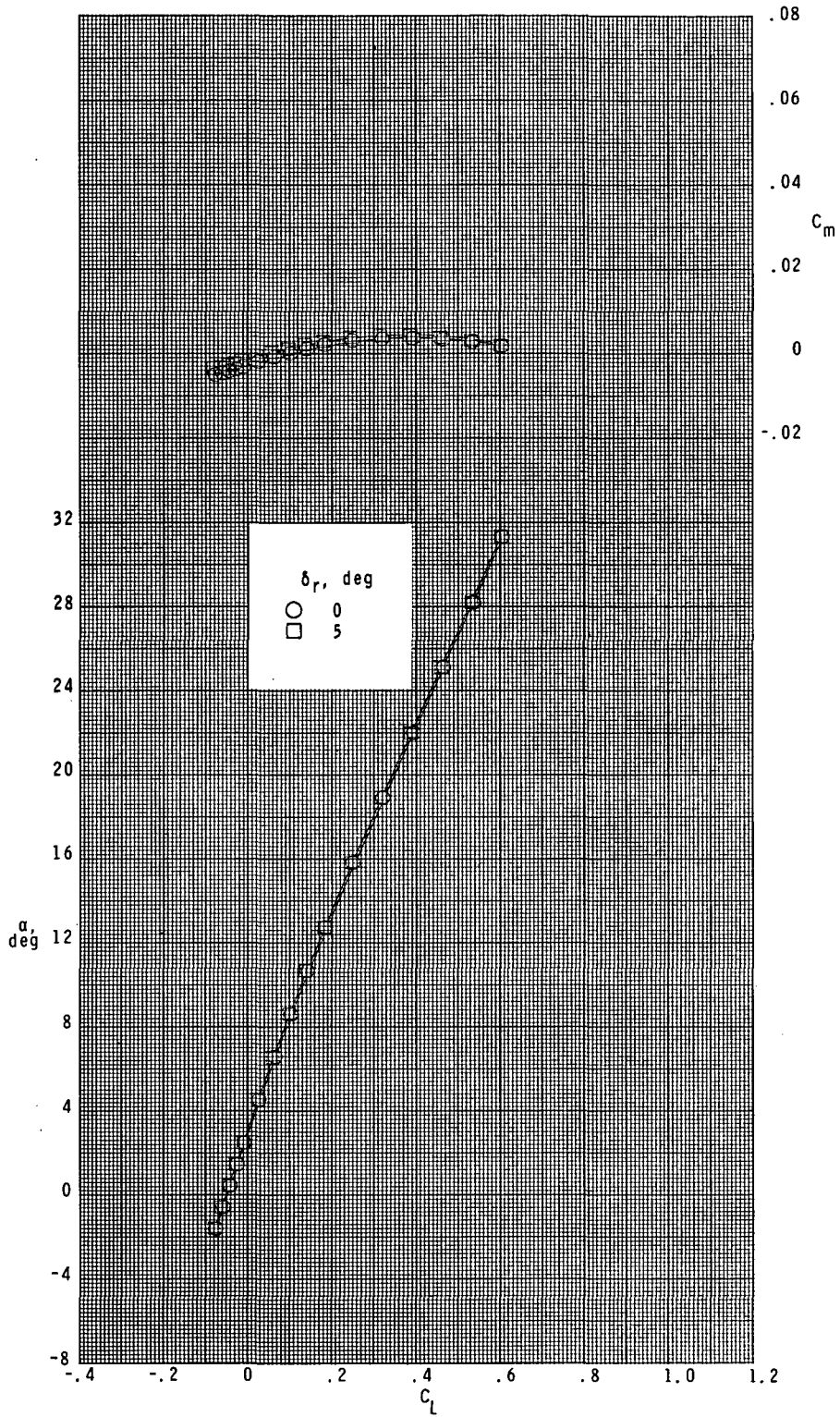
Figure 9.- Continued.
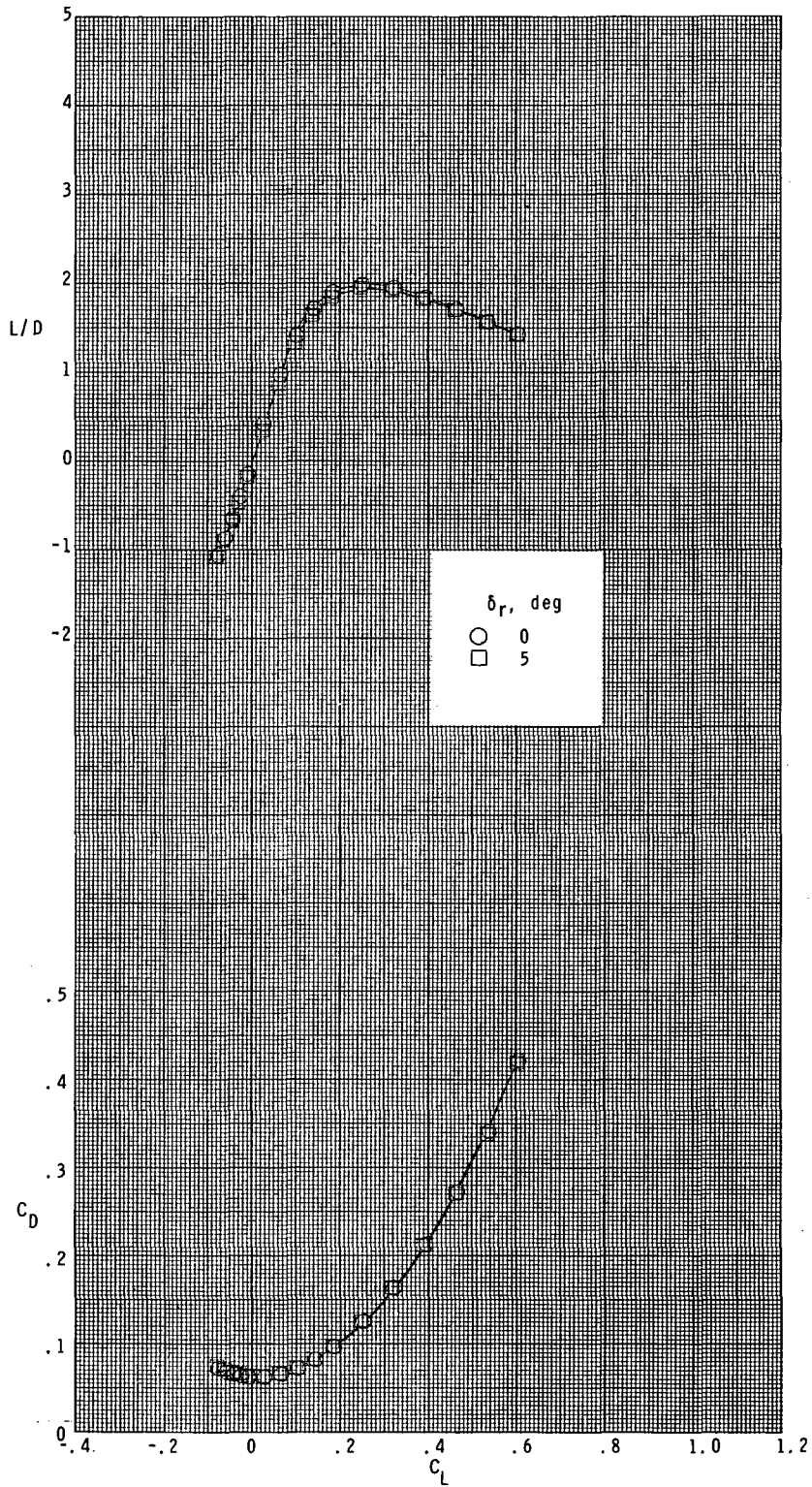
(f) Concluded.

Figure 9.- Concluded.

(a) $\alpha \approx 0^{O}$.
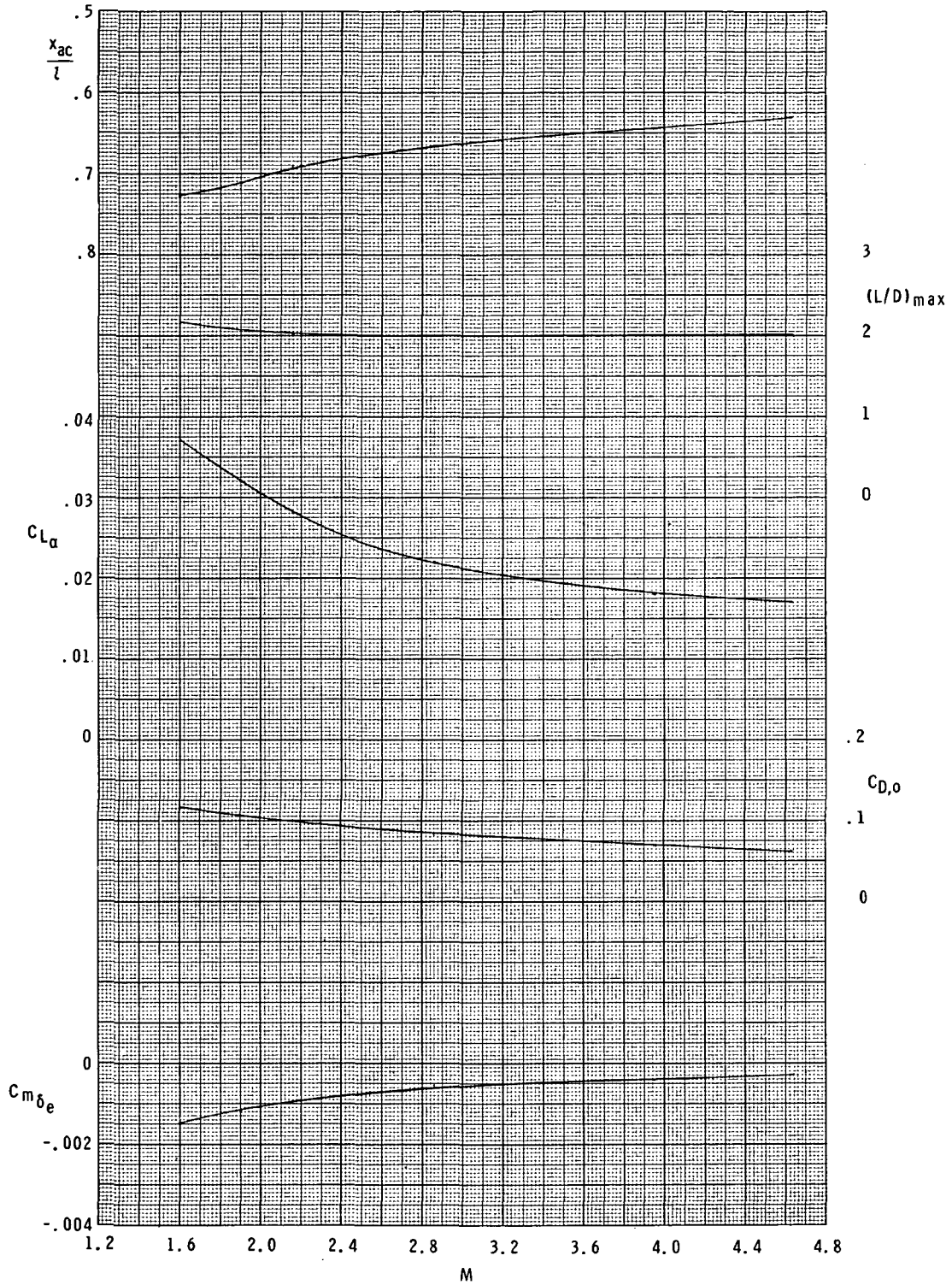
Figure 10.- Summary of longitudinal aerodynamic characteristics. $\delta_{rf} = 30^{O}$.
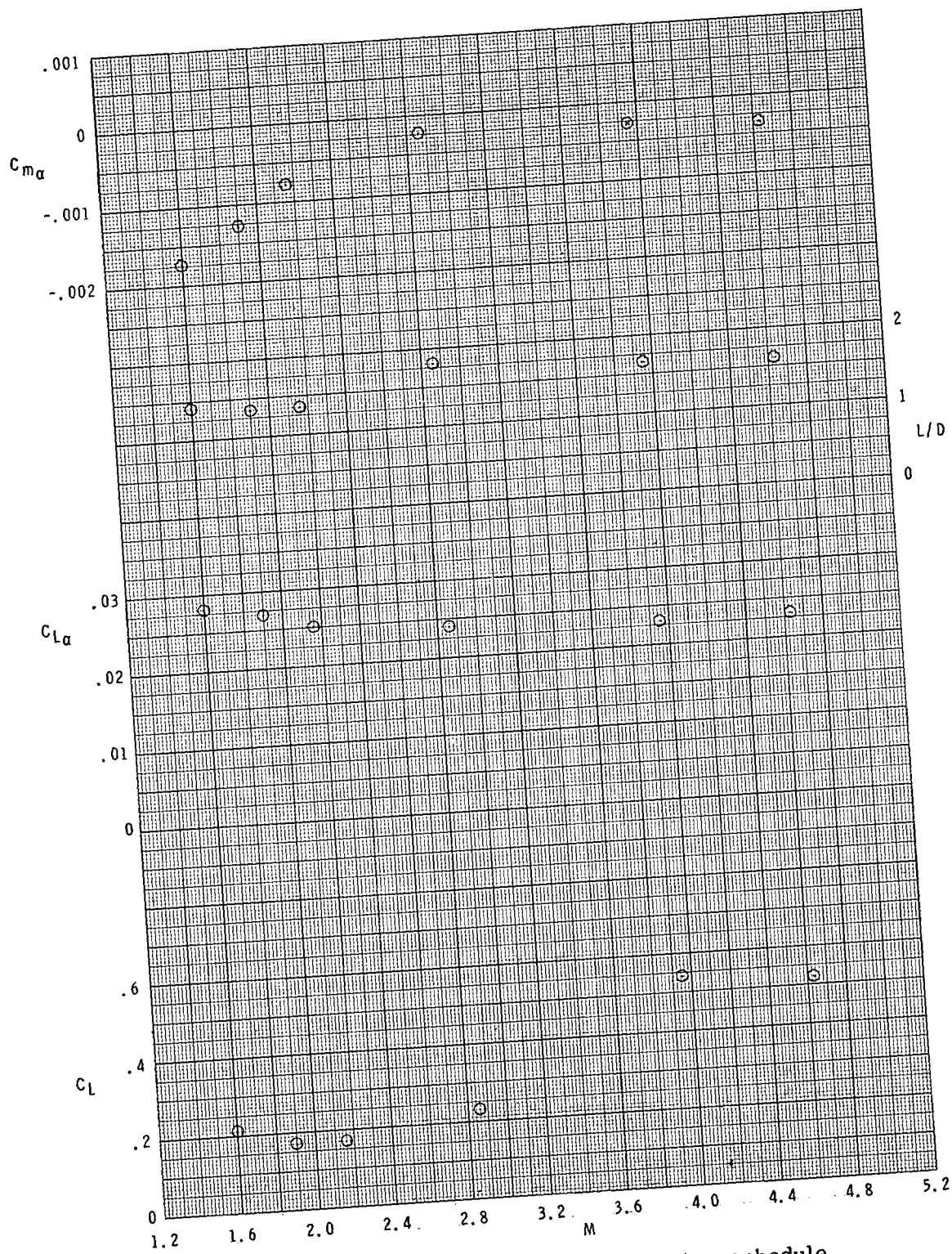
(b) Trimmed conditions for the flight α-schedule.

Figure 10.- Concluded.
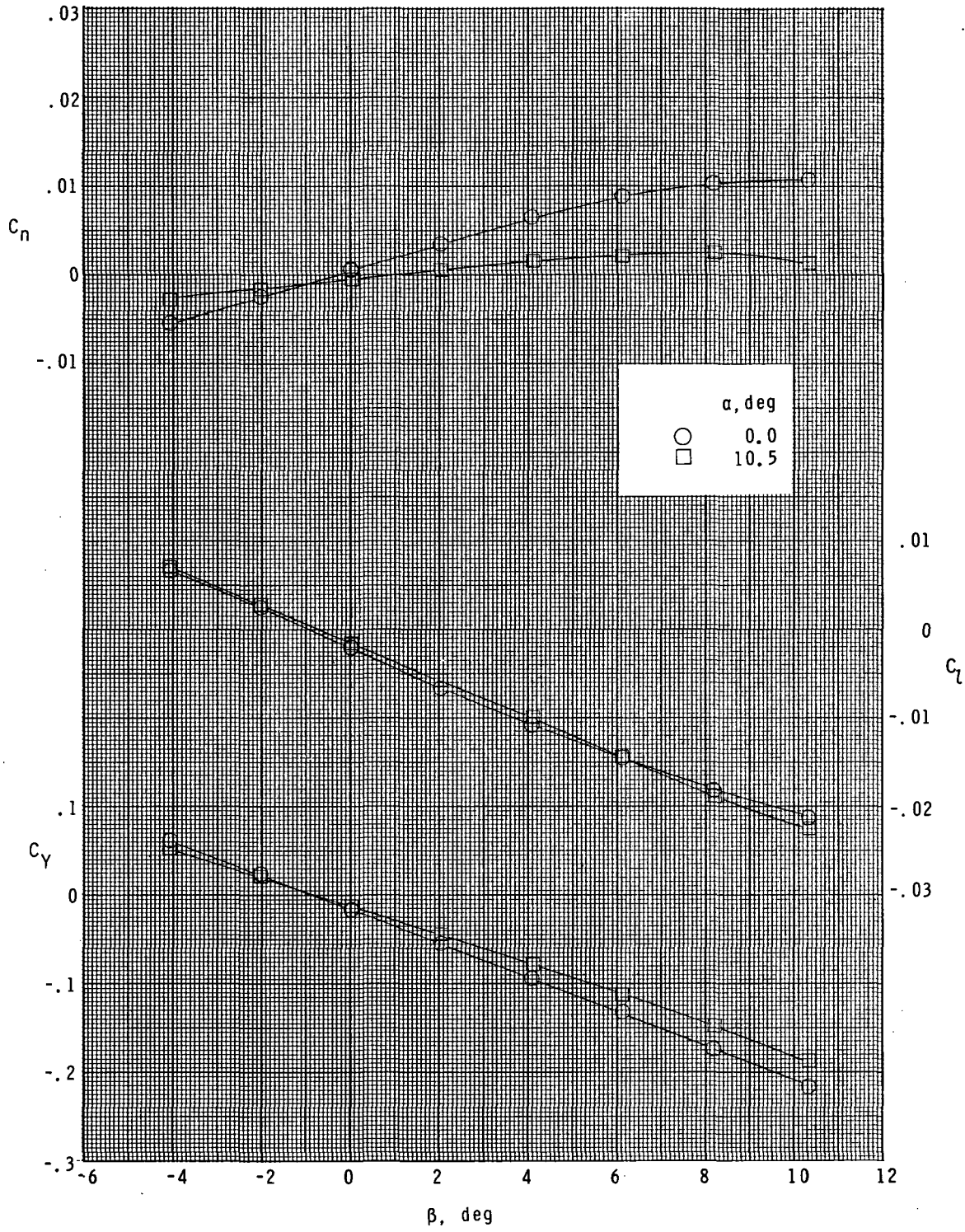
(a) M = 1.60; $\delta_{rf} = 0^O$.

Figure 11.- Lateral characteristics in sideslip. $\delta_{e_L} = \delta_{e_R} = 0^O$.
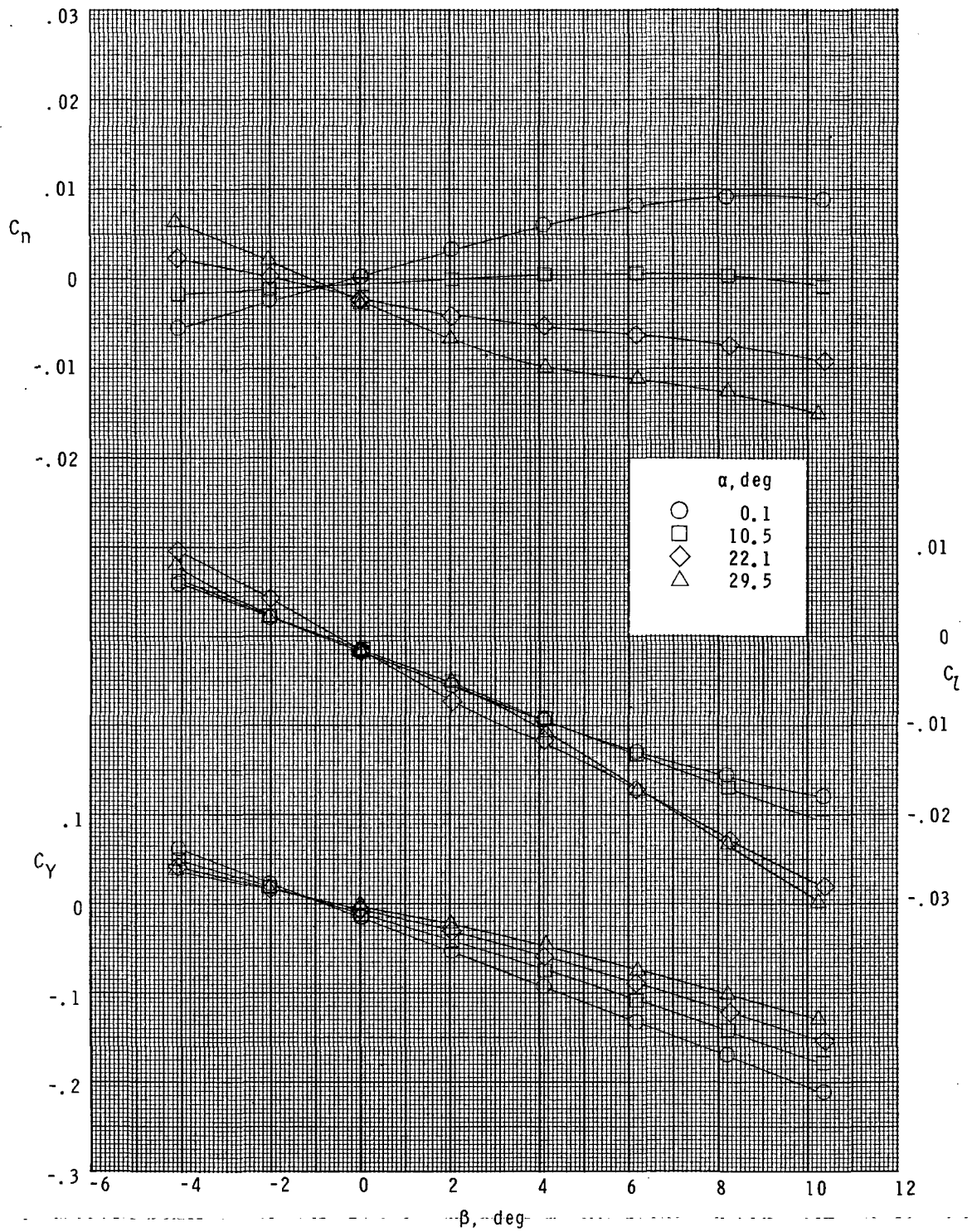
(b)   M = 1.90; $\delta_{rf} = 0^O$.

Figure 11.- Continued.
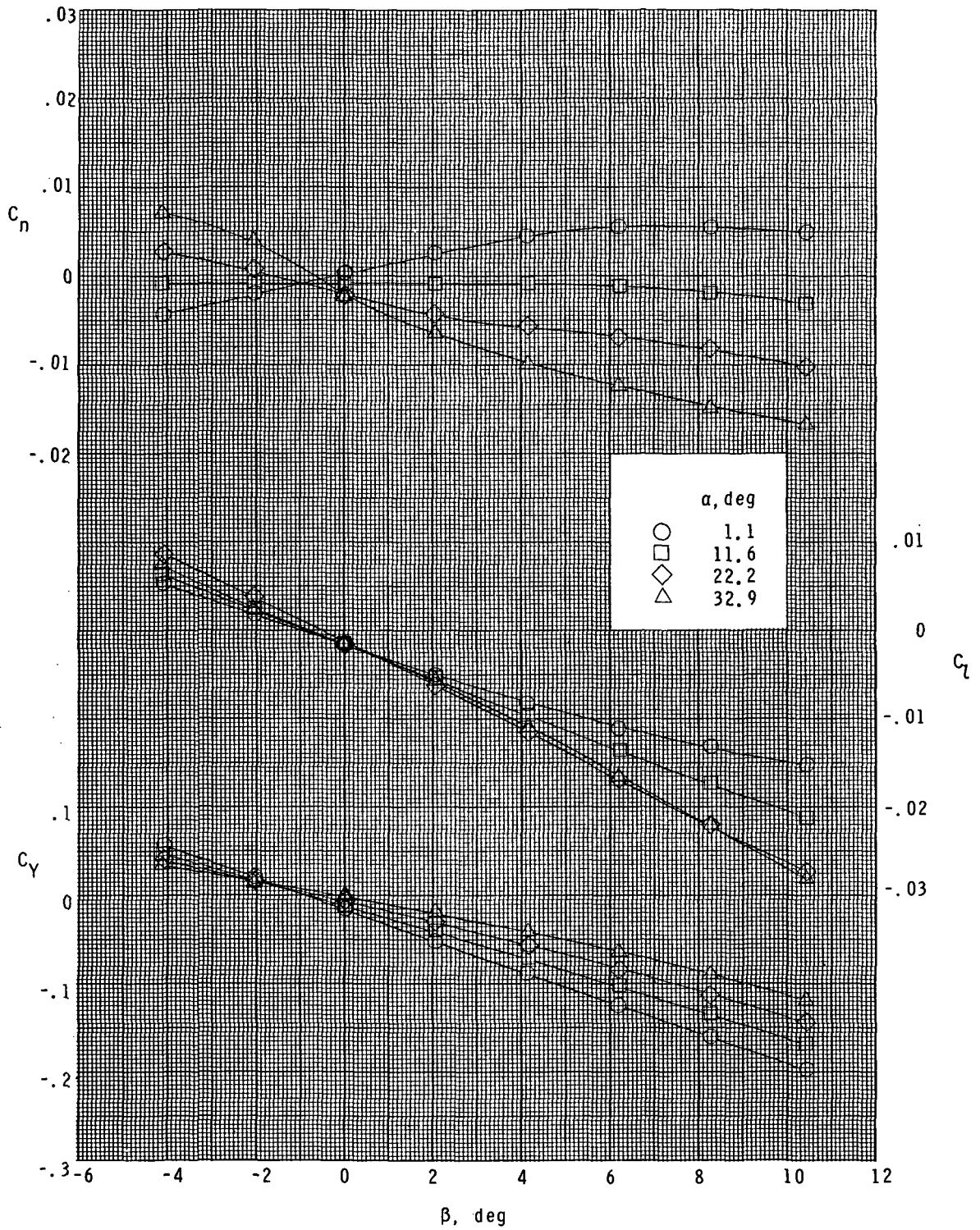
(c) $M = 2.16;$ $\delta_{rf} = 0^{o}$.

Figure 11.- Continued.

(d)   M = 2.86; δ_{rf} = 30°.
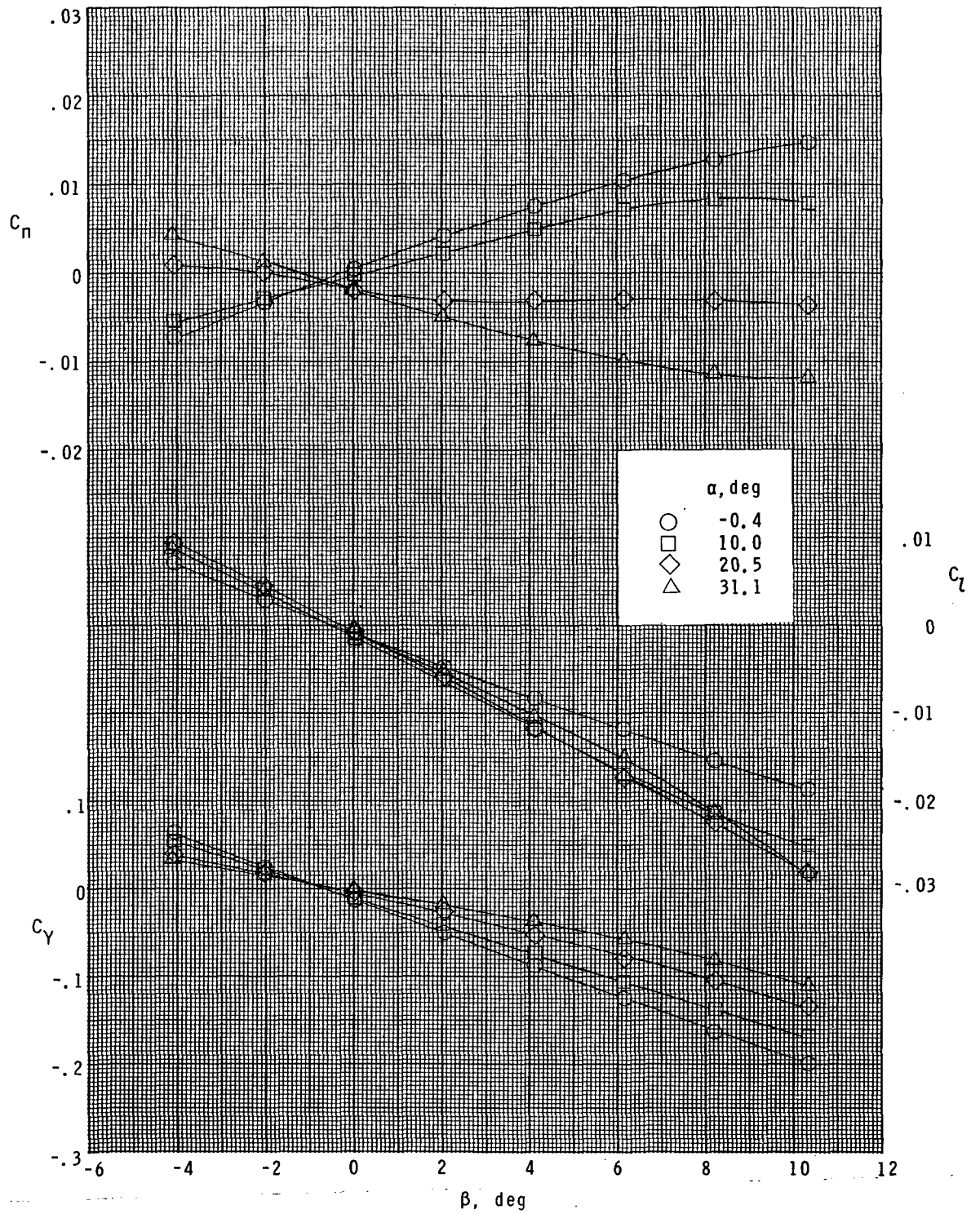
Figure 11.- Continued.
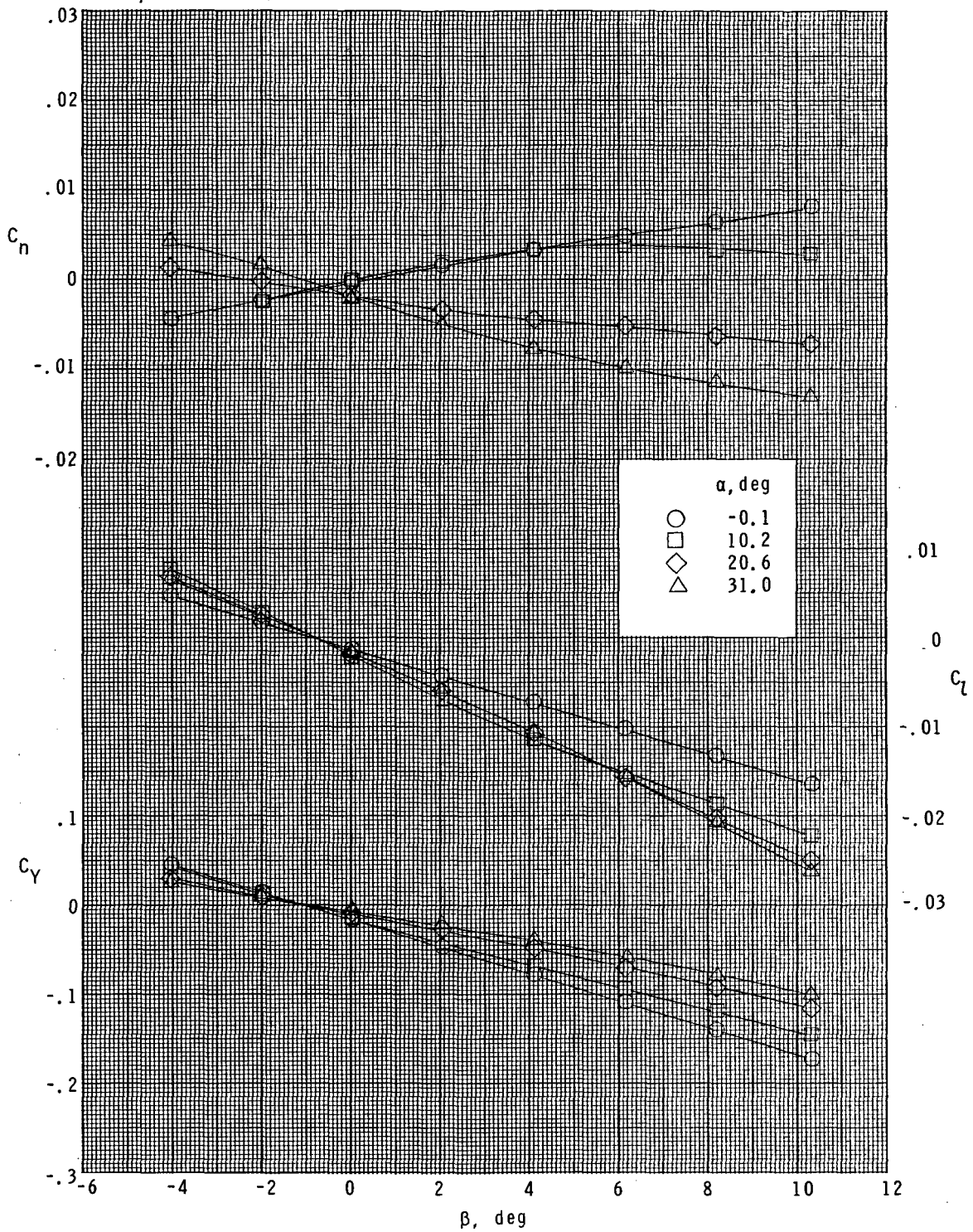
(e) M = 3.95; δ_{rf} = 30°.

Figure 11.- Continued.
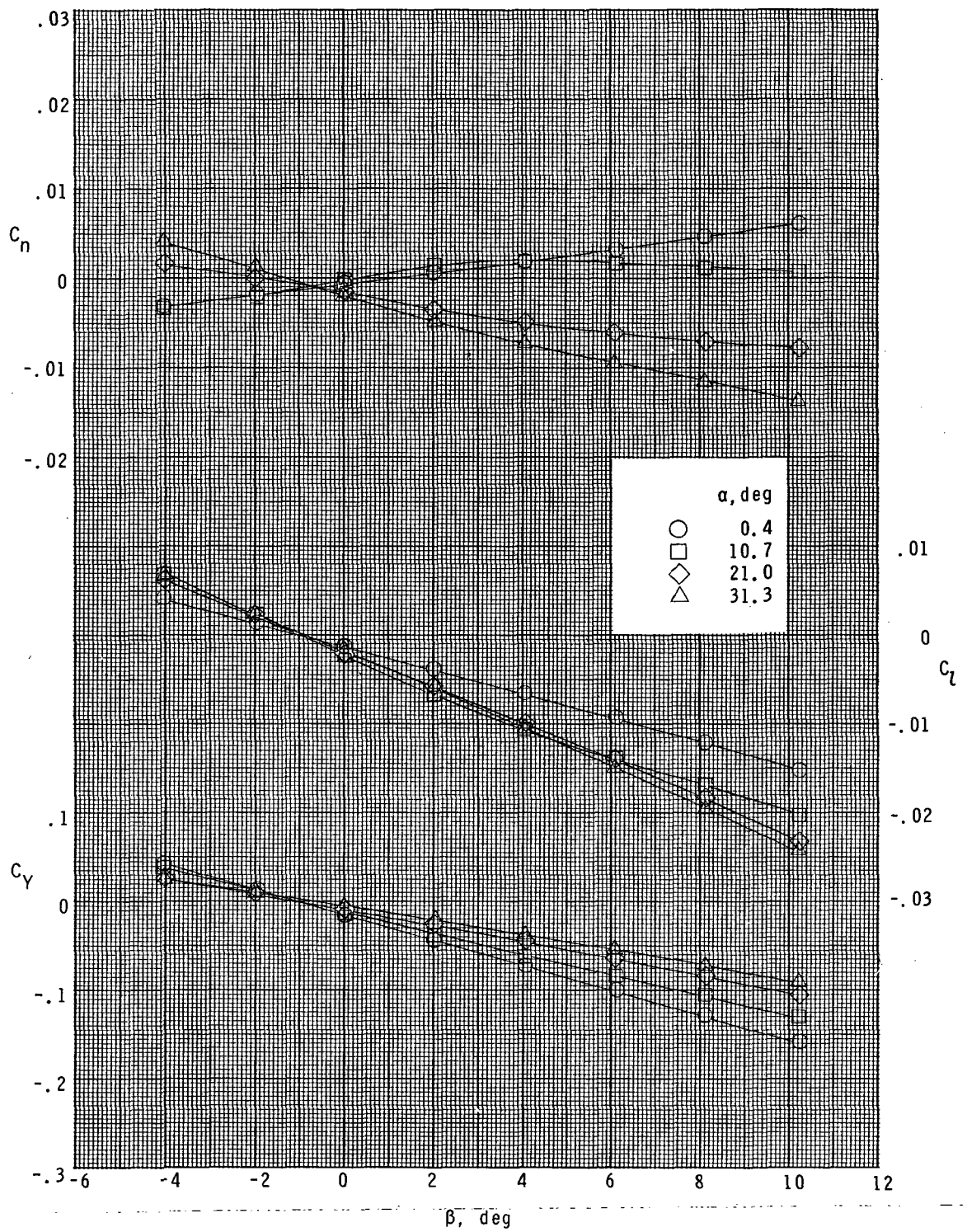
(f) M = 4.63; $\delta_{rf} = 30^O$.

Figure 11.- Concluded.
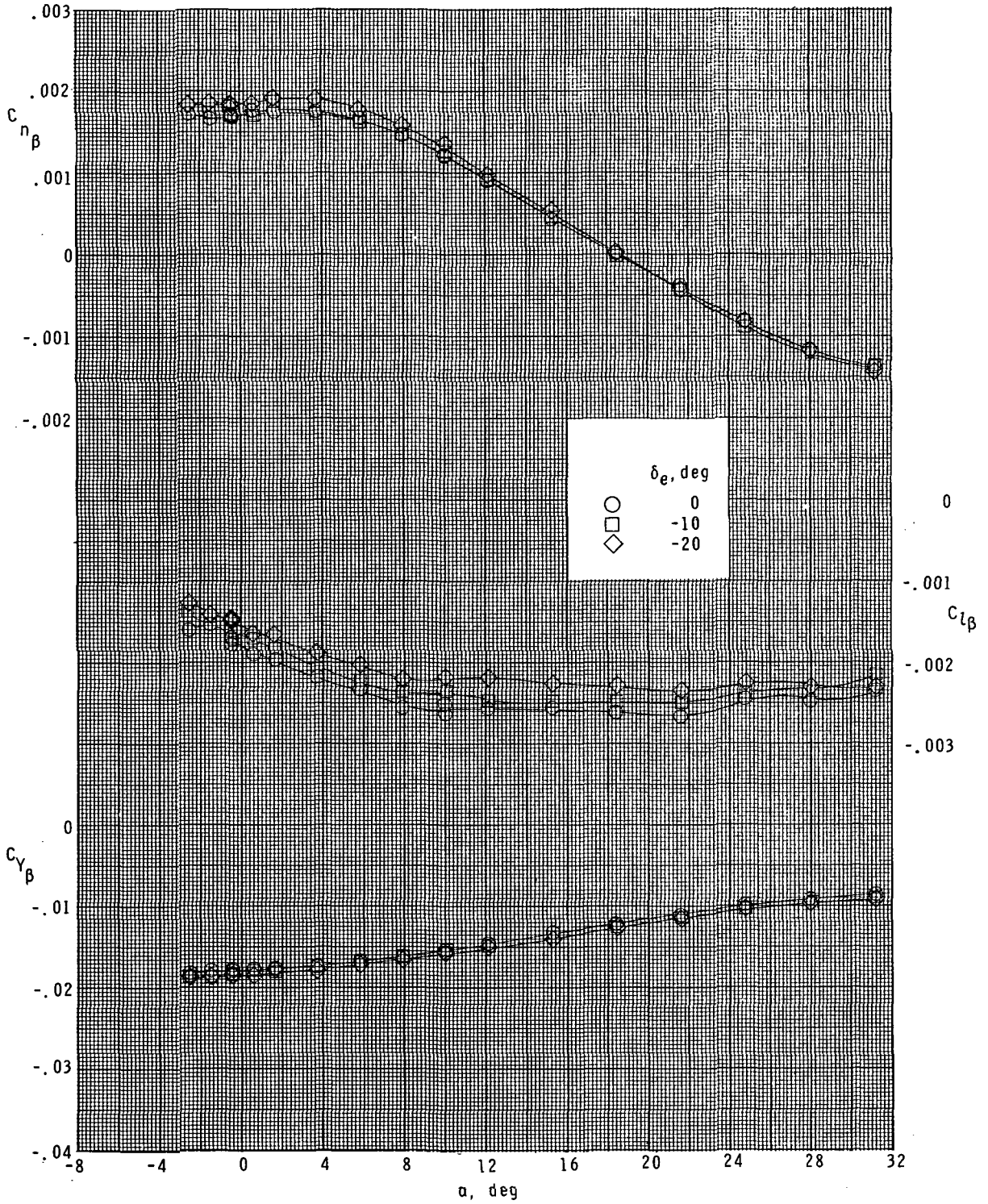
(a) M = 2.86.

Figure 12.- Effect of elevon deflection on lateral parameters. $\delta_{rf} = 30^{o}$.
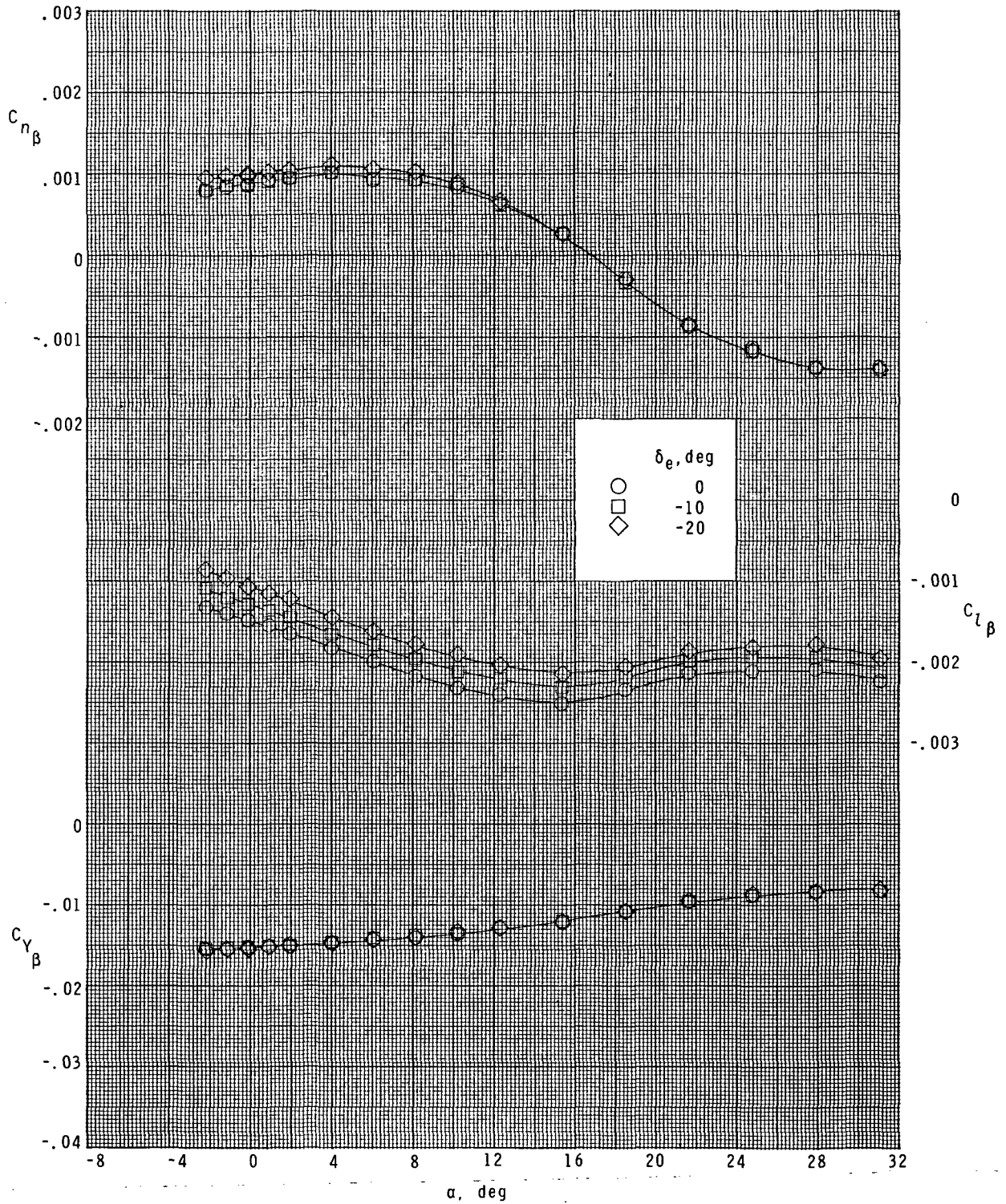
(b) M = 3.95.

Figure 12.- Continued.
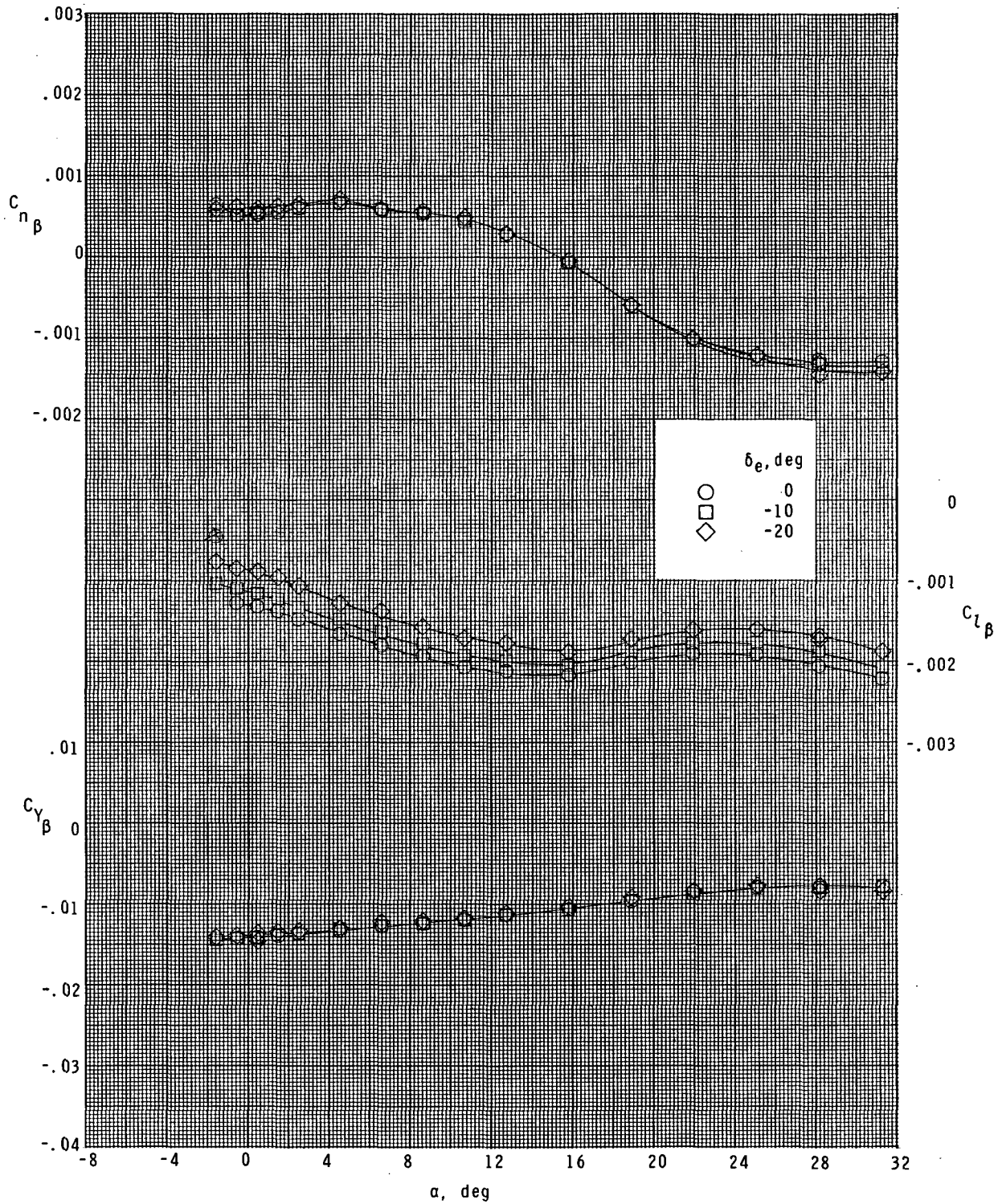
(c)   M = 4.63.

Figure 12.- Concluded.
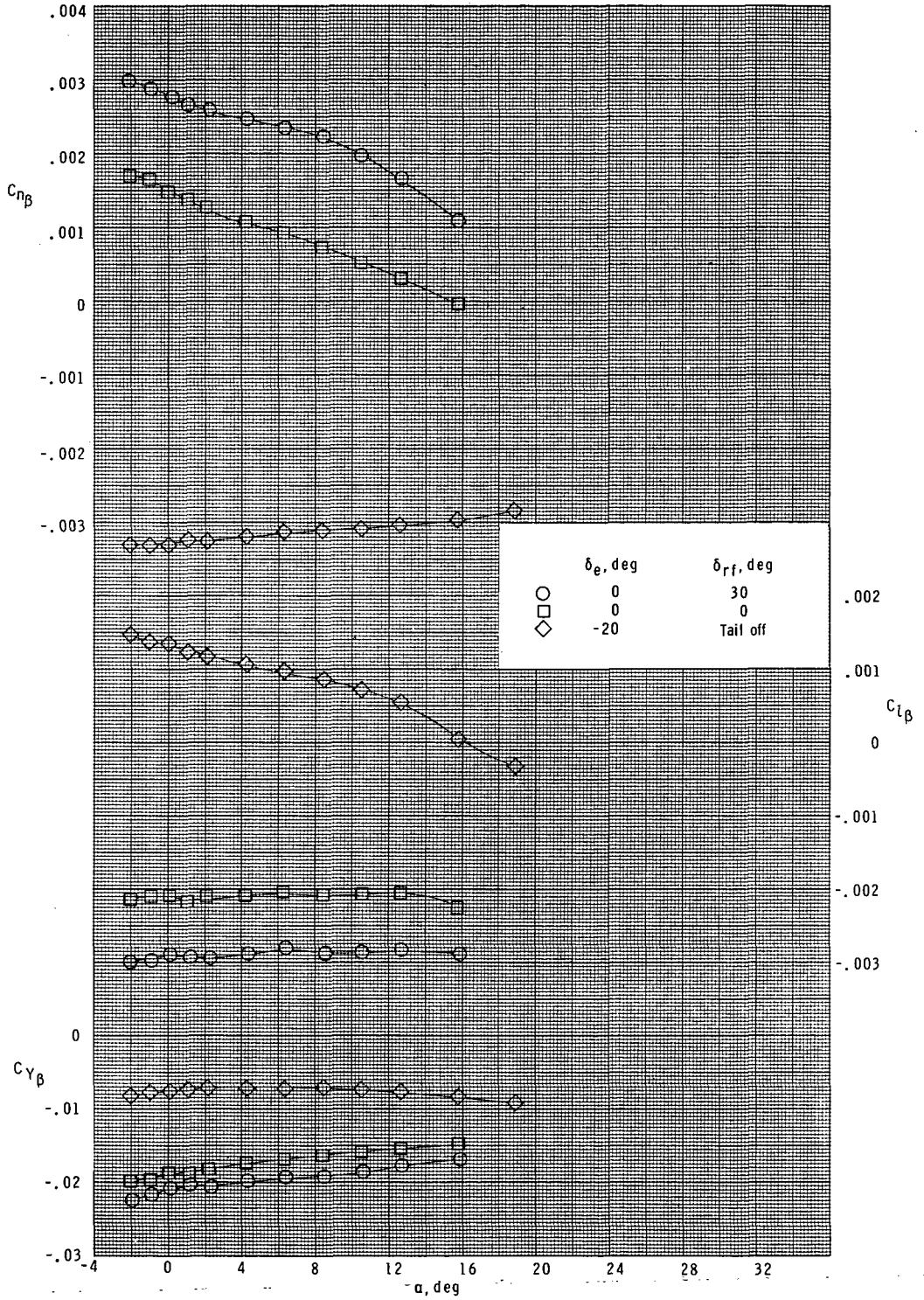
(a)   M = 1.60.

Figure 13.- Effect of rudder flare on lateral parameters.
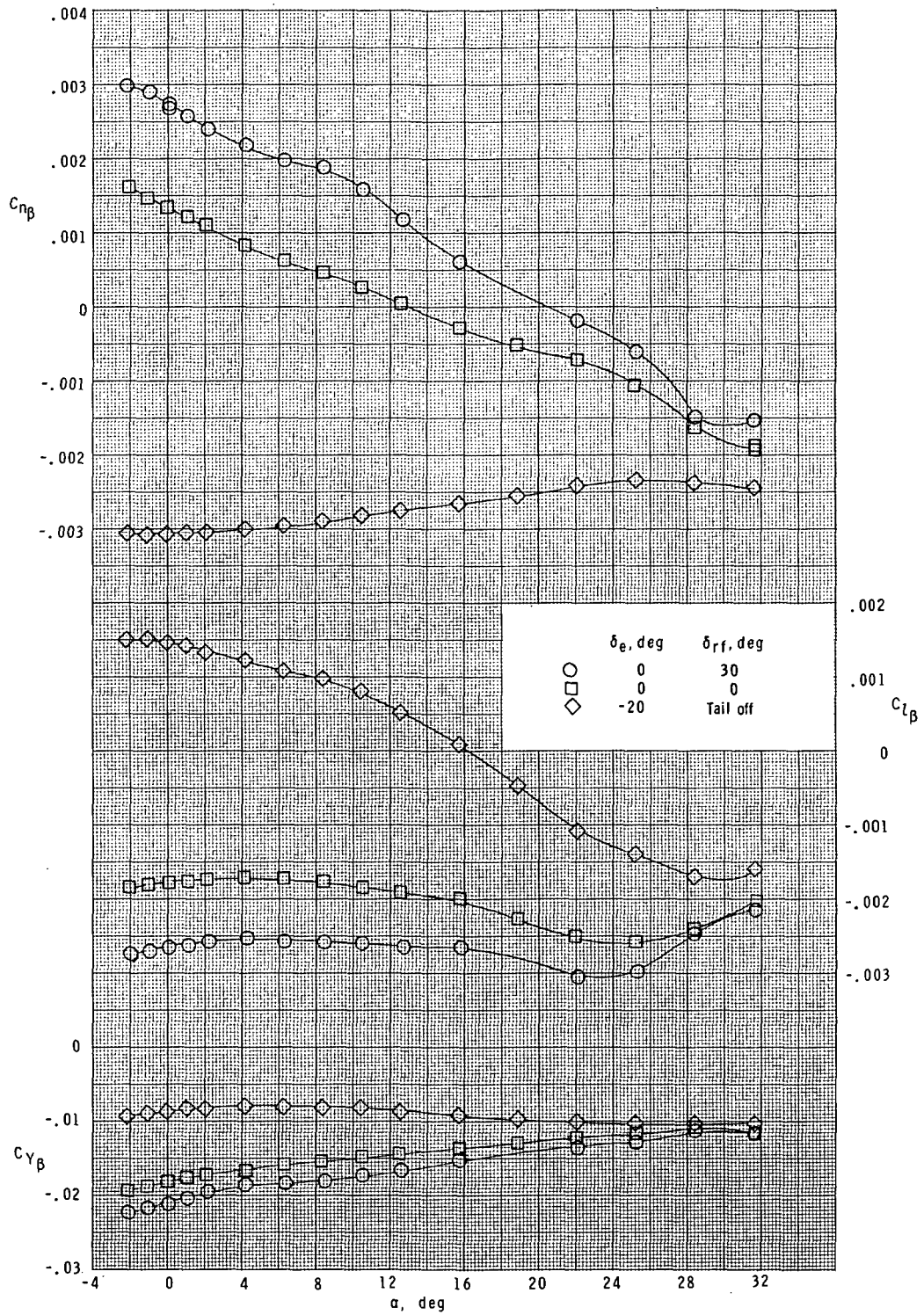
(b) M = 1.90.

Figure 13.- Continued.
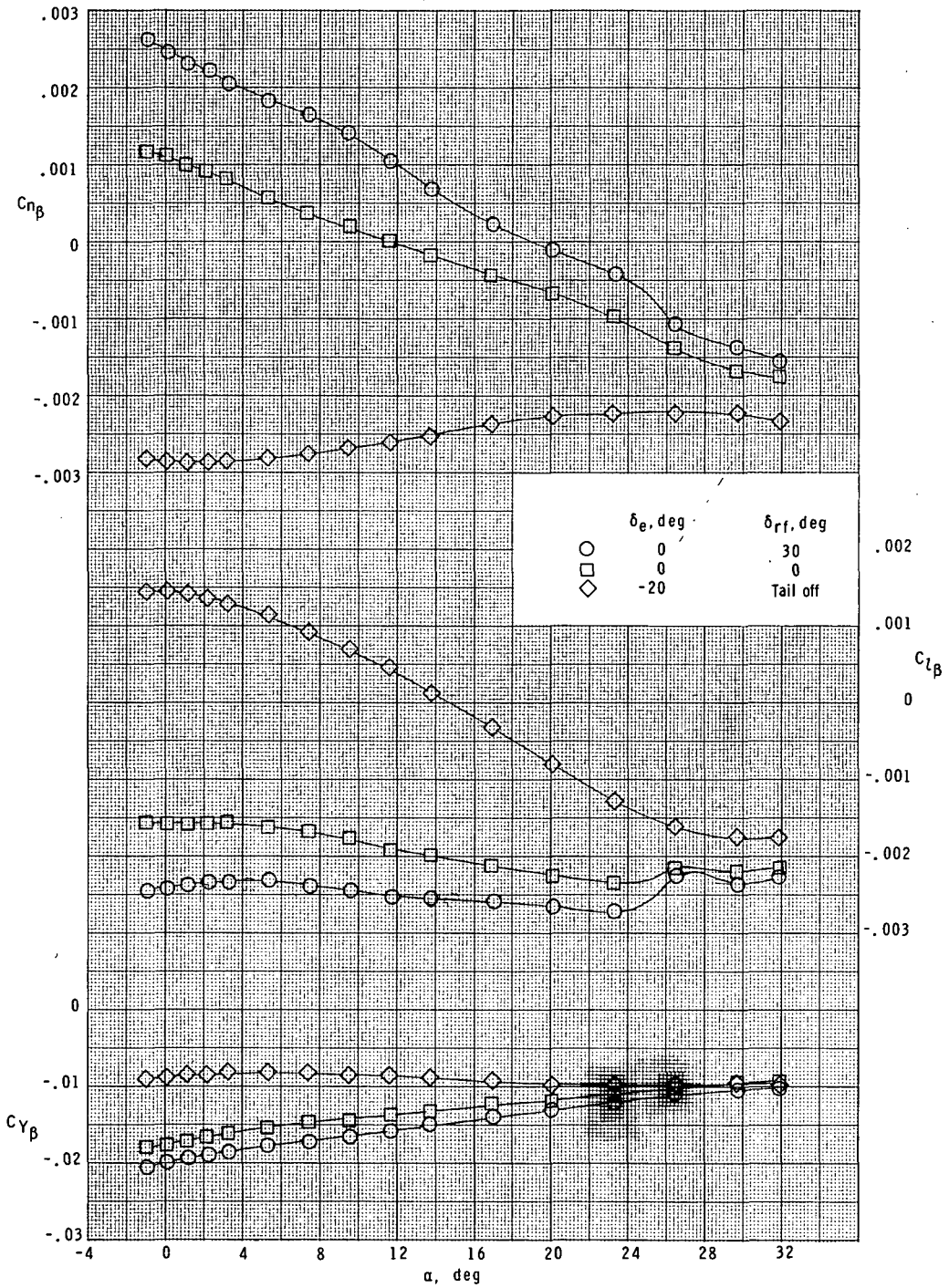
(c) M = 2.16.

Figure 13.- Concluded.
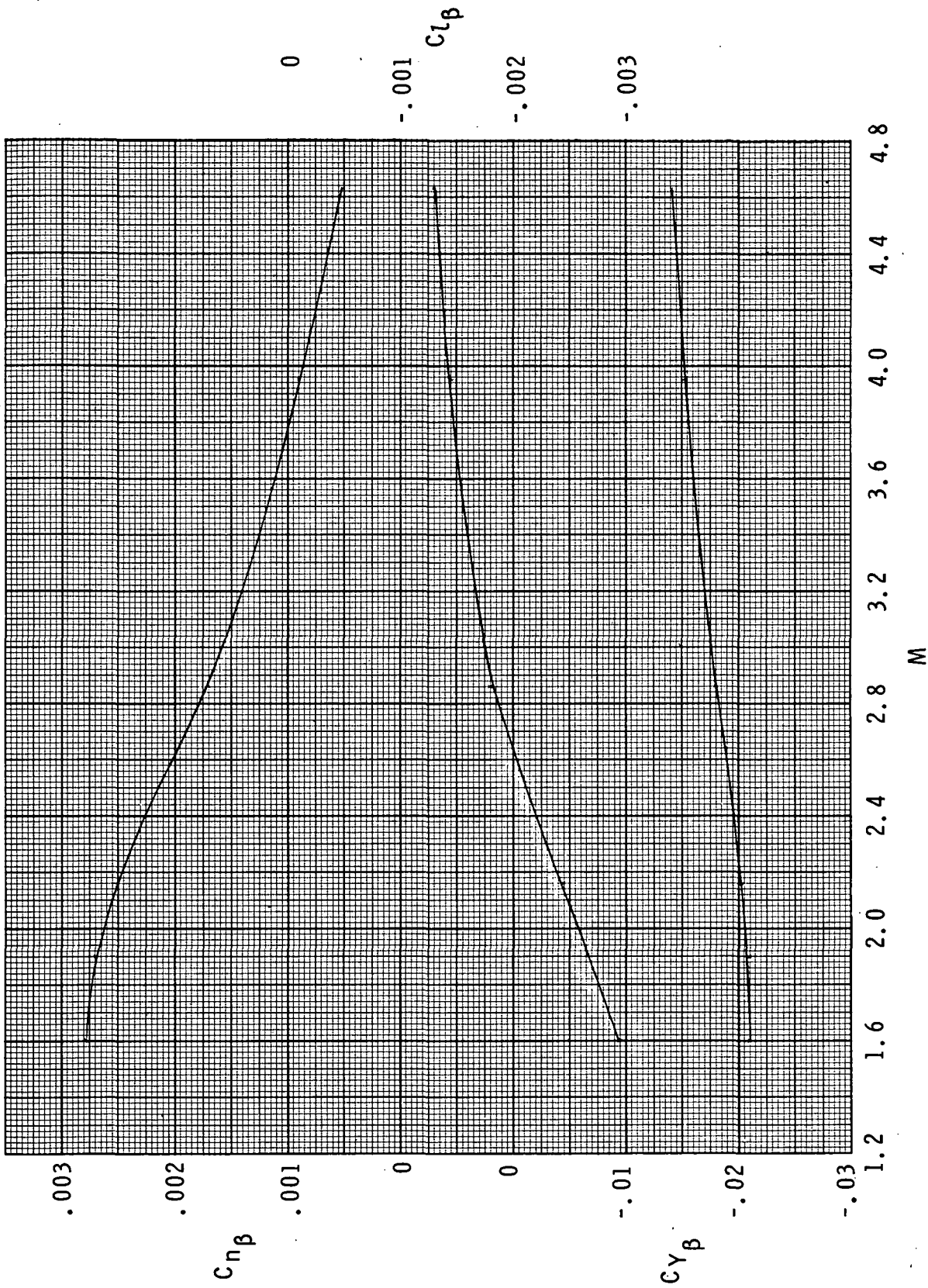
Figure 14.- Summary of lateral and directional stability parameters. $\delta_{rf} = 30^{o}$.

(a) $\alpha = 0^{o}$.

81
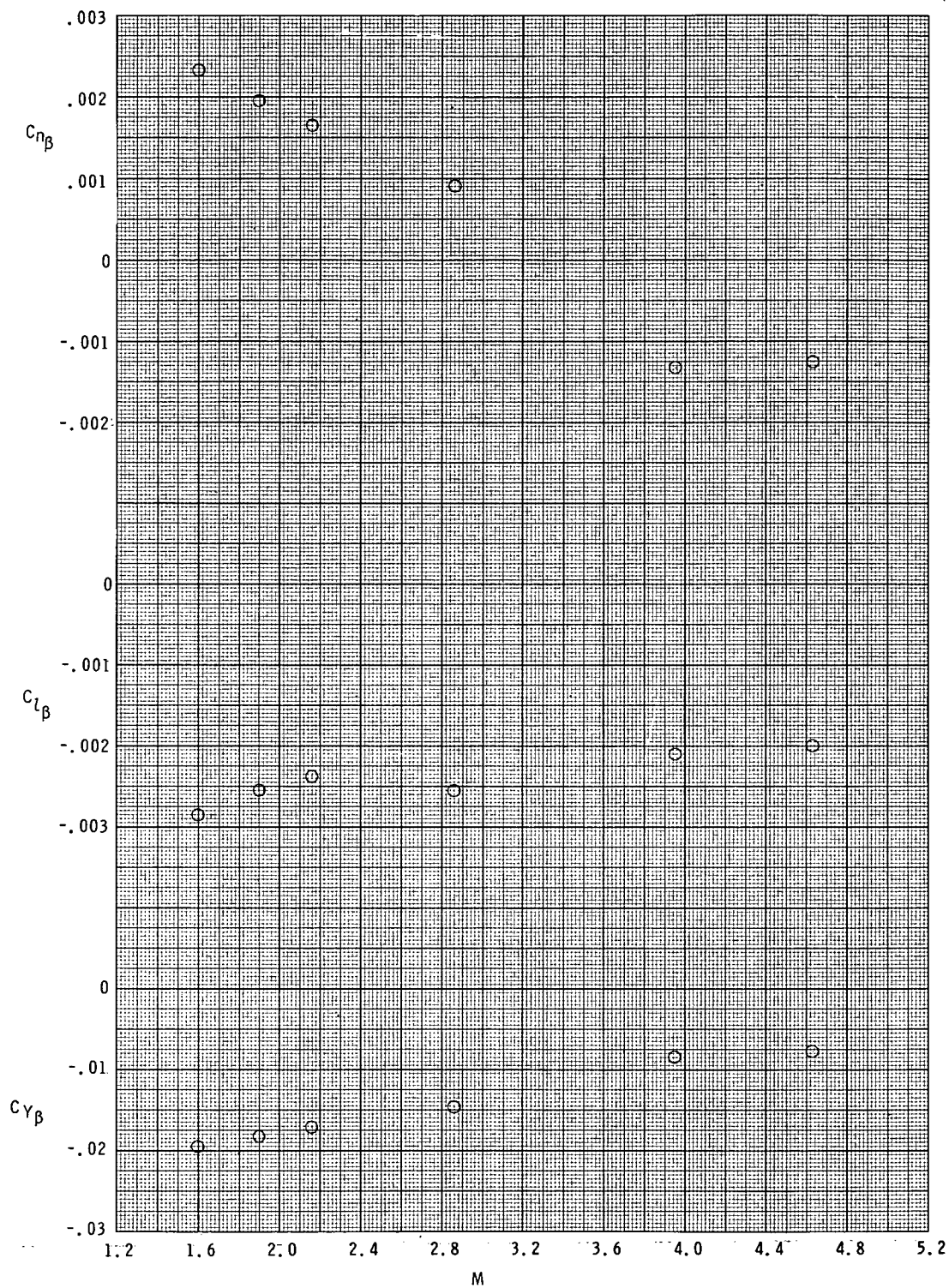
(b) Flight α-schedule.

Figure 14.- Concluded.
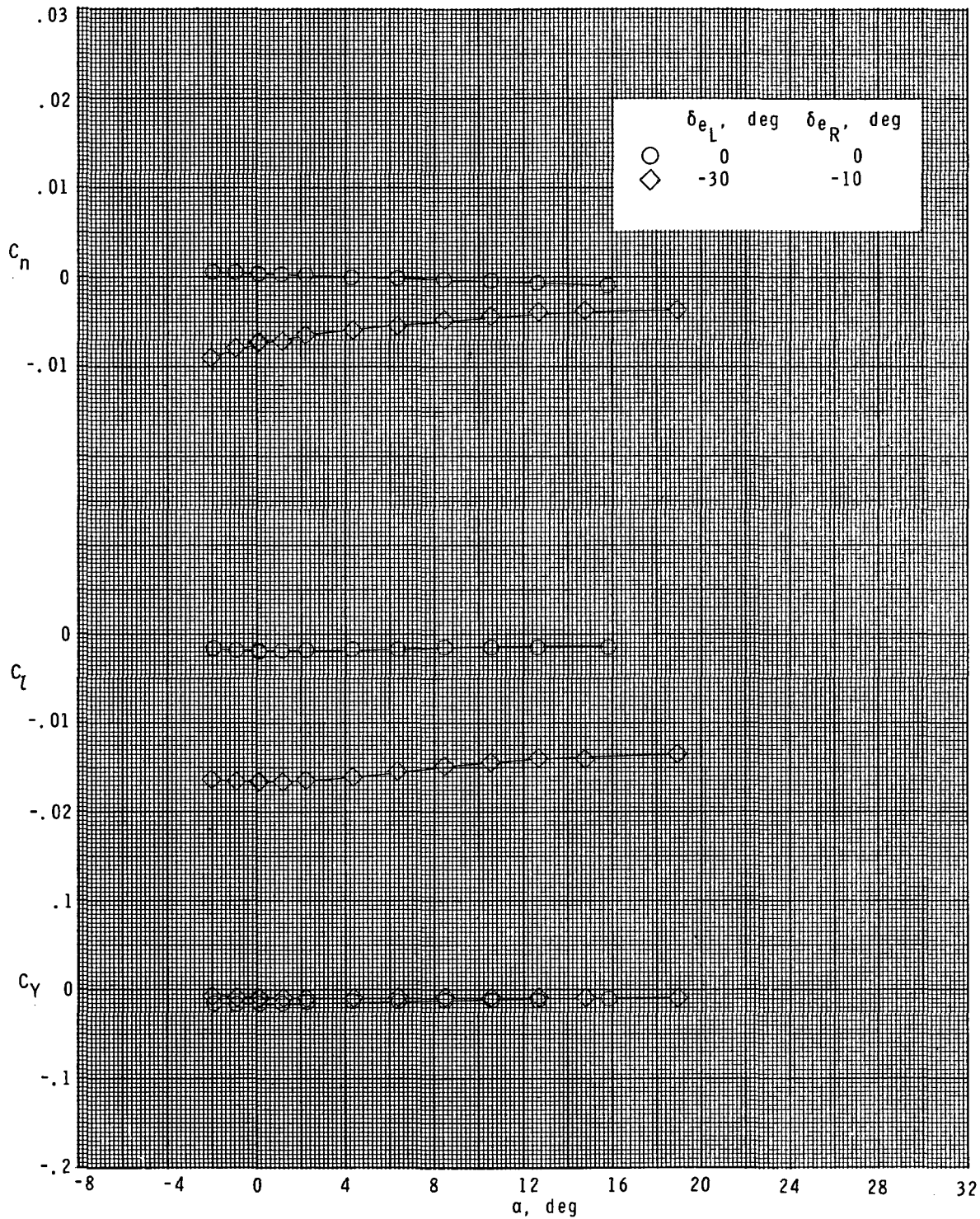
(a)   M = 1.60.

Figure 15.- Elevon effectiveness in roll. $\delta_{rf} = 30^o$.
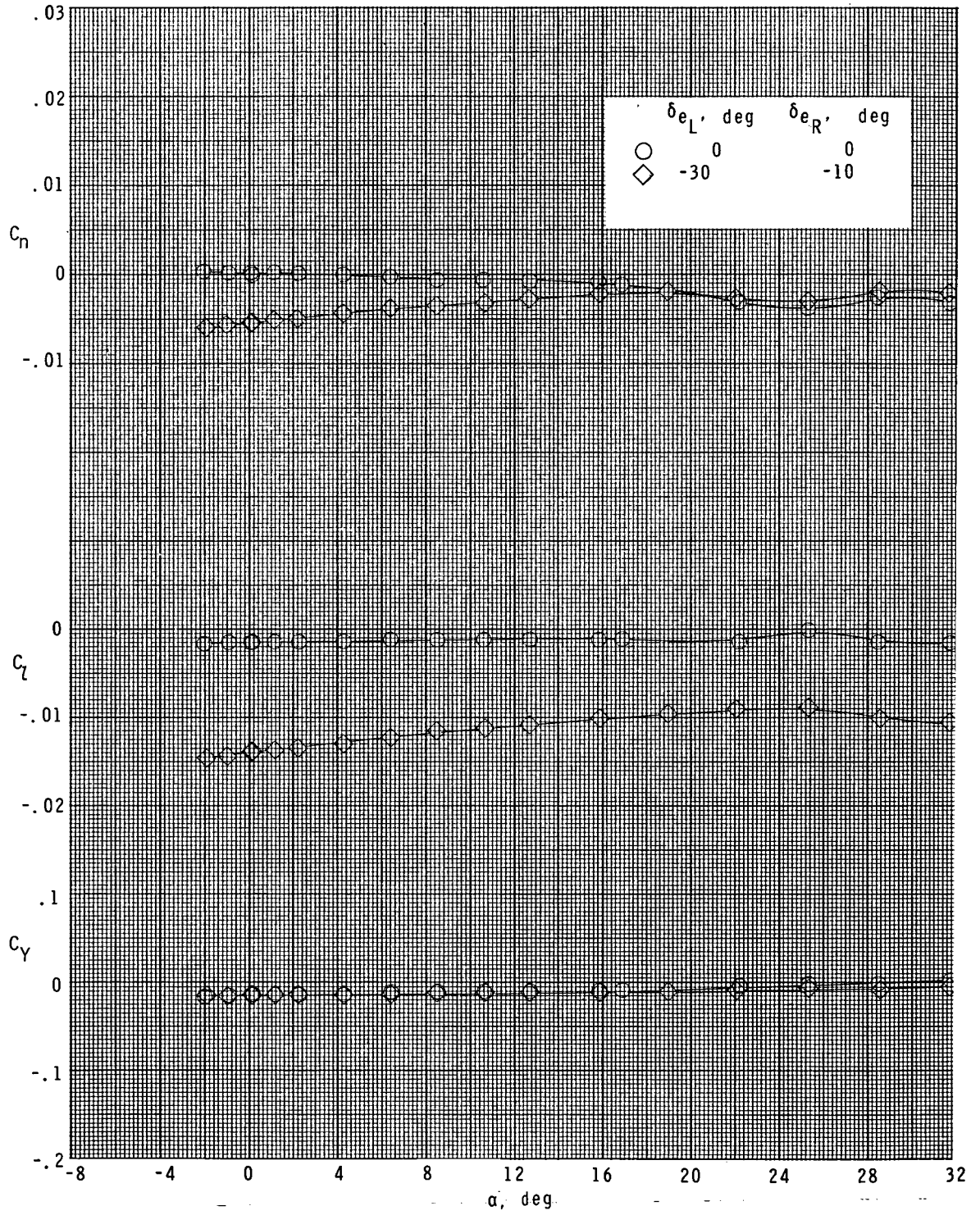
(b) M = 1.90.

Figure 15.- Continued.
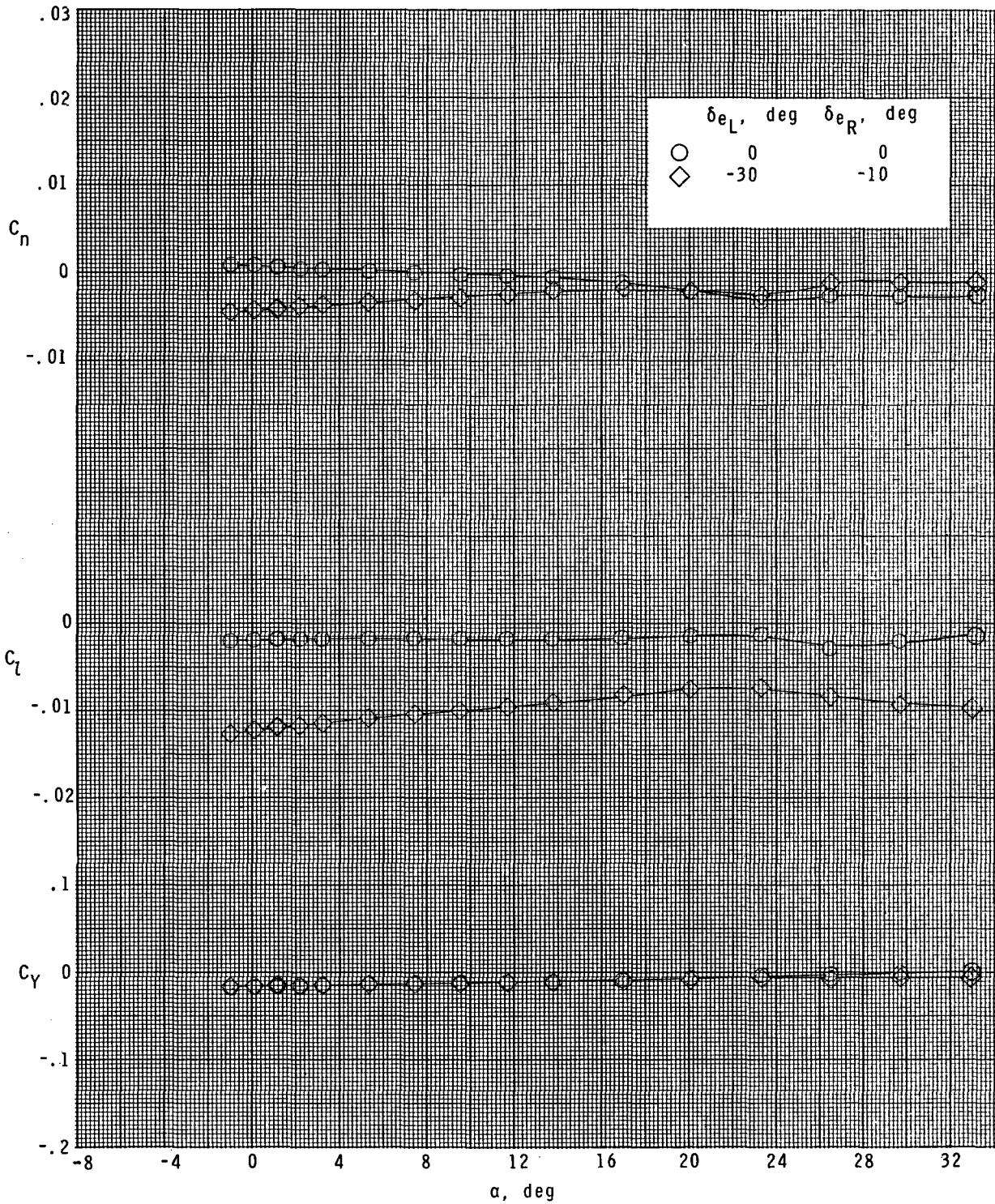
(c) M = 2.16.

Figure 15.- Continued.
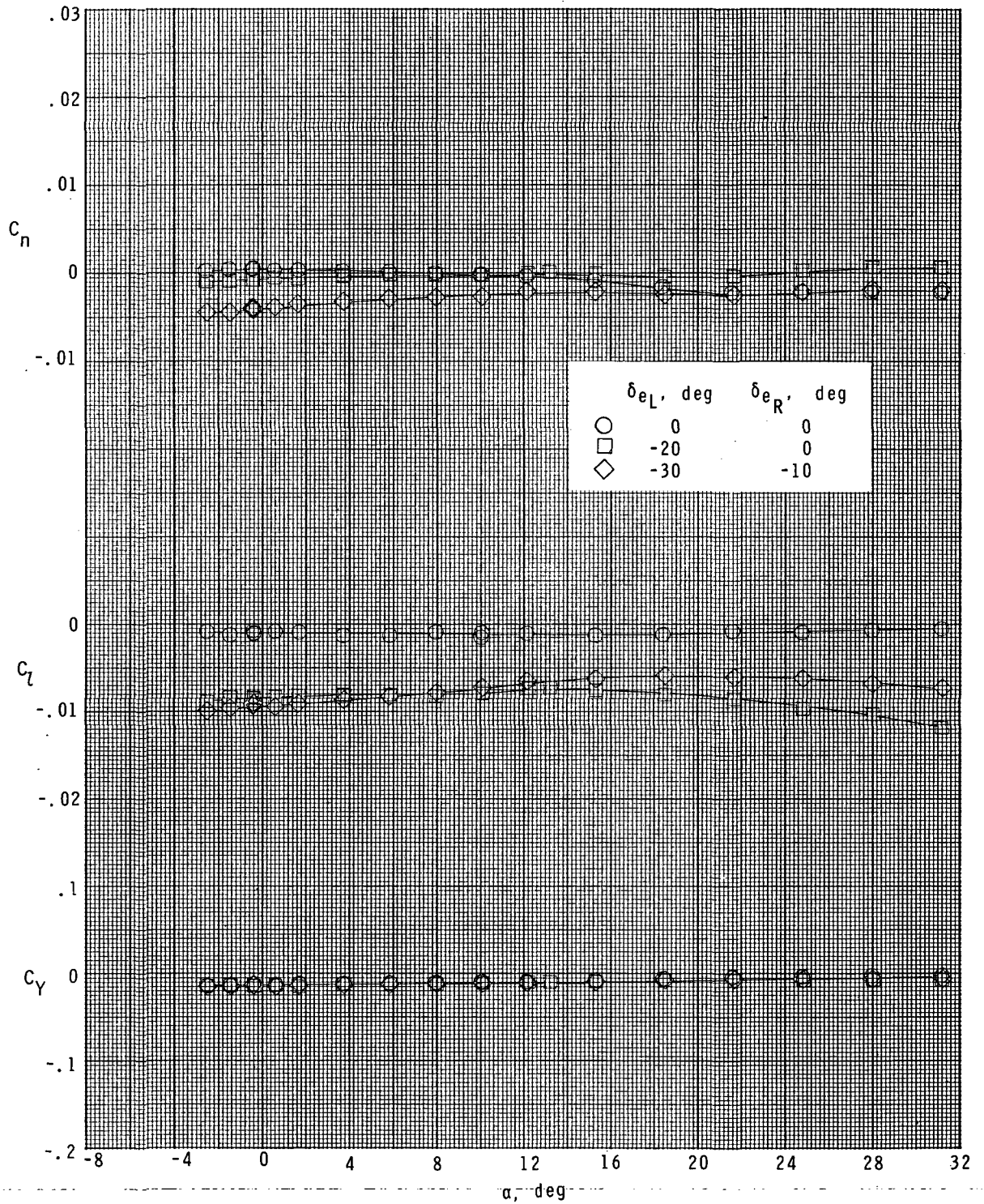
(d)   M = 2.86.

Figure 15.- Continued.
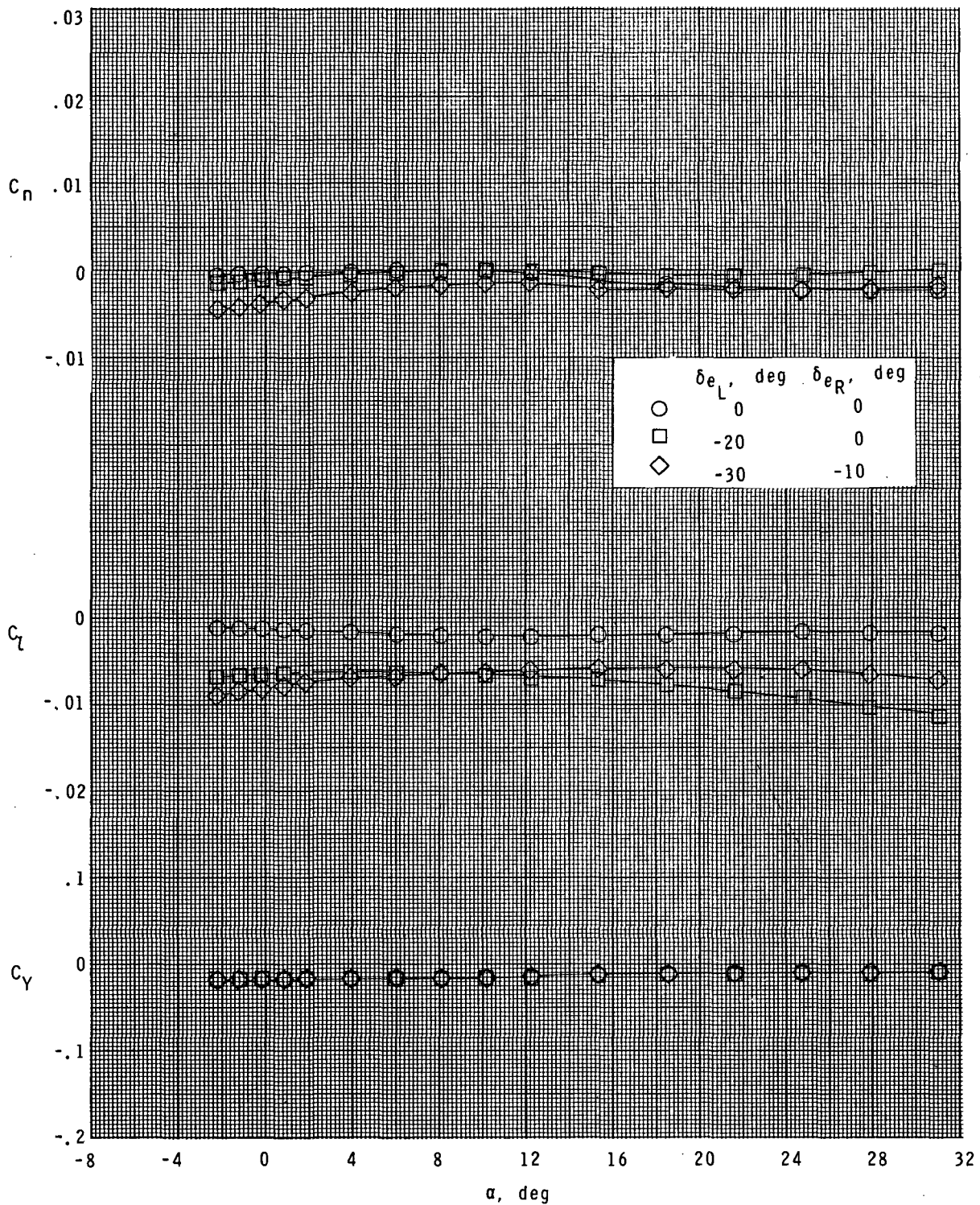
(e) M = 3.95.

Figure 15.- Continued.
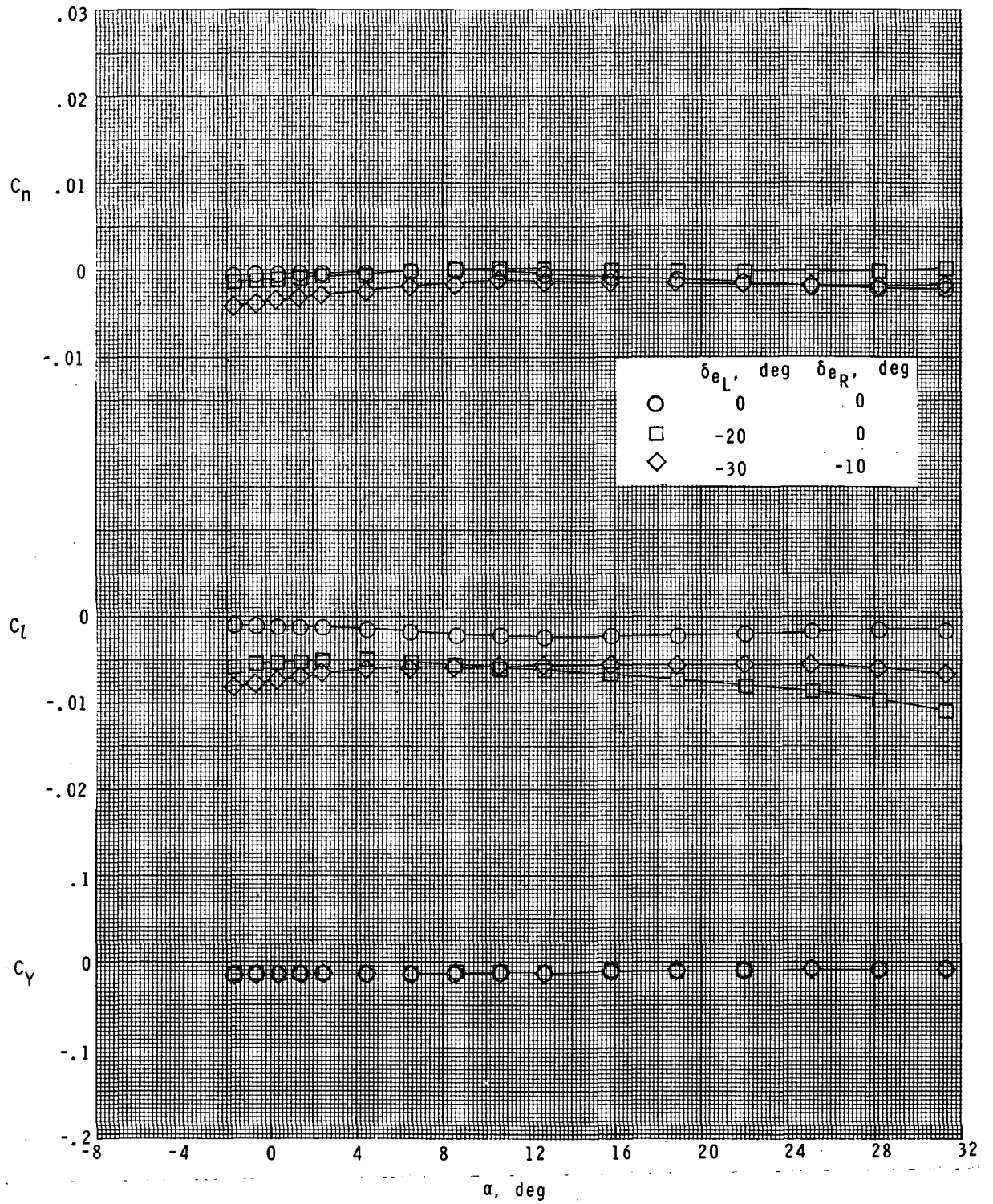
(f) M = 4.63.

Figure 15.- Concluded.

(a) M = 1.60; δ_e = -20°.
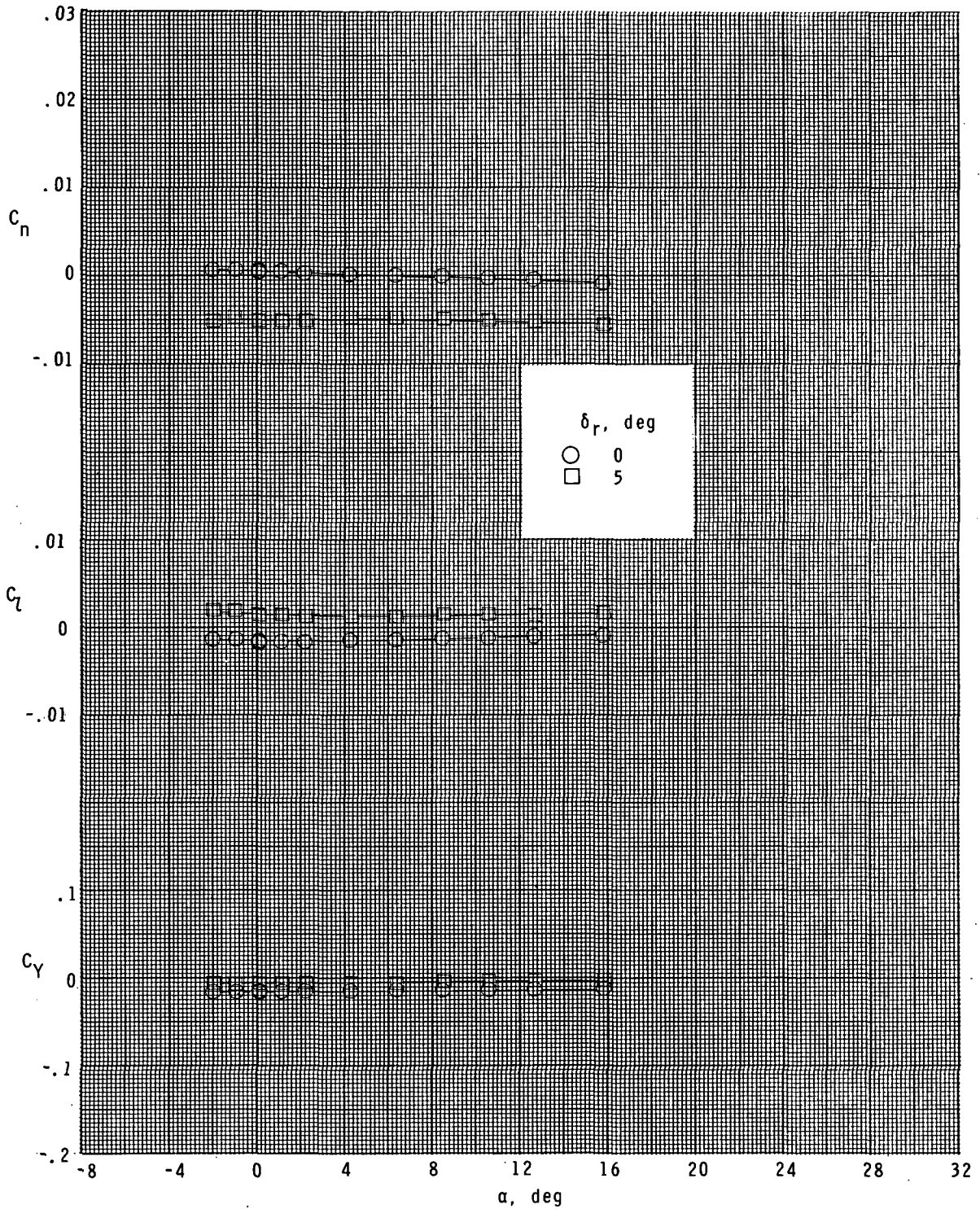
Figure 16.- Effect of rudder deflection on lateral characteristics. δ_{rf} = 30°.

(b)   M = 1.90; δ_e = -20°.
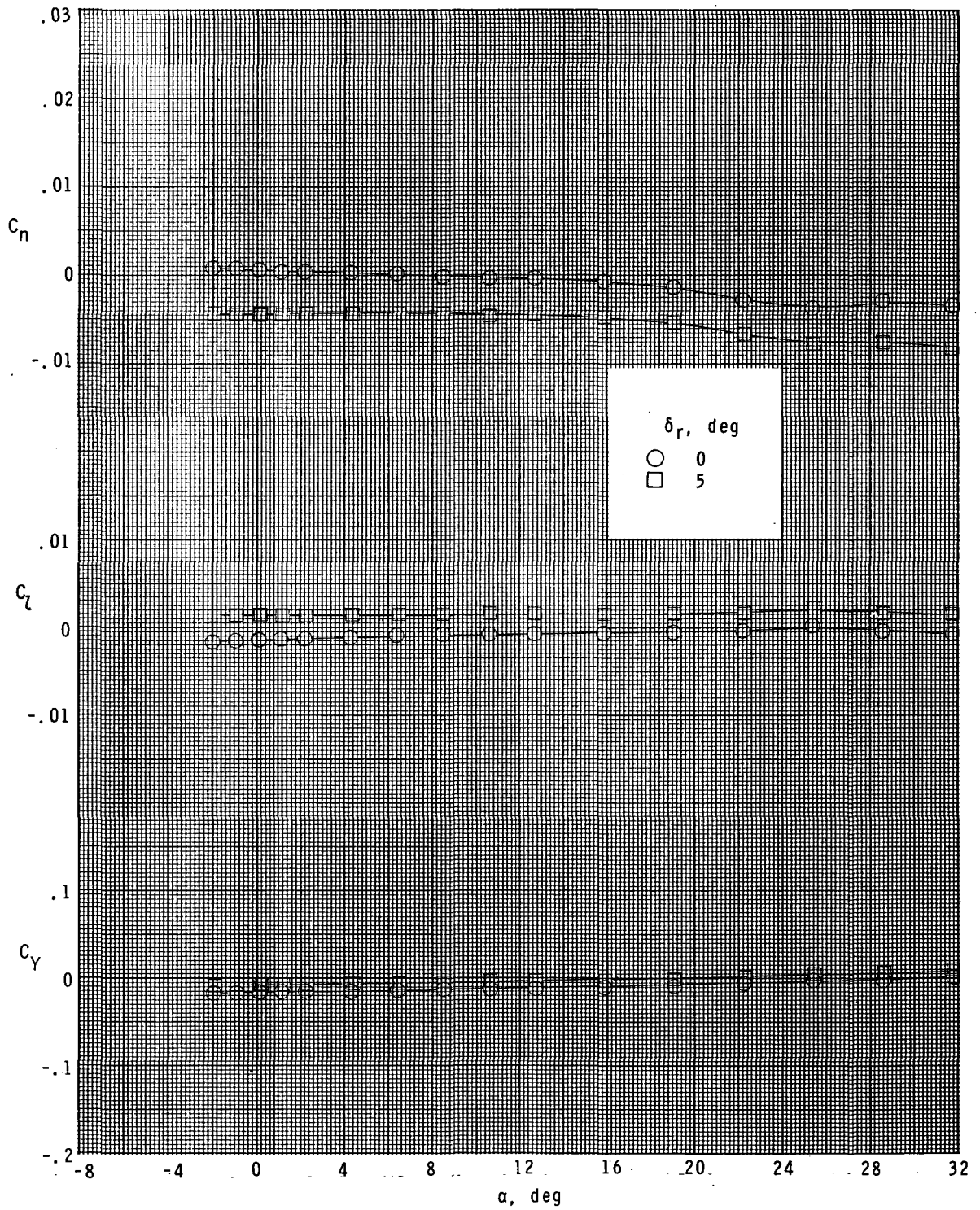
Figure 16.- Continued.
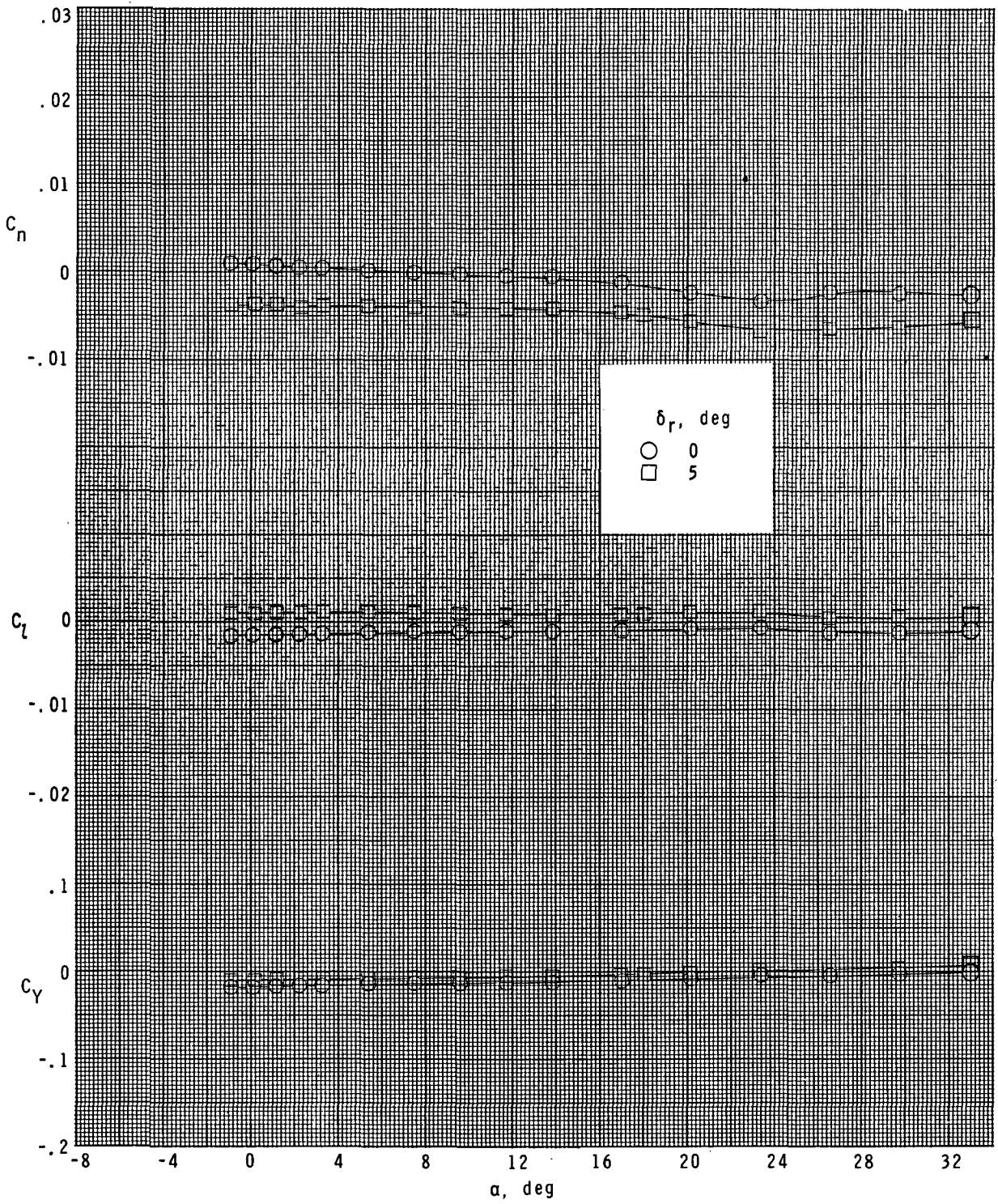
(c)   M = 2.16; δ_e = -20°.

Figure 16.- Continued.

(d) M = 2.86; δ_e = -10°.
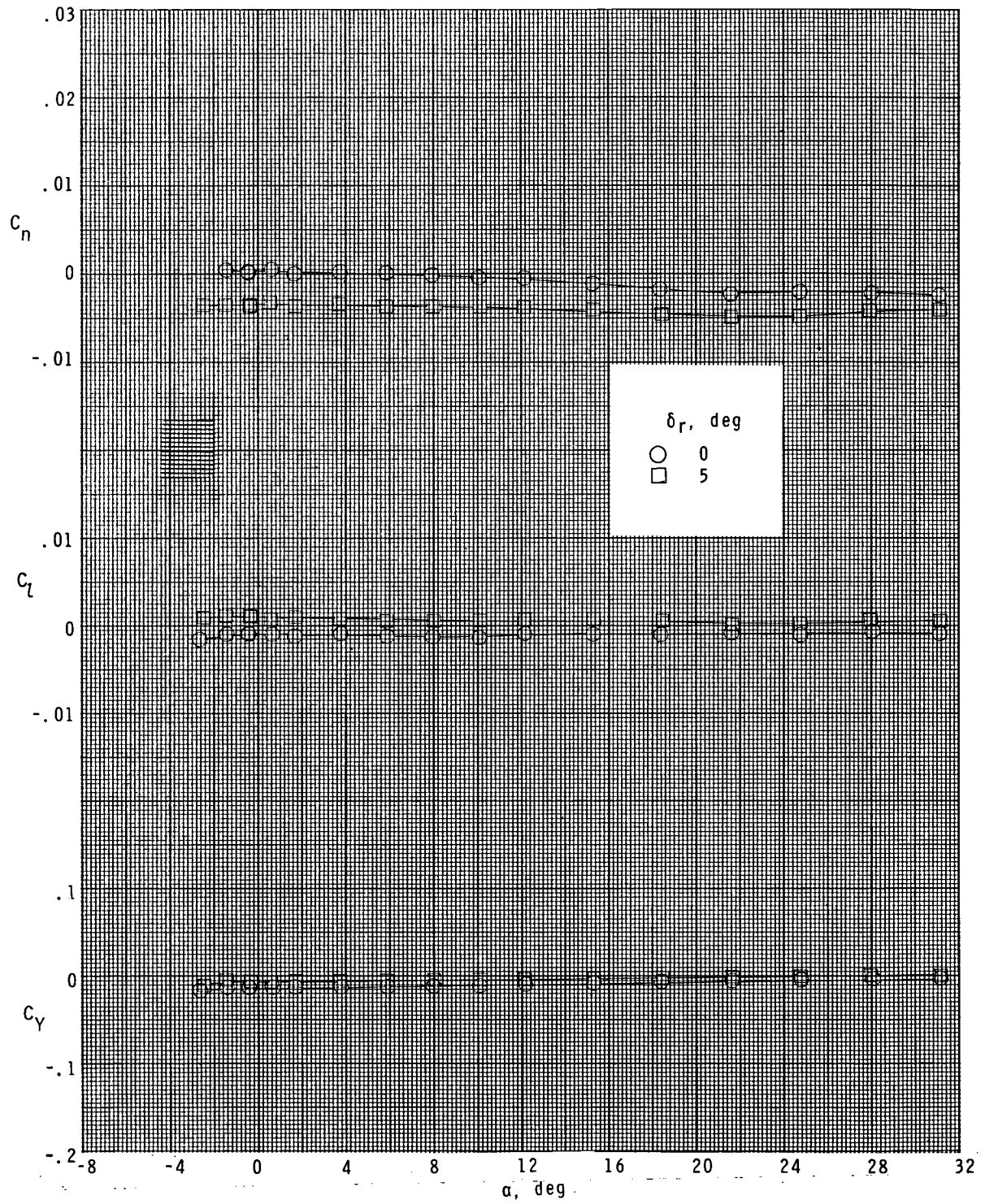
Figure 16.- Continued.

(e) M = 3.95; δ_e = -10°.
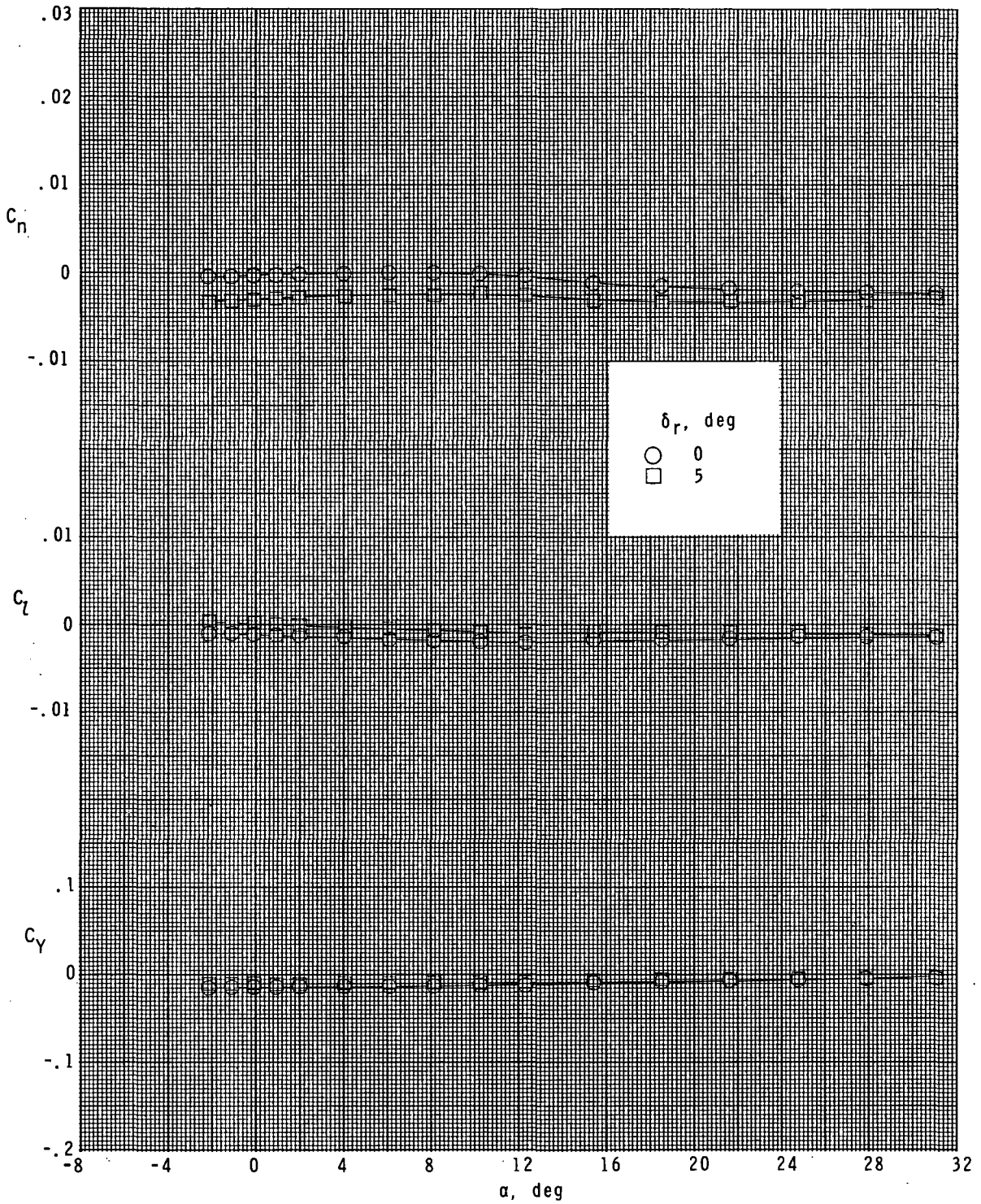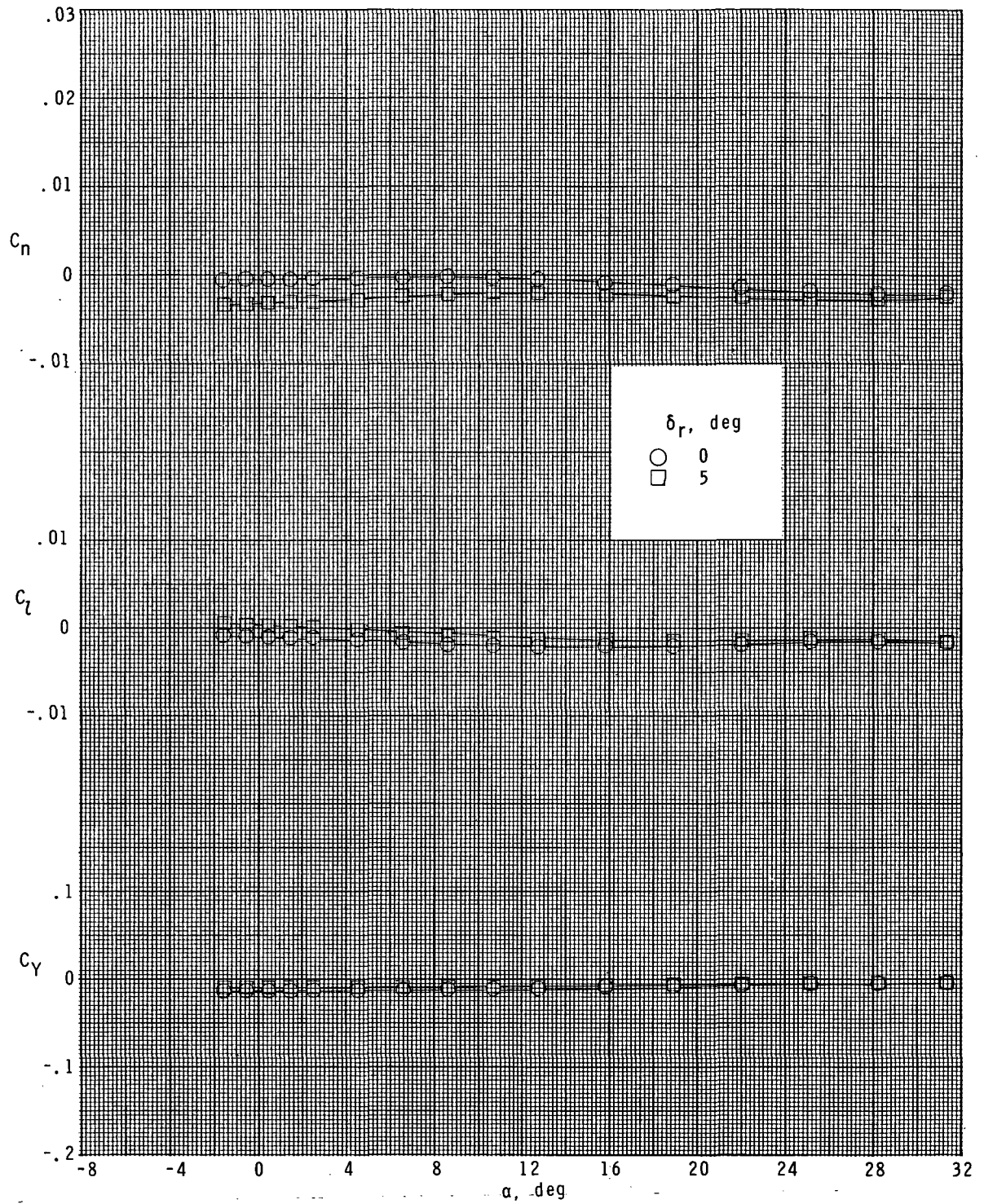
Figure 16.- Continued.

(f)   M = 4.63; δ_e = -10°.

Figure 16.- Concluded.

*"The aeronautical and space activities of the United States shall be
conducted so as to contribute . . . to the expansion of human knowl-
edge of phenomena in the atmosphere and space. The Administration
shall provide for the widest practicable and appropriate dissemination
of information concerning its activities and the results thereof."*
—NATIONAL AERONAUTICS AND SPACE ACT OF 1958

NASA SCIENTIFIC AND TECHNICAL PUBLICATIONS

TECHNICAL REPORTS: Scientific and
technical information considered important,
complete, and a lasting contribution to existing
knowledge.

TECHNICAL NOTES: Information less broad
in scope but nevertheless of importance as a
contribution to existing knowledge.

TECHNICAL MEMORANDUMS:
Information receiving limited distribution
because of preliminary data, security classifica-
tion, or other reasons. Also includes conference
proceedings with either limited or unlimited
distribution.

CONTRACTOR REPORTS: Scientific and
technical information generated under a NASA
contract or grant and considered an important
contribution to existing knowledge.

TECHNICAL TRANSLATIONS: Information
published in a foreign language considered
to merit NASA distribution in English.

SPECIAL PUBLICATIONS: Information
derived from or of value to NASA activities.
Publications include final reports of major
projects, monographs, data compilations,
handbooks, sourcebooks, and special
bibliographies.

**TECHNOLOGY UTILIZATION
PUBLICATIONS:** Information on technology
used by NASA that may be of particular
interest in commercial and other non-aerospace
applications. Publications include Tech Briefs,
Technology Utilization Reports and
Technology Surveys.

Details on the availability of these publications may be obtained from:

SCIENTIFIC AND TECHNICAL INFORMATION OFFICE

NATIONAL AERONAUTICS AND SPACE ADMINISTRATION
Washington, D.C. 20546